

Lentiviral vector-mediated gene transfer to  
ependymal cells in primary culture

Gentransfer in primäre ependymale Zellkulturen  
durch lentivirale Vektoren

**DISSERTATION**

**der Fakultät für Chemie und Pharmazie  
der Eberhard-Karls-Universität Tübingen**

zur Erlangung des Grades eines Doktors  
der Naturwissenschaften

2008

vorgelegt von

**Bhavani Shankar Kowtharapu**

**Tag der mündlichen Prüfung: 4. Juli 2008**

**Dekan: Prof. Dr. Lars Wesemann**

**1. Berichterstatter: Prof. Dr. Bernd Hamprecht**

**2. Berichterstatter: PD Dr. Stephan Verleysdonk**

# Acknowledgements

I would like to convey my sincere gratitude to all those who gave me the opportunity, support and encouragement to complete this thesis.

I would like to thank Prof. Dr. Bernd Hamprecht for giving me the opportunity to work in his group. His valuable suggestions, including his constructive critical remarks during the seminars, and his commitment improved my interest in science. His wide knowledge and way of thinking have been of great value for me.

Successful mentors, with their creativity and inspiring talks, indeed generate enthusiasm concerning the specified tasks, and I was fortunate enough to have PD Dr. Stephan Verleysdonk as my mentor, whose interest, help, motivating suggestions and continuous encouragement helped me a lot to solve the problems in my research and during the writing of this thesis. I am grateful to him for spending countless hours in teaching and explaining things to me with patience. I would have been lost without him and this work would not have been possible without his supervision and valuable support. What ever I inscribe here about him is too short and words cannot explain my gratitude towards him.

I wish to thank Prof. Dr. Günther Jung for making the peptides for my research and Dr. Mirna Rapp for the provision of thrombin.

I would like to thank Prof. Dr. Gabriele Dodt for her support during my qualifying exam in biochemistry at the beginning of my research and her group for providing plasmids and allowing me to use their microscope and X-ray film developing machine during my work.

I am thankful to Dr. M. Kittel, Dr. J.M. Schibel and G. Tiedemann for their continuous support and help during my work in the S2 lab at the Verfügungsgebäude.

I am thankful to Dr. Brigitte Pfeiffer-Guglielmi for introducing me to different laboratory safety instructions and for her support in providing antibodies and ordering animals.

I would like to thank Prof. Dr. Gabriele Dodt, Prof. Dr. Karl Forchhammer and PD Dr. Sven Gemballa for their encouragement and creating a friendly atmosphere during my thesis defence.

I would like to express my thanks to Ulrike Thieß for providing her technical expertise in the real-time RT-PCR analyses.

My warm and sincere thanks go to Barbara Birk for her excellent technical support in preparing primary cultures, media and also in doing several experiments like ELISA, Western blotting, and immunostaining for me. Also I am thankful to her for her personal help and patience with translating my letters, with my shopping and with my online bookings, travel etc.

I am really fortunate to have Dr. Wolfgang Hirschner and Daniela Scheible as my colleagues. I would like to thank them for their attention, cooperation and creating a wonderful working environment in the lab with their discussions, suggestions, encouragement and often with some gossips.

My special and sincere thanks go to Dr. Radovan Murin for posing his simple questions, for spending time with me in excellent discussions, for his valuable suggestions concerning my career, and my work. I especially thank him for giving me the opportunity to contribute to his research.

I am thankful to Dr. Benedikt Dolderer for his willingness to discuss my work and his support, especially in the planning of S2 experiments and his valuable company during my work in the S2 lab.



I wish to thank the staff of the Biochemistry chair I, Claudia Heberle, Hermann Liggesmeyer, Katharina Rehn, Ruth Schmid, Heide Schmid and Erika Mikeler for their constant support and help.

I also would like to thank all the employees of the Interfaculty Institute for Biochemistry and especially the Technical Director, Dr. Klaus Möschel for extending my contract during the last days of my thesis writing and providing official letters to solve my problems of Visa extensions.

I would like to acknowledge Journals Rights & Permissions Controller, Blackwell Publishing Ltd as well as Elsevier Limited for giving me permissions to use their copy righted material in this thesis.

I would like to thank all of my friends who made my time memorable during my stay in Tuebingen during this thesis.

My sincere gratitude goes to my beloved parents and family members for their continuous support throughout my studies. Especially to my dear babai K. Venkateswara Rao, for joining his M. Tech and supporting me during my M. Tech, without him may be I would have not thought of doing my PhD.

Specially and finally, I would like to express my deep and sincere gratitude to the subjects of my research, the new born rats, who sacrificed their lives for the sake of my research.



*to my Mentor  
Stephan Verleysdonk*



# Abbreviations

The following list does not contain abbreviations that do not require definition according to the instructions for authors of the FEBS Journal available online at the web address <http://www.blackwellpublishing.com/products/journals/suppmat/ejb/ejbtab4.htm>. Such abbreviations are used in the text and the legends of figures and tables without prior definition.

AAV	adeno-associated virus
Ad	adenovirus
AI	apoptosis inhibitor
AMV	avian myeloblastosis virus
ANP	atrial natriuretic peptide
AP	alkaline phosphatase
APS	ammonium peroxodisulfate
AQP	aquaporin
ATCC	American Type Culture Collection
BLAST	Basic Local Alignment Search Tool
CIAP	calf intestine alkaline phosphatase
CMV	cytomegalovirus
CNS	central nervous system
CVO	circumventricular organs
CP	crossing point
CSF	cerebrospinal fluid
Cy3	carbocyanin 3
CXCR	chemokine receptor
DAPI	4',6-diamidino-2-phenylindole
ddH <sub>2</sub> O	doubly deionized water

DIG	digoxigenin
DIV	day(s) in vitro
DMEM	Dulbecco's modified Eagle's medium
DMSO	dimethyl sulfoxide
dNTP	deoxyribonucleoside triphosphate
DTT	dithiothreitol
E	efficiency of PCR reaction
Ebola-Z	Ebola-Zaire
E1	early region 1
ECL	enhanced chemiluminescence
EF1 $\alpha$	elongation factor 1 alpha
EGFP	enhanced green fluorescent protein
EPC	ependymal primary culture
EST	expressed sequence tag
FCS	fetal calf serum
Fig	Figure
FITC	fluorescein isothiocyanate
FOXJ1	forkhead box J1
g	earth's gravitational acceleration (9.81 m/s <sup>2</sup> )
GFP	green fluorescent protein
HBS	HEPES-buffered saline
HEPES	N-2-hydroxyethylpiperazine-N'-2-ethanesulfonic acid
HIV-1	human immunodeficiency virus type 1
HSV	herpes simplex virus
IFT	intraflagellar transport
IFN- $\gamma$	interferon-gamma
KLH	keyhole limpet hemocyanin
LB	Luria-Bertani broth
LINE	long interspersed nuclear element
LTR	long terminal repeat
LV	lentiviral vector
MEM	Minimal Essential Medium

MOI	multiplicity of infection
MoMLV	moloney murine leukaemia virus
NCBI	National Center for Biotechnology Information, Bethesda, USA
NPs	natriuretic peptides
OD	optical density (absorbance/extinction)
ODA	outer dynein arm
ODA-DC	outer dynein arm docking complex
ORF	open reading frame
pAK-7	putative adenylate kinase 7
PBS	phosphate-buffered saline
PC	personal computer
PEI	polyethylenimine
PFA	paraformaldehyde
PS	penicillin/streptomycin
RNAi	RNA interference
rpm	revolutions per minute
RT	1. reverse transcriptase 2. reverse transcription 3. room temperature
SCO	subcommissural organ
shRNA	short hairpin RNA
SOC	superoptimal broth for catabolite repression (medium for bacterial liquid culture)
Spag6	sperm-associated antigen 6
SV40	simian virus 40
SVZ	subventricular zone
TEMED	N,N,N',N'-tetramethylethylenediamine
TNF- $\alpha$	tumour necrosis factor alpha
Tris	tris(hydroxymethyl)aminomethane
TU	transducing unit
VSV-G	vesicular stomatitis virus G protein





# Contents

<b>1. Introduction .....</b>	<b>1</b>
1.1. The ventricular system.....	1
1.2. The cerebrospinal fluid .....	1
1.3. The ependyma .....	2
1.3.1. Development of the ependyma.....	3
1.3.2. Ependymal responses to injury and antigens.....	3
1.4. Specialised ependymal organs.....	4
1.4.1. The subcommissural organ .....	4
1.4.2. The choroid plexus.....	4
1.5. Functions of the ependyma .....	5
1.5.1. The ependyma as neural stem cells.....	5
1.5.2. Participation of the ependyma in cerebral energy metabolism.....	6
1.5.3. The ependyma in brain water and osmoregulation .....	6
1.5.4. The ependyma as a secretory organ.....	7
1.5.5. The role of the ependyma in disease: Hydrocephalus .....	8
1.6. Cilia.....	9
1.6.1. Functions of cilia .....	10
1.7. Ependymal cells in primary culture .....	11
1.8. Methods of gene transfer to cells of the nervous system.....	11
1.8.1. Viral vectors .....	12
1.8.1.1. Adenoviral vectors .....	12
1.8.1.2. Adeno-associated viral vectors .....	12
1.8.1.3. Lentiviral vectors.....	13
1.8.1.4. Other viral vectors .....	13
1.8.1.5. Vector choice .....	14
1.9. Cell-specific promoters and their importance in gene transfer vectors .....	14
1.10. Scope of the thesis.....	15
<b>2. Results .....</b>	<b>17</b>
2.1. Identification of ependyma-specific cDNA fragments.....	17
2.2. Bioinformatic characterisation of the potentially ependyma-specific E71 protein .....	19
2.3. Analysis of the E71 transcription profile by real-time RT-PCR .....	21
2.3.1. E71 tissue-specific transcription profile .....	21
2.3.2. E71 transcription kinetics in ependymal primary cultures.....	21
2.4. Determination of immunoreactivity and specificity of the E71 antiserum.....	23
2.4.1. ELISAs for E71 antisera.....	23
2.4.2. Detection of E71 by Western blotting .....	24
2.5. Transfection of ependymal primary cultures .....	27
2.5.1. Calcium phosphate precipitation method .....	27
2.5.2. Polyethylenimine-mediated gene transfer.....	27
2.6. Lentiviral vector-mediated gene transfer .....	28
2.6.1. Production of lentiviral vectors .....	28
2.6.2. Titration of lentiviral vectors .....	29
2.6.3. p24 ELISA.....	31

2.6.4. Production of pseudotyped lentiviral vectors .....	32
2.6.5. Lentiviral vector-mediated transfection of ependymal cells in primary culture...	32
2.6.5.1. Transfection of differentiated ependymal cells in primary culture .....	32
2.6.5.2. Transfection of undifferentiated ependymal primary cultures.....	33
2.6.6. Transfection of ependymal primary cultures with different pseudotypes .....	35
2.6.7. Effect of virus on ependymal primary cultures .....	35
2.6.8. Transfection of ependymal primary cultures in the presence of	
apoptosis inhibitor II (NS3694) .....	37
2.6.8.1. Transfection in the presence of apoptosis inhibitor II (NS3694).....	37
2.6.8.2. Effect of apoptosis inhibitor II (NS3694) on the ependymal primary cultures	
.....	38
2.6.9. Transfection of ependymal primary cultures with virus encoding GFP under the	
control of kinociliated-cell specific promoters .....	39
2.6.9.1. Lentivirus encoding GFP under the control of the FOXJ1 promoter .....	40
2.6.9.2. Lentivirus encoding GFP under the control of the wdr16 promoter.....	41
2.6.9.3. Specificity of the FOXJ1 and wdr16 promoters .....	42
2.6.9.4. Transfection efficiencies in ciliated cells under the control of different	
promoters .....	44
2.6.9.5. FOXJ1 and wdr16 promoters drive the expression of transgenes in different	
species.....	45
2.6.10. Analysis of proviral DNA integration .....	47
2.6.11. Transfection of EPC with lentiviruses bearing transgenes tagged with GFP .....	49
2.6.11.1. Localisation of the Spag6-GFP fusion protein.....	50
2.6.12. Analysis of different small hairpin RNAs targeting Wdr16 .....	51
2.6.12.1. HEK-wdr16 cell line .....	51
2.6.12.2. Analysis of different anti-wdr16 shRNAs with the HEK-wdr16 cell.....	52
2.6.12.3. Analysis of the effect of different anti-wdr16 shRNAs on ependymal primary	
cultures .....	53
2.6.13. Transfection of HepG2 cells with HIV/VSV-G/GFP under the control of the wdr16	
promoter .....	55

### **3. Discussion ..... 57**

3.1. Quality of the employed subtractive ependymal cDNA libraries .....	57
3.2. E71 and the occurrence of coiled-coil proteins in ciliated cells .....	57
3.3. Transfection of ciliated epithelial cells .....	58
3.3.1. Nonviral vector-mediated gene transfer .....	58
3.3.2. Lentiviral vector-mediated gene transfer .....	59
3.4. Titration of lentiviral vectors .....	61
3.5. Lentiviral vector-mediated gene transfer to ependymal cells in primary culture .....	62
3.6. Effect of lentivirus on the ependymal primary cultures.....	63
3.7. Expression of transgenes in ciliated cells using ciliated cell-specific promoters.....	65
3.7.1. The FOXJ1 promoter .....	65
3.7.2. The wdr16 promoter, a novel ciliated cell-specific promoter .....	66
3.7.3. Specificity of the FOXJ1 and wdr16 promoters .....	67
3.8. Integration of proviral DNA .....	67
3.9. Expression of Wdr16 in the hepatocarcinoma cell line HepG2 .....	68
3.10. Effect of apoptosis inhibitors on virus-infected EPC .....	68

3.11. Wdr16 silencing in ependymal primary culture .....	69
3.12. Localisation of cilia-specific, GFP-tagged proteins .....	70
3.13. Outlook .....	71

## **4. Materials and methods ..... 73**

4.1. Materials .....	73
4.1.1. Devices .....	73
4.1.2. General material .....	75
4.1.3. Chemicals .....	77
4.1.4. Kits .....	78
4.1.5. Reagents for molecular biology .....	79
4.1.6. Enzymes for molecular biology .....	79
4.1.7. Constituents and reagents for bacterial and mammalian cell cultures .....	80
4.1.8. Antibodies .....	81
4.1.8.1. Primary antibodies .....	81
4.1.8.2. Secondary antibodies .....	81
4.1.9. Bacterial strains .....	82
4.1.10. Mammalian cell lines .....	82
4.1.11. Animals .....	82
4.1.12. Vectors .....	83
4.1.12.1. Prokaryotic expression vectors .....	83
4.1.12.2. Lentiviral vectors .....	83
4.2. Methods .....	86
4.2.1. Cell culture .....	86
4.2.1.1. Media and solutions for cell culture .....	86
4.2.1.2. Ependymal primary cultures .....	87
4.2.1.3. Cultures of the human embryonic kidney cell line HEK293T .....	89
4.2.2. Production of lentiviral vectors in HEK293T cells .....	90
4.2.3. Concentration of lentiviral vectors .....	91
4.2.4. Titration of lentiviral vectors .....	91
4.2.5. Transfection of ependymal primary cultures .....	92
4.2.5.1. Calcium phosphate precipitation method .....	92
4.2.5.2. Polyethylenimine-mediated gene transfer .....	93
4.2.5.3. Lentiviral vector-mediated gene transfer .....	93
4.2.6. Isolation of genomic DNA from the transfected ependymal primary cell cultures .....	94
4.2.7. Analysis of proviral DNA integration .....	94
4.2.8. Immunostaining of the transfected ependymal primary cultures .....	95
4.2.9. Production of cell lines .....	95
4.2.10. Analysis of the efficiency of different shRNA constructs .....	96
4.2.11. Cultures of the human hepatocarcinoma cell line HepG2 .....	96
4.2.12. Harvesting of cells from culture dishes for Western blotting .....	97
4.2.13. Screening of subtracted ependymal cDNA libraries .....	97
4.2.14. Other molecular biology techniques .....	97
4.2.14.1. Preparation of medium for bacterial cultures .....	97
4.2.14.2. Preparation of agar plates .....	98
4.2.14.3. Bacterial liquid cultures .....	98

4.2.14.4. Preparation of bacterial glycerol stocks .....	98
4.2.14.5. "Mini" scale preparation of plasmid DNA from bacterial liquid cultures.....	98
4.2.14.6. Isolation of total cellular RNA from cultured cells.....	99
4.2.14.7. Isolation of genomic DNA from cultured cells.....	100
4.2.14.8. Extraction of DNA from agarose gels.....	100
4.2.14.9. Direct purification of PCR products .....	101
4.2.14.10. Photometric determination of nucleic acid concentration .....	102
4.2.14.11. Cloning of the E71 PCR products into the pDNR-1r vector .....	102
4.2.14.12. Cloning of the Spag6 PCR products into the pWPXL vector .....	104
4.2.14.13. Cloning of shRNAs into the pLVTHM vector .....	105
4.2.14.14. Replacement of the promoter in the pWPXL vector .....	106
4.2.14.15. Restriction digestion of DNA.....	108
4.2.14.16. Phenol / chloroform / isoamyl alcohol extraction of DNA with subsequent ethanol precipitation .....	108
4.2.14.17. Dephosphorylation of vector DNA.....	109
4.2.14.18. Agarose gel electrophoresis .....	109
4.2.14.19. Ligation of PCR products into vector DNA.....	110
4.2.14.20. Preparation of E.coli competent cells.....	110
4.2.14.21. Transformation of competent bacterial cells with plasmid DNA .....	111
4.2.15. Reverse transcription of RNA.....	111
4.2.16. Real-time PCR.....	112
4.2.17. Generation of E71 peptide antibodies.....	112
4.2.18. ELISA for determining the peptide antibody titer .....	113
4.2.19. ELISA for determining HIV-1-p24 antigen.....	114
4.2.20. Protein assay (Bradford assay) .....	115
4.2.21. Discontinuous SDS-PAGE .....	116
4.2.22. Coomassie blue staining of polyacrylamide gels .....	117
4.2.23. Western blot analysis with chemiluminescence detection .....	118
<b>5. References .....</b>	<b>121</b>
<b>6. Summary .....</b>	<b>151</b>

# 1. Introduction

## 1.1. The ventricular system

The mammalian ventricular system consists of a series of four interconnecting, fluid-filled cavities which are called the lateral, third and fourth ventricles. The two large lateral ventricles open into the third ventricle through the interventricular foramina of Monro. The third ventricle is connected with the fourth ventricle through the aqueduct of Sylvius. The fourth ventricle narrows caudally into the central canal of the spinal cord. The cisterna magna of the subarachnoid space is reached from the fourth ventricle through the median aperture (foramen of Magendie). At its distal end, the central canal of the spinal cord becomes dilated; this dilatation has been designated the terminal ventricle or ampulla caudalis. The ventricles are filled with cerebrospinal fluid, the majority of which is produced by the choroid plexus (Nicholson, 1999). The CSF percolates through the ventricular system, flows into the subarachnoid space and is eventually absorbed by arachnoid villi and thus returned to the venous circulation (Purves et al., 2001). A small part of the CSF in the fourth ventricle also enters the central canal of the spinal cord (Cifuentes et al., 1992).

## 1.2. The cerebrospinal fluid

The epithelial cells of the choroid plexus secrete the CSF by a process involving the transport of  $\text{Na}^+$ ,  $\text{Cl}^-$  and  $\text{HCO}_3^-$  from the blood into the ventricles of the brain (Brown et al., 2004). In humans, the total CSF volume is about 140 ml, which is replaced by freshly secreted fluid every 8 hours (Davson and Segal, 1996). The directional beating of ependymal cilia may play a role in the circulation of CSF (Davson and Segal, 1996), as evidenced by the development of hydrocephalus in small animals suffering from primary ciliary dyskinesia (Greenstone et al., 1984; Afzelius, 1985). The CSF acts as a medium of communication within the CNS by carrying hormones and transmitters between different areas of the brain (Spector and Eells, 1984; Preston, 2001).

### 1.3. The ependyma

The term *ependyma* was introduced by Virchow to name the epithelium covering the walls of the ventricular system. It consists of cells with particular structural and functional properties named ependymocytes (Mestres, 1998). Their kinocilia facilitate the rostral-to-caudal flow of cerebrospinal fluid (CSF) through the ventricular system, while their large surface area provides an avenue for the exchange of metabolites. The ependymal cells have been suggested to prevent the re-entry of toxic substances from the CSF into the neuropil, and to help to regulate the composition of the neuronal microenvironment (Del Bigio, 1995).

In vivo, the ependyma forms a continuous but heterogeneous epithelial layer composed of several cell types, including those particular to the circumventricular organs (Knowles, 1972; Oksche, 1973; Rodriguez, 1976; Leonhardt, 1980; Del Bigio, 1995). These cell types can be distinguished by their specific location in relation to the ventricular cavities, by the types of their cell-cell junction complexes, and by the presence or absence of kinocilia on their apical surface. Generally, the ependymocytes of the ventricular epithelia bear bundles of kinocilia. However, on the floor of the third ventricle, the local ependymal cells that are called tanycytes lack those cell appendages. Ciliated and nonciliated ependymocytes generally lack functional tight junctions. However, so-called leaky tight junctions between ciliated ependymal cells have been described (Lippoldt et al., 2000). Ependymal cells in possession of completely sealed, truly functional tight junctions, in the sense of a diffusion barrier, are found in circumventricular organs (CVOs) such as the choroid plexus, the median eminence, and the subcommissural organ (Leonhardt, 1980). The tanycytes of the ventrolateral walls of the third ventricle are a special kind of nonciliated ependymal cell with a long basal process that occasionally contacts the blood–brain barrier (Wittkowski, 1998). The specialized ependymocytes of the choroid plexus are identified by their cuboidal shape, numerous apical, long, club-shaped microvilli, functional tight junctions and their exclusive location (Maxwell and Pease, 1956; Milhorat, 1976; Peters and Swan, 1979). Other discrete populations of specialized ependymal cells are formed by those of the secretory CVOs, such as the subcommissural organ (Rodriguez et al., 1984) or the subfornical organ (Dellmann and Simpson, 1979).

The main characteristic feature of the most abundant, “normal”, apparently unspecialised ependymal cells is a bundle of approximately 40 kinocilia on the apical surface (Manthorpe et al., 1977) which are approximately 8 µm long and project into the CSF, beating with a frequency of 40 Hz in rat (O'Callaghan et al., 1999).

### **1.3.1. Development of the ependyma**

During development, ependymal cells originate from radial glial cells (Spassky et al., 2005) and are the first cells to differentiate from the embryonic neuroepithelium at 5 weeks of gestation. The ventricular surface becomes completely covered by the ependymal precursors at 22 weeks of gestation (Sarnat, 1992). In the course of development, the ependyma begins its fetal existence as a pseudostratified columnar epithelium, which ensures an adequate supply of ependymal cells to cover the complete ventricular surfaces of the brain in later stages of development, even though the mature ependymocytes generally lack proliferative capacity (Sarnat, 1995). Gradually the epithelial layers become thinner until only a single layer of differentiated ependymal cells lines the ventricular system (Sarnat, 1998).

### **1.3.2. Ependymal responses to injury and antigens**

The ependyma, once differentiated from the neuroepithelium, is postmitotic (Spassky et al., 2005) and does not regenerate when injured (Sarnat, 1995). This becomes apparent by the lack of synthesis of intermediate filament and secretory proteins by the ependyma at the site of damage, and by the absence of proliferation markers from the cells (Sarnat, 1995). Enhanced expression of major histocompatibility complex class II genes after IFN-γ injection into the lateral ventricles (Lampson et al., 1994) and synthesis of tumour necrosis factor-α (Tarlow et al., 1993) by the ependymal cells show their participation in the initiation of an immune response to certain bacterial and viral infections.

## **1.4. Specialised ependymal organs**

### **1.4.1. The subcommissural organ**

The phylogenetically ancient and conserved subcommissural organ (SCO) is located in the dorsocaudal region of the third ventricle at the entrance of the Sylvian aqueduct and covers the ventral facet of the posterior commissure (Oksche, 1969). It is the first brain secretory structure to differentiate. The cells of the SCO, which release their secretory material into the ventricular CSF, are arranged in two layers, ependyma and hypendyma (Leonhardt, 1980; Rodriguez et al., 1992). The SCO secretes glycoproteins of high molecular mass (Nualart et al., 1991), which condense to form a thread-like structure called Reissner's fiber (Sterba, 1969; Meiniel et al., 1996). The SCO contains the receptors for peptides linked to hydromineral balance, such as angiotensin II, bradykinin and ANP (Leonhardt, 1980; Rodriguez and Caprile, 2001). The Reissner's fiber complex may play a role in basic morphogenetic mechanisms of the CNS (Rodriguez et al., 1998).

### **1.4.2. The choroid plexus**

The choroid plexus is formed by a specialized columnar ependymal epithelium surrounding a core of loose mesenchyme with a capillary convolute. This arrangement protrudes into the lumen of the ventricles (Keep and Jones, 1990; Muller and O'Rahilly, 1990). The choroidal cells have numerous microvilli with a small group of kinocilia on their apical surfaces (Peters and Swan, 1979). The choroid plexus is mainly involved in the production and secretion of CSF (Sarnat, 1998; Nicholson, 1999) and also forms one of the blood-brain barrier interfaces (Dziegielewska et al., 2001). Even though the macroscopic surface area of the choroid plexus appears small, the infolding of the choroidal cell membranes vastly increases the area for the exchange of substances (Keep and Jones, 1990; Segal, 2001).



## **1.5. Functions of the ependyma**

The role of the ependyma in normal brain function has by no means been fully understood even after more than a century of research carried out on this kinociliated cell type of the brain. Nevertheless, a number of putative functions have been postulated and investigated. Ependymal cells are at the interface between the brain parenchyma and the ventricular cavities and play an essential role in maintaining the flow of CSF through the ventricular system (Worthington and Cathcart, 1963; Cathcart and Worthington, 1964). Ependymal malfunction often leads to disturbances of CSF flow and causes hydrocephalus (Brody et al., 2000; Taulman et al., 2001; Kobayashi et al., 2002). Therefore, it has been suggested that ependymal cells divert the bulk flow of CSF in a particular direction and optimize the dispersion of neural messengers in the CSF (Roth et al., 1985). Apart from this, the ependyma has been implicated in additional roles as detailed below.

### **1.5.1. The ependyma as neural stem cells**

It has been proposed that the multiciliated ependymal cells lining the lateral wall of the lateral ventricle in adult mice act as slowly proliferating neural stem cells (Johansson et al., 1999). However, this possibility has been ruled out, since several groups were unable to produce multipotent stem cells from purified ependymal cells (Chiasson et al., 1999; Laywell et al., 2000; Capela and Temple, 2002; Doetsch et al., 2002). Instead, it has been shown that the astrocytes of the subventricular zone (SVZ), located in the lateral walls of the lateral ventricles, serve as neural stem cells. They generate neuroblasts that migrate in the SVZ (Doetsch and Alvarez-Buylla, 1996) in the direction of the CSF flow, which is generated by the coordinated beating of ependymal cilia (Sawamoto et al., 2006). The migrating neuroblasts enter the olfactory bulb via the rostral migratory pathway and finally differentiate into interneurons (Luskin, 1993; Lois and Alvarez-Buylla, 1994; Doetsch and Alvarez-Buylla, 1996). During development, the majority of ependymal cells are generated between embryonic days 14 (E14) and E16, and the formation of their cilia occurs later during the first postnatal week. Due to their postmitotic nature these matured ependymal cells do not divide after their differentiation and therefore cannot function as neural stem

cells (Spassky et al., 2005). They may, however, have a role in supplying the SVZ stem cells with nutrients and growth factors.

### **1.5.2. Participation of the ependyma in cerebral energy metabolism**

Ependymal cells contain the highest amount of glycogen among all the cell types of the central nervous system (Cataldo and Broadwell, 1986; Prothmann et al., 2001), along with a high level of glycogen phosphorylase protein and activity (Cataldo and Broadwell, 1986; Pfeiffer et al., 1990). Glycogen was shown to be a functional energy store in ependymal cells, and glycogenolysis was observed after exposure of EPC to serotonin or noradrenaline (Prothmann et al., 2001). The observed increase in the beating frequency of the ependymal cilia after stimulation with serotonin (Nguyen et al., 2001) indicates that ependymal glycogen may participate in energizing kinocilia.

Glucokinase as well as glucose transporter GLUT2 play an important role in brain glucose sensing (Leloup et al., 1998; Dunn-Meynell et al., 2002). GLUT4 mediates insulin-responsive glucose uptake (Furtado et al., 2002) and is also expressed in mammalian brain (Sankar et al., 2002). The presence of glucokinase in ependymal cells (Jetton et al., 1994), together with the facilitative glucose transporter GLUT2 in addition to GLUT1 (Maekawa et al., 2000), supports a role of the ependyma in brain glucose sensing. Besides glucose sensing, ependymal cells also need to take up the glucose required for energising their other functions, including movement of CSF by ciliary beat. They do so via signal-induced recruitment of glucose transporter GLUT1 to the plasma membrane, a process which was found to be more sensitive to insulin-like growth factor 1 than to insulin in the ependymal cell culture model (Verleysdonk et al., 2004).

### **1.5.3. The ependyma in brain water and osmoregulation**

The mature ependyma forms an interface between CSF and the brain extracellular fluid that may regulate the transport of ions and water. The water-regulatory hormone vasopressin plays an important role in brain osmoregulation by increasing the passage of water through

the ependymal layer (Rosenberg et al., 1986; Chen et al., 1992). Ependymal cells also possess angiotensin II receptors, which are further important regulators of brain water and electrolytes (Oldfield et al., 1994; Bruni, 1998). In addition, the presence of the water transport proteins, aquaporins (AQP) 4 and 9, on ependymal cells (Lehmann et al., 2004) supports the assumption that the ependyma may be involved in water homeostasis of the CNS (Del Bigio, 1995). Of the two aquaporins strongly expressed in brain, AQP1 is present in the choroid plexus and plays an important role in CSF secretion. The other, AQP4, has been implicated in the pathogenesis of brain edema (Papadopoulos et al., 2002). Besides aquaporins, natriuretic peptides (NPs) are considered to participate in cerebral osmoregulation. Ependymal cells carry the receptors for the NPs, and treatment of cultured ependymal cells with NPs elicits an increase in intracellular levels of guanosine 3',5' -cyclic monophosphate levels (cGMP; Wellard et al., 2003, 2006), indicating a responsiveness of the ependyma toward NPs. Also in choroid plexus epithelial cells, the atrial natriuretic peptide (ANP) induces the generation of cGMP and plays a role in regulating the rate of CSF formation (Johanson et al., 2006), thereby participating in CSF homeostasis. The concentration of ANP in the CSF appears to be less than that in the plasma (Marumo et al., 1987), and the ventricular peptide stems mainly from the anteroventral third ventricle (Geiger et al., 1989; Gundlach and Knobe, 1992). Ventricular ANP levels have been reported to be increased in intracranial diseases like intracerebral hematoma, subarachnoid hemorrhage and obstructive hydrocephalus (Diringer et al., 1990).

#### **1.5.4. The ependyma as a secretory organ**

The presence of secretory droplets at the apical surface of ependymal cells prior to the acquisition of cilia implicates them in a secretory role (Del Bigio, 1995). The presence of granulophysin, a membrane protein linked to exocytosis, in human ependymal cells also supports the idea of their secretory functions (Hatskelzon et al., 1993). Further evidence in this direction is provided by the presence of the mRNAs for chromogranin B, secretogranin (Gee et al., 1993) and sulfated glycoprotein-2 in rat ependymal cells (Senut et al., 1992; Danik et al., 1993). In the case of the ependymal cells of the subcommissural organ, they

secrete SCO-spondin into the CSF, where this glycoprotein aggregates and forms Reissner's fiber (Meinzel, 2007).

### **1.5.5. The role of the ependyma in disease: Hydrocephalus**

Hydrocephalus is a disorder characterised by dilation of the cerebral ventricles and abnormalities in the flow or resorption of cerebrospinal fluid (Zhang et al., 2006). It occurs at the rate of about 3-4 per 1000 live births (Pattisapu, 2001), of which approximately 20% are caused by aqueductal stenosis (Sarnat and Menkes, 2000). Hydrocephalus can be classified into a communicating and a non-communicating form. The communicating hydrocephalus is characterised by an increase of CSF volume in the ventricles due to increased production or impaired resorption in the absence of CSF flow obstruction. Non-communicating hydrocephalus, on the other hand, originates from the pathophysiological obstruction of CSF flow, e.g. at the aqueduct of Sylvius or the foramen of Monro (Perez-Figares et al., 2001).

Hydrocephalus may be caused by congenital insults, genetic mutations, tumors or infections (Crews et al., 2004). Inoculation of mammalian brains with myxo- or reoviruses causes ependymal damage and leads to hydrocephalus (Nielsen and Baringer, 1972; Ogata, 1992; Takano et al., 1993). Destruction or malformation of the ependyma lining the aqueduct normally leads to aqueduct closure resulting in non-communicating hydrocephalus (Perez-Figares et al., 2001). Experimentally, administration of neuraminidase into the ventricles of adult rats results in the immediate loss of the ependymal layer and the generation of hydrocephalus (Grondona et al., 1996). Hydrocephalus can also be caused by the mutation of genes (Perez-Figares et al., 2001), and experiments *in vitro* and *in vivo* are in progress to identify them and to discover the molecular mechanisms of their actions. The products of hydrocephalus-associated genes often are direct constituents of the axoneme, e.g. sperm-associated antigen 6 (Sapiro et al., 2002), polaris (Banizs et al., 2005) and Mdnah5 (Ibanez-Tallon et al., 2004). Furthermore, knockdown of the *wdr16* gene, the product of which has not been shown to be present in the axoneme but nevertheless is tightly correlated with the presence of kinocilia and which is highly expressed in rat EPC, also causes hydrocephalus in

zebrafish (Hirschner et al., 2007). This demonstrates the involvement of ependyma-specific genes in the pathogenesis of this disease.

## **1.6. Cilia**

Cilia are membrane protruberances of polarized cells supported by a microtubular cytoskeleton called the axoneme, which originates from a centriole-derived basal body (Satir and Christensen, 2007). Generally, there are different types of cilia and mammalian ciliary axonemes are formed with two major patterns. In the 9+2 pattern, nine outer microtubule doublets surround a central pair of singlet microtubules, as seen in the kinocilia of ependymal cells and respiratory epithelium. In the 9+0 pattern, the central pair is absent. The corresponding cilia are called primary cilia (Fliegauf and Omran, 2006) if they also lack the molecular motors (dynein arms) and are therefore immotile. Alternatively, if the molecular motors are present they are called 9+0 kinocilia. The immotile primary cilia are solitary and participate in various sensory functions (Ibanez-Tallon et al., 2003; Afzelius, 2004). Motile 9+0 kinocilia are found on one subpopulation of the cells at the embryonic node (McGrath et al., 2003). While immotile 9+0 monocilia are present on renal and photoreceptor cells (Fliegauf and Omran, 2006), vestibular cells possess cilia with a 9+2 axoneme of uncertain mobility status. A recently found novel type of axoneme composed of 9 outer microtubule doublets and 4 inner singlets (9+4 axonemal structure) from the notochordal plate of the rabbit embryo further illustrates the widely varied architecture of axoneme structures in vertebrates (Feistel and Blum, 2006).

In cross section, the structure of 9+2 kinocilia is characterised by 9 outer microtubule doublets that surround a central apparatus. The central apparatus is composed of two bridged, single microtubules encircled by the central sheath. The outer microtubule doublets are connected to each other by nexin links. Dynein arms attached to the microtubules generate the driving force for ciliary movement by cleavage of ATP. Radial spokes project from the outer microtubule doublets towards the centre of the axoneme and are equipped with several kinases (Lindemann and Kanous, 1997). Regulation of ciliary motility is accomplished by the interplay of the radial spokes and the central apparatus

(Smith and Lefebvre, 1997). The ciliary axoneme, the microtubule-based cytoskeleton of the cilium, grows from and continues the ninefold symmetry of a centriole at the centre of the ciliary basal body. The ciliary membrane surrounding the axoneme contains specific receptors and ion channels that initiate signaling pathways controlling cell motility, differentiation, migration and growth. At the base of the cilium, the “ciliary necklace” forms the assembly region for transport of cargos into the cilium (Satir and Christensen, 2007). The basal body lies closely attached under the cell surface, separating the transition between the cytoplasm and the ciliary compartment (Dutcher, 2003). The cilium is built and maintained by an evolutionarily conserved process called intraflagellar transport (IFT). During ciliogenesis, preassembled protein complexes dock to an IFT raft, a multiprotein platform, and are transported into the cilium from the proximal end to the distal tip by heterotrimeric kinesin II motor proteins, whereas the retrograde transport is facilitated by cytoplasmic dynein (Rosenbaum and Witman, 2002; Snell et al., 2004). Recent findings present strong evidence supporting the role of IFT not only in ciliogenesis and maintenance but also in ciliary signal transduction (Marshall and Nonaka, 2006; Scholey and Anderson, 2006; Wang et al., 2006).

### **1.6.1. Functions of cilia**

Motile kinocilia beat rapidly in a coordinated fashion to generate a directed fluid flow and participate in different functions like mucociliary clearance of the respiratory tract and movement of CSF in the ventricles of the brain. Primary cilia are capable of detecting a variety of stimuli and transmitting the signal into the intracellular compartment, thus acting as sensory antennae (Poole et al., 1985). Mutations in ciliary proteins lead to ciliopathies such as primary ciliary dyskinesia, polycystic kidney disease, retinitis pigmentosa, and hydrocephalus (Banizs et al., 2005; Fliegauf and Omran, 2006). Motile 9+0 nodal cilia create a leftward flow of morphogens which is critical for left-right asymmetry development in the body (McGrath et al., 2003).

## 1.7. Ependymal cells in primary culture

In EPC, polyciliated, monociliated and non-ciliated epithelial cells are found. Some non-epithelial cells are also present, including undefined precursor cells with long processes occasionally seen on top of the epithelial cell layer (Fig. 1).

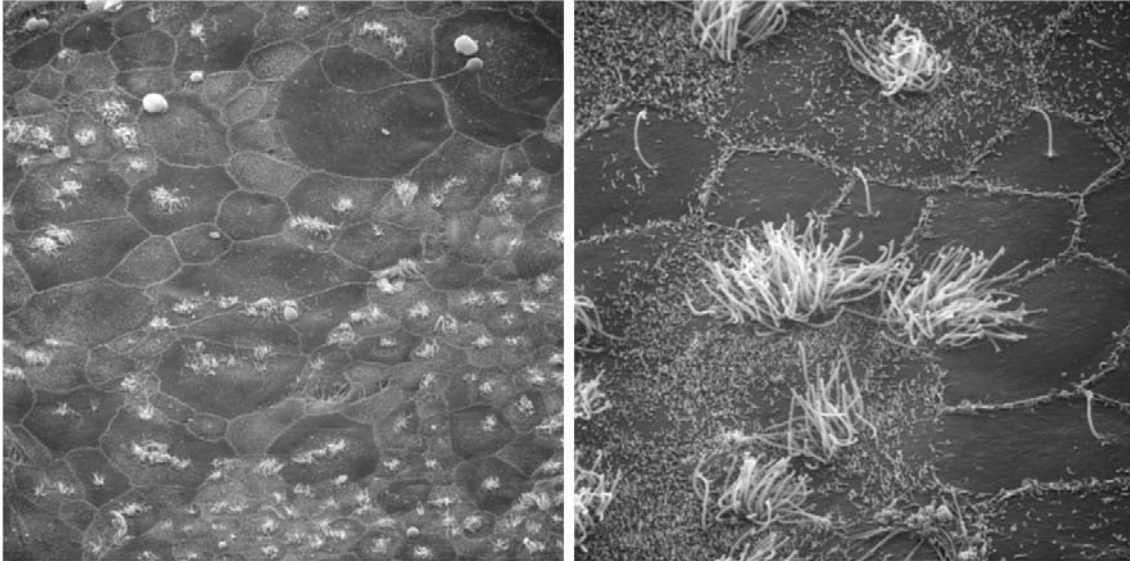


**Fig. 1.** S.E.M. micrographs of a 15-day-old EPC showing a lawn of epithelial cells with variation in cell size and and number of cilia. Only a few non-epithelial cells are also visible [taken with permission from Prothman et al., 2001].

## 1.8. Methods of gene transfer to cells of the nervous system

Gene delivery to mammalian cells is generally achieved by using vectors derived from either viruses (viral vectors) or nonviral elements (nonviral vectors). The most frequently used nonviral gene transfer vectors are plasmids containing the gene of interest behind a suitable promoter sequence. In general, the plasmid DNA is complexed with different formulations that may assist to transfer them into the nuclei of mammalian cells. Unfortunately, gene transfer with naked plasmids has not been very successful in neural cells, necessitating more efficient ways of delivery (Mata et al., 2003).

### **1.8.1. Viral vectors**

Development of viral vectors as gene transfer agents, by exploitation of the nature of some viruses to deliver DNA to the target cell nucleus, made possible gene transfer to almost all types of cells (Mata et al., 2003). Design of the viral vectors by manipulation of their core nucleic acids may reduce pathogenicity while leaving the basic characteristics of the virus intact. Different viruses have been tailored to create the vectors that are used in most of the gene transfer studies reported to date.

#### **1.8.1.1. Adenoviral vectors**

Adenoviral (Ad) vectors are derived from a relatively nonpathogenic virus that causes infections of the respiratory tract. The first-generation recombinant Ad vectors, rendered replication-defective by removal of the early region 1 (E1) gene (Berkner, 1988), accommodate an insert of up to approximately 8 kb. Adenoviruses have been shown to infect neurons, astrocytes, oligodendroglia, ependymal cells, microglia and the choroidal epithelium (Akli et al., 1993; Davidson et al., 1993). The extreme adjuvant properties of the adenovirus capsid protein (Dubensky, 2002) makes Ad vectors ineffective for long-term gene expression in living animals. In contrast, so-called 'gutless' Ad viral vectors, containing only the packaging signal with non-coding inverted terminal repeats, have an increased transgene capacity of up to 36 kb with diminished immune activation. Therefore they are able to confer long-term gene expression (Morrall et al., 1998; Thomas et al., 2000; Hartigan-O'Connor et al., 2002).

#### **1.8.1.2. Adeno-associated viral vectors**

Adeno-associated viral (AAV) vectors, derived from a nonpathogenic parvovirus, are naturally replication-defective and need a helper virus such as Ad virus or herpes simplex virus (HSV) for a productive infection (Grimm and Kleinschmidt, 1999). In brain-directed gene transfer, different serotypes of AAV vectors show distinct cell tropism. AAV serotype 2 (AAV2) preferentially infects neurons (Bartlett et al., 1998), AAV4 transduces into



ependymal cells (Davidson et al., 2000) and AAV5 transduces into Purkinje cells in the cerebellum (Alisky et al., 2000) with high efficiency. Even though AAV vectors are highly effective for gene delivery and are non-toxic, their low insert capacity (4–5 kb) often limits their applicability (Davidson and Breakefield, 2003).

### **1.8.1.3. Lentiviral vectors**

Lentiviruses are enveloped RNA viruses, the genomes of which are reverse-transcribed into double-stranded DNA by viral reverse transcriptases after entering the target cell. The reverse transcripts are then integrated into the host genome by the viral integrase. Lentiviral vectors (LV) are replication-defective hybrid viral particles containing the core proteins and enzymes of HIV-1 (human immunodeficiency virus type 1) pseudotyped with the envelope of a different virus (Dull et al., 1998). Vectors derived from some retroviruses, such as Moloney murine leukaemia virus (MoMLV), are unable to deliver genes to non-dividing cells. In contrast, vectors derived from HIV, with a modest packaging capacity of approximately 8 kb, are highly efficient in transducing into cells of the brain, nervous system and infect dividing as well as non-dividing cells, including neurons (Naldini et al., 1996; Blomer et al., 1997; Brooks et al., 2002; Vogel et al., 2004). Transgene expression begins within 24-48 h after infection. With the many modifications possible by changing the envelope glycoproteins, LVs permit the manipulation of viral tropism (Cronin et al., 2005), which is especially broad in case of the G-glycoprotein from vesicular stomatitis virus (Alisky et al., 2000; Brooks et al., 2002). In vivo, when introduced into brain parenchyma or ventricles, LV provide long-term gene expression at high levels (Blomer et al., 1997; Vigna and Naldini, 2000; Brooks et al., 2002).

### **1.8.1.4. Other viral vectors**

Several other vectors have also been developed and their potential for delivering genes to the nervous system has been verified by several investigators. The DNA virus vectors that have been tested include simian virus 40 (SV40) and Herpes simplex virus (HSV). SV40 shows high potency to infect neurons and microglia (Kimchi-Sarfaty et al., 2002), and the HSV

vector applications have been directed toward neurons because of their neurotropic nature (Fink et al., 1996; Burton et al., 2001). Other RNA virus vectors successfully tested for gene transfer to neurons include the alphaviruses (Ehrensgruber, 2002) and poliovirus (Bledsoe et al., 2000). The main factor limiting the usability of these vectors in gene transfer is their toxicity, which can already manifest itself within 8 h after infection (Davidson and Breakefield, 2003).

#### **1.8.1.5. Vector choice**

Kinociliated cells are considered to be terminally differentiated (Randell, 1992), and the ependymal cells lining the ventricles of the brain are post-mitotic (Spassky et al., 2005). The main aim of the present study was to transfect ependymal cells in primary culture for studying the location and function of ependyma-specific transcripts with different methods including RNA interference. It is well known that lentiviral vectors are able to transfect post-mitotic as well as non-dividing cells (Naldini, 1998). As it was also shown that vesicular stomatitis virus glycoprotein (VSV-G)-pseudotyped lentiviral vectors are capable of transducing into ependymal cells *in vivo* (Watson et al., 2005), a lentivirus was chosen as gene transfer vector for ependymal cells in primary culture.

### **1.9. Cell-specific promoters and their importance in gene transfer vectors**

The objective of gene transfer vectors is the introduction of genes of interest into cells of interest. One of the potential limitations of such vectors is lack of specificity. The use of highly active viral or cellular promoters which are recognised by many cell types, like the CMV (cytomegalovirus) or the  $\beta$ -actin promoters, for driving transgene expression may have deleterious effects in target cells that do not normally express the transgene of choice (Nicklin et al., 2001). On the other hand, attenuation of promoter function in the target cell may cause silencing of the transgene, as observed in lung (Baskar et al., 1996). The pertinent mechanism may be transcriptional silencing. The CMV enhancer/promoter, which is one of the strongest and most widely used, is known to undergo transcriptional inactivation in

several tissues (Baskar et al., 1996; Loser et al., 1998) and appears to be unable to direct persistent transgene expression in airway epithelial cells (Lee et al., 1996).

Transcriptional targeting allows the restriction of mRNA and protein synthesis to a specific cell type (Lotti et al., 2002), even if the gene transfer vector was introduced into multiple cell types. It can be accomplished by using promoters that are specific to particular tissues or cells (Dai et al., 2004). Utilization of cell type-specific promoter sequences for expressing transgenes in the appropriate cell type enhances efficiency and stability of gene expression. Cell-type-specific expression in leukocytes has been achieved by using the CD11a promoter (Cornwell et al., 1993). By using the promoter for phosphoenolpyruvate carboxykinase, the transgene expression was directed exclusively to liver and kidney (McGrane et al., 1988). Further examples involving cell-type-specific promoters are available for almost all tissues. Such promoters can be used in viral as well as nonviral vectors for directed transgene expression in the appropriate target tissues (Walther and Stein, 1996). By using the ciliated cell-specific promoter, FOXJ1, transgene expression may be directed exclusively to cells with kinocilia (Ostrowski et al., 2003). FOXJ1 is a member of the forkhead/winged helix family of transcription factors and only active in cells possessing motile cilia (Hackett et al., 1995; Lim et al., 1997; Blatt et al., 1999). This vector encoding GFP under the control of FOXJ1 promoter leads to transgene expression only in ciliated ependymal cells, ciliated epithelial cells of the oviduct, developing sperm, and in the ciliated cells of the respiratory tract (Ostrowski et al., 2003).

## **1.10. Scope of the thesis**

Even though the existence of the ependymal cells has been well known for more than a century, their exact roles in health and disease remain speculative. Identification of transcripts expressed exclusively in the ependyma by generation and screening of subtractive ependymal cDNA libraries was chosen as one way towards elucidating their function. For functional studies of the identified ependyma-specific transcripts, it is highly desirable to find a means of gene transfer into ependymal cells which would facilitate, among other things, localisation studies with GFP-tagged fusion proteins and RNA

interference (RNAi) gene knockdown experiments. Various nonviral- as well as viral vector-mediated gene transfer methods were therefore to be tested in order to identify a way of transferring genes into kinociliated ependymal cells.

## 2. Results

### 2.1. Identification of ependyma-specific cDNA fragments

As a first step in understanding the differential gene expression pattern of the ependyma, it is necessary to identify those genes the transcripts of which are temporally or spatially restricted to it. To identify genes specifically transcribed by the ependyma, two subtractive bovine ependymal cDNA libraries, ependyma minus brain and SCO minus brain, were generated and screened. The obtained sequences of putatively ependyma-specific targets were subjected to bioinformatic analyses using the BLAST (**B**asic **L**ocal **A**lignment **S**earch **T**ool) computer program from the NCBI (**N**ational **C**enter for **B**iotechnology **I**nformation), Bethesda, USA. The initially promising candidates are listed in Table 1. Unambiguously false-positives, namely genomic DNA and clones without an open reading frame, are omitted.

The aim of the subtractive library screening was to identify cDNA sequences that are specific for the ependyma. The candidate clones identified in the present screening were designated as E2, E8, E27, E29, E71, E72, E88, S22 and S57 (Table 1). Clone E8 corresponds to dynein intermediate chain 1, one of the main components of the axonemal dynein arms, which are essential for ciliary and flagellar beating. They consist of several heavy, intermediate and light chains. Mutations in the gene for axonemal dynein intermediate-chain 1 result in primary ciliary dyskinesia (Guichard et al., 2001).

Clones E27 and S57 correspond to WD-repeat domain-containing proteins. Clone E27, already identified in a previous screening of the subtractive ependymal cDNA library (Hirschner et al., 2007), encodes the WD40-repeat protein, Wdr16. This protein is abundantly expressed in testis and cultured ependymal cells and is a marker protein for kinocilia-bearing cells (Hirschner et al., 2007). Clone S57 encodes a protein similar to WD-repeat domain protein 52. The WD-repeat protein family is characterised by the presence of conserved, approximately 40 amino acids long repetitive sequences which normally end

with the amino acids tryptophan (W) and aspartate (D). The list of WD40 protein functions includes, but is not limited to signal transduction, cytoskeleton assembly and the processing of pre-mRNA (Li and Roberts, 2001). WD40 proteins are well known to fulfill their diverse range of functions by engaging in protein-protein interactions (Smith et al., 1999).

**Table 1.** Preliminary analysis of clones identified by screening of the subtractive ependymal cDNA libraries according to the results of their sequencing. False-positive sequences corresponding to fragments of genomic DNA are not listed. E, S in the designation of clones corresponds to the ependyma and SCO, respectively. The numbers in the designation results from the consecutive numbering of all clones that have been analysed.

Clone No	Designation	Accession number	Species	Comment
1	E2	NM_001076315	Bos taurus	hypothetical protein LOC614187
2	E8	XM_001097717	Macaca mulatta	dynein, axonemal, intermediate polypeptide 1
3	E27	XM_582249	Bos taurus	similar to WDR16 (LOC505885)
		NM_145054	Homo sapiens	WD repeat domain 16 (WDR16)
4	E29	XM_614198	Bos taurus	hypothetical protein LOC534432
		XM_001099378	Macaca mulatta	similar to coiled-coil domain containing protein 39
5	E71	XM_001099378	Macaca mulatta	similar to coiled-coil domain containing protein 39
		AL122120	Homo sapiens	hypothetical protein from testis; DKFZp434A128
6	E72	NM_001038185	Bos taurus	sperm-associated antigen 6 (Spag6)
		XM_001097245	Macaca mulatta	sperm-associated antigen 6
7	E88	NM_174301	Bos taurus	chemokine (C-X-C motif) receptor 4
		M86739	Bos taurus	cow neuropeptide Y receptor from brain
8	S22	XM_606535	Bos taurus	hypothetical protein LOC528123
		DQ323735	Homo sapiens	wntless protein
9	S57	XM_001099684	Macaca mulatta	similar to WD repeat domain 52 (LOC710973)
		BC113553	Homo sapiens	WD repeat domain 52

Clone E72 corresponds to sperm-associated antigen 6, a kinocilia marker protein like Wdr16 and a constituent of the axonemal central apparatus (Sapiro et al., 2000).

Clone E88 corresponds to chemokine receptor 4 (CXCR4; also known as "fusin") the ligand of which is a chemokine known as CXCL12 (stromal cell-derived factor 1). CXCR4 is abused by HIV-1 to gain entry into target cells (Yi et al., 2004). This receptor has a wide cellular distribution, with expression on most immature and mature hematopoietic cell types including vascular endothelial cells and neuronal or nerve cells. It has a pivotal role in the directional migration of cancer cells during the metastatic process (Arya et al., 2007).

Clone S22 corresponds to wntless (WLS) protein, a conserved membrane protein of the Wnt signalling pathway (Banziger et al., 2006).

Clones E29 and E71 correspond to the same mRNA encoding a hypothetical protein similar to coiled-coil domain containing protein 39. A coiled coil is a structural motif in proteins, in which 2 to 7 alpha helices are coiled together like the strands of a rope. Many coiled coil proteins are involved in protein-protein interactions regulating important biological functions such as gene expression or membrane trafficking (Lupas, 1996; Lupas and Gruber, 2005).

The genes corresponding to clones E8, E27 and E72 are typically expressed in ciliated cells and might therefore be regarded as ependyma-specific with respect to neural cells. Because all these genes have already been characterised earlier and their putative functions are well known, their further investigation has not been considered within the scope of this thesis. Clones E88 and S22 were ignored in the context of the present study, since these genes are not specific for the ependyma. Among the remaining clones, E29 and E71 were chosen for further study due to their duplicate appearance in the present screening. They represent one and the same gene encoding a protein with coiled-coil domains.

## **2.2. Bioinformatic characterisation of the potentially ependyma-specific E71 protein**

The full length sequence of rat E71 cDNA was amplified by RT-PCR using RNA from testis, an organ in which the gene is expressed at high level. The E71 open reading frame encodes a

protein of 935 amino acids with a molecular mass of 110 kDa. A protein motif scan reveals the E71 protein to bear coiled-coil repeats, features for which it was already previously made entry 39 in the list of proteins from the coiled-coil domain-containing family (Fig. 2) at the NCBI conserved domain database (Marchler-Bauer et al., 2007).

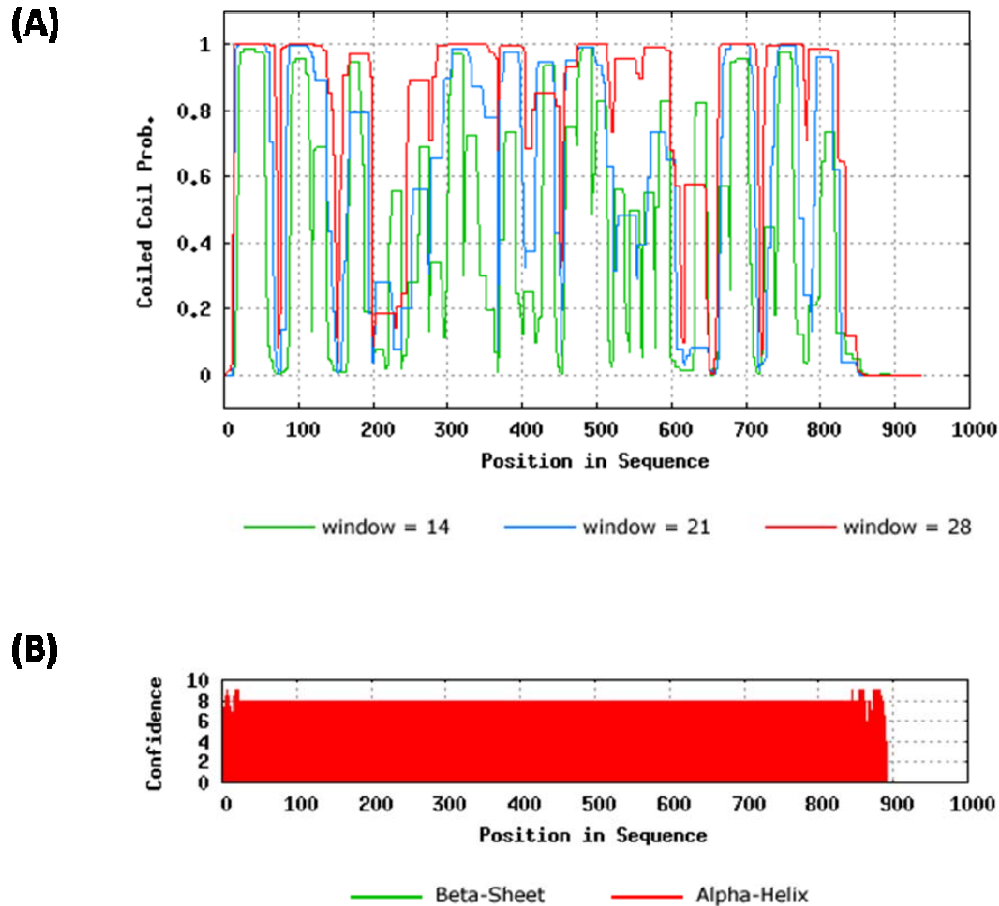


**Fig. 2.** Results of analysis of E71 with the computer program PCOILS available at <http://toolkit.tuebingen.mpg.de/pcoils>. PCOILS compares a single sequence or a sequence alignment to a database of known coiled-coil proteins, derives a similarity score and calculates the probability of the submitted sequence to adopt a coiled-coil conformation (Lupas, 1996; Lupas et al., 1991). The ordinate in A indicates the probability of forming alpha-helical coiled-coils in the predicted protein sequences (window size = 28). A: The coiled-coil prediction shows the coiled-coil probability over the sequence. Calculations for window size 28 are depicted in red, for 21 in blue and for 14 in green. B: The secondary structure prediction shows the probability of forming alpha-helices (red) or beta sheets (green). No beta sheet content is indicated for E71.



## 2.3. Analysis of the E71 transcription profile by real-time RT-PCR

### 2.3.1. E71 tissue-specific transcription profile

The tissue-specific transcription profile of the E71 gene was analysed by real-time RT-PCR using RNA from several rat organs and cell culture systems. The specificity of the individual reactions was verified by agarose gel electrophoresis and melting point analysis (not shown). High levels of the E71 transcript in comparison to those of cyclophilin were detected in testis and in 13-day old rat EPC. Weak signals for E71 mRNA were also found in lung and brain. The E71 transcript was not observed in liver, kidney, small intestine (“gut”) and spleen (Fig. 3).

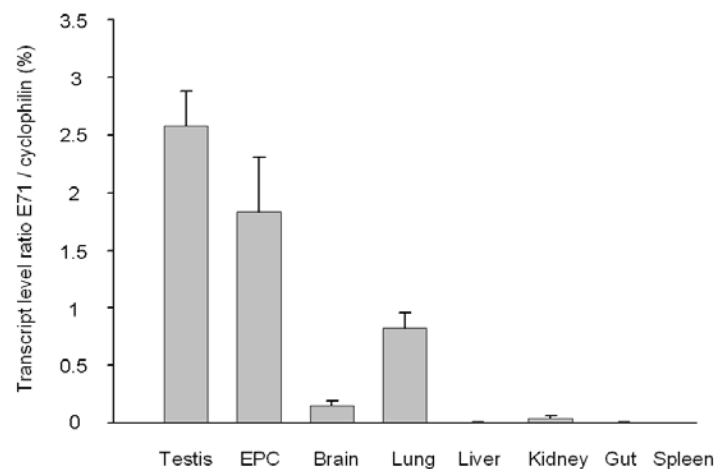


**Fig. 3.** Real-time RT-PCR quantification of E71 mRNA in different rat organs relative to cyclophilin mRNA. The housekeeping gene cyclophilin encodes a peptidyl-prolyl cis-trans isomerase that is transcribed constitutively and independently from developmental stage and can therefore be used as a standard for comparison with the E71 mRNA levels. One microgram of total RNA was reverse-transcribed and subjected to the PCR in a LightCycler® instrument over 45 cycles using the FastStart DNA Master SYBR Green I system. Each bar indicates the mean  $\pm$  standard error of the mean of the relative amount of target mRNA measured in three independent rat organs, respectively (EPC, ependymal primary culture).

### 2.3.2. E71 transcription kinetics in ependymal primary cultures

In developing EPC, E71 transcript levels increase gradually with time. The level of E71 mRNA starts to increase after day in vitro (DIV) 6 and reaches its maximum in the matured EPC at

DIV 13 (Fig. 4), similar to the mRNA levels for the cilia-specific proteins, Spag6 and Wdr16, as shown by Hirschner et al. (2007).

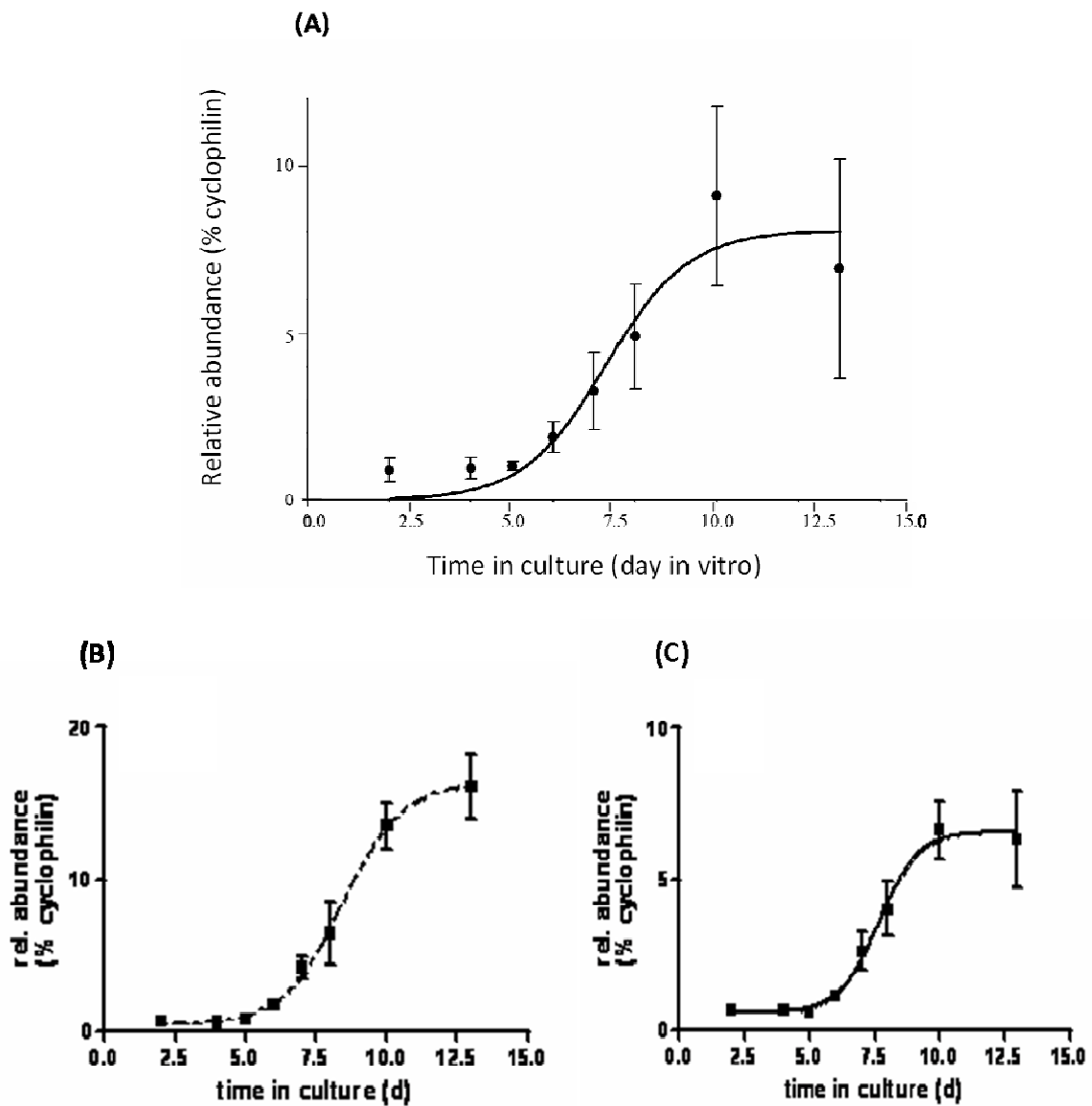


**Fig. 4.** A: Real-time RT-PCR analysis of the time-dependent change in E71 mRNA levels as compared to that of cyclophilin mRNA in EPC. Graphs B and C show the time-dependent changes in mRNA levels for Spag6 and Wdr16 in EPCs, respectively. One microgram of total RNA was reverse-transcribed and subjected to the PCR in a LightCycler® instrument over 45 cycles using the FastStart DNA Master SYBR Green I system. Each data point indicates the mean  $\pm$  standard error of the mean of the relative amount of target mRNA measured in three independent EPC, respectively, at the indicated age. (Diagram B and C taken with permission from Hirschner et al., 2007).

## **2.4. Determination of immunoreactivity and specificity of the E71 antiserum**

Since it was desirable to analyse the expression of E71 at the protein level, antibodies were raised against specific peptides, the sequences of which were derived from the primary structure of the putative rat E71 ortholog. Four antigenic peptides (SSEFLSELHWEDGFAIC, QKLKHHNEIVKHKLKC, CEDSIPISPPTAKVIELR, and CSSGSNSNIPKGKKLNK) corresponding to the positions 2-17, 347-366, 891-907, and 921-936 respectively, were coupled each to the hapten carrier keyhole limpet hemocyanin (KLH) and sent to a commercial company for immunisation of rabbits. For each peptide, two rabbits were immunised and the antisera were analysed for their antibody titers by an Enzyme-Linked ImmunoSorbent Assay (ELISA).

### **2.4.1. ELISAs for E71 antisera**

ELISA analysis of E71 antisera revealed high titers in all four cases. The preimmune sera exhibited no affinity for E71 (Fig. 5).

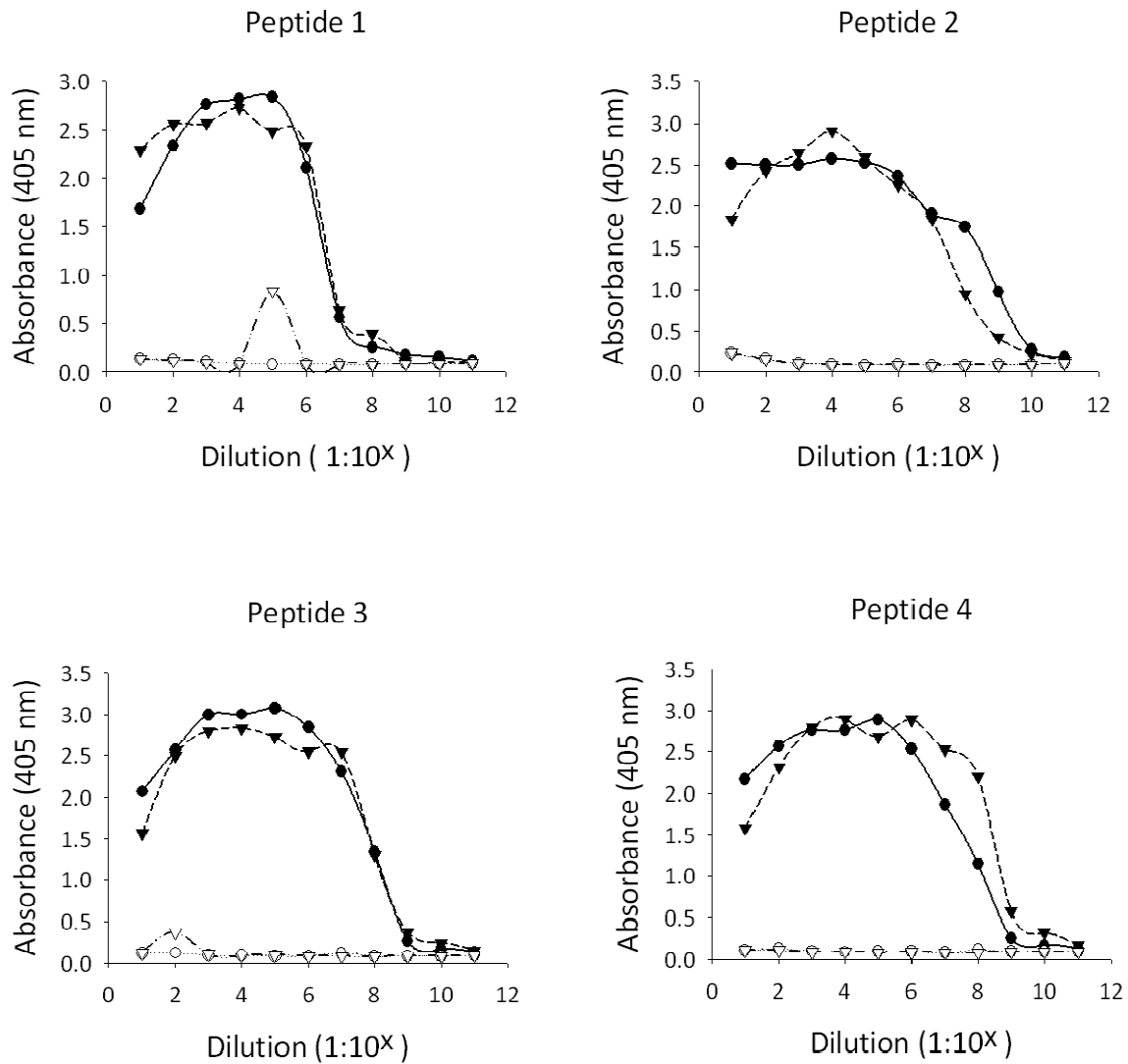


**Fig. 5.** ELISAs demonstrating the immunoreactivity of the rabbit E71 antisera towards the respective antigenic peptide. A 96 well plate was coated with 250 ng of BSA-conjugated peptide against which the antiserum was raised. Serum samples resulting from immunisation of a rabbit with keyhole limpet hemocyanin-conjugated antigenic peptide were applied to the BSA-conjugated peptide in a dilution series ranging from 1:10 up to 1:10<sup>6</sup>. Incubation time was 2 h. Goat anti-rabbit IgG-alkaline phosphatase conjugate (1:1,000) was applied as secondary antibody for 1 h. The conjugated phosphatase converted p-nitrophenylphosphate into the p-nitrophenolate ion, the absorbance of which was measured at a wavelength of 405 nm in an ELISA reader. The inflection point of the curve connecting the individual data points represents the titer of the respective antiserum. ●, rabbit 1 antiserum; ○, rabbit 1 preimmune serum; ▼, rabbit 2 antiserum; ▽, rabbit 2 preimmune serum.

#### 2.4.2. Detection of E71 by Western blotting

After determination of antibody titers by ELISA, reactivity and specificity of the different E71 antisera were checked by immunoblotting experiments. Since it had been learned from RT-

PCR analysis that E71 mRNA is abundant in EPC and testis, homogenates from these two protein sources were probed with the E71 antiserum from different animals together with homogenate from liver as a control. None of the antisera raised against the four different antigenic peptides was specific for E71 according to the immunoblotting results. No specific band corresponding to the molecular mass of E71 (110 kDa) was observed in the homogenates from the EPC. The antisera raised against peptides 1, 2 and 3 produced several non-specific bands in the range between 100-130 kDa when used against homogenates from testis, but not with homogenates from EPC (Fig. 6).

A specific antibody against E71 was not obtained, but remains highly desirable to further analyse the tissue- and time-specific expression pattern of E71. For want of the antibody, it became the main focus of this work to develop an alternative tool with which at least part of the information obtainable through antibody-based methods would become accessible. The ability to express transgenes in the ependymal cells, e.g. wdr16 fused to the open reading frame (ORF) of GFP was considered most crucial in this respect and therefore a method for efficient transfection of EPC was searched.

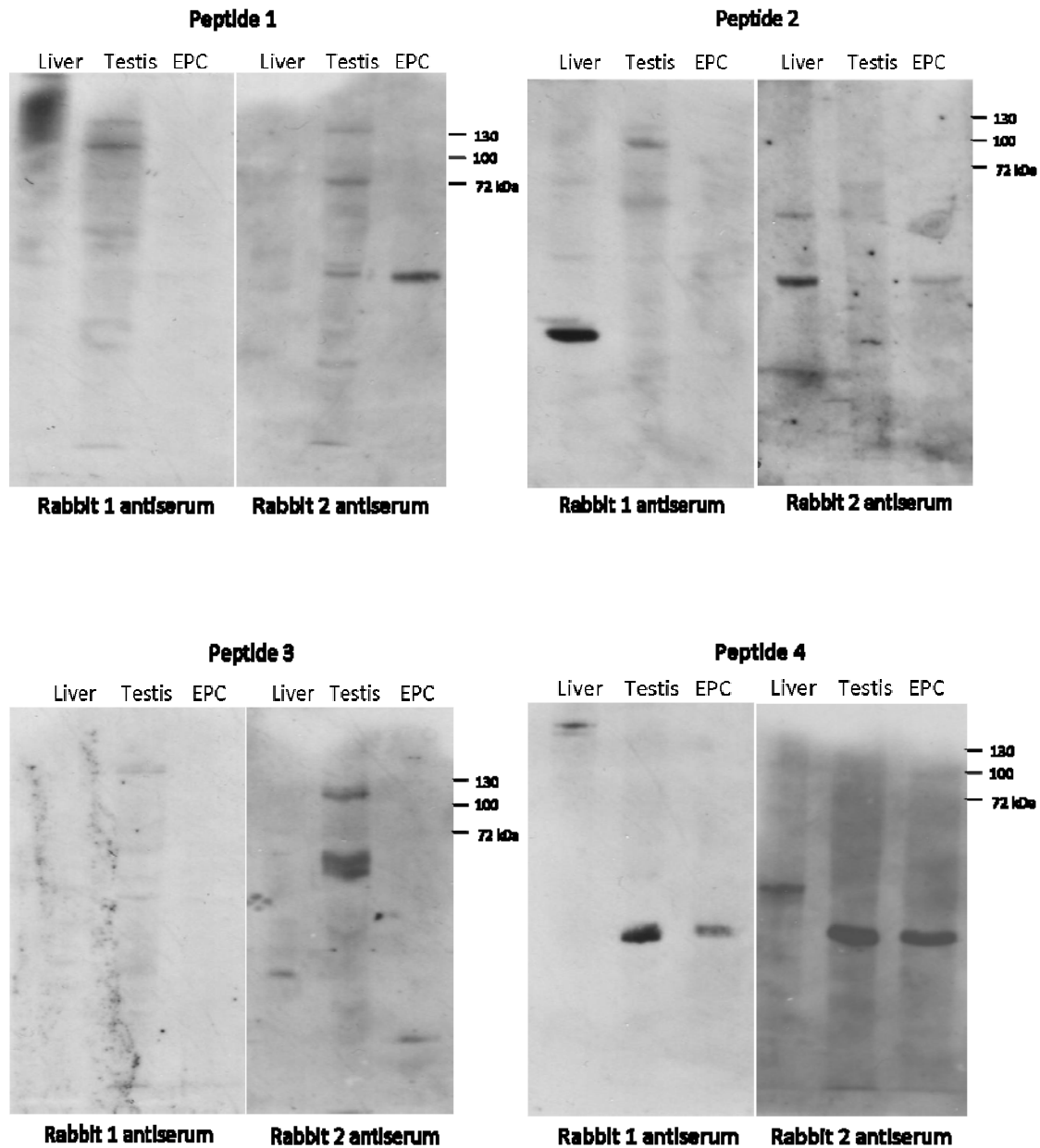


**Fig. 6.** Western blots with E71 antisera raised against different peptides of the rat E71 ortholog. The expected molecular mass of the E71 protein is 110 kDa. Two rabbits were immunised for each peptide. Each lane of the gel was loaded with 20  $\mu$ g protein from the homogenates of either EPC, testis or liver. Proteins were separated by SDS-PAGE and transferred to nitrocellulose membranes by electroblotting. Each membrane was probed for 2 h with the indicated antiserum diluted 1:3,000. The secondary antibody, donkey anti-rabbit IgG-peroxidase conjugate diluted 1:10,000, was applied for 1 h. Detection was performed with the ECL ("Enhanced Chemiluminescence System") from Amersham Biosciences.

## 2.5. Transfection of ependymal primary cultures

### 2.5.1. Calcium phosphate precipitation method

Attempts to transfect EPC with a plasmid vector encoding enhanced green fluorescent protein (EGFP) as a marker by the traditional calcium phosphate precipitation method (Jordan et al., 1996) on either DIV 6, 8 or 10 resulted in the transfection of only a few non-epithelial cells along with major alterations of general culture morphology. The cultures did not grow properly after the transfection attempt even when it was performed on DIV 2 or DIV 4, and the transfection efficiency was almost negligible (below 1%). Ciliated cells were never observed to be transfected by this method (Fig. 7).

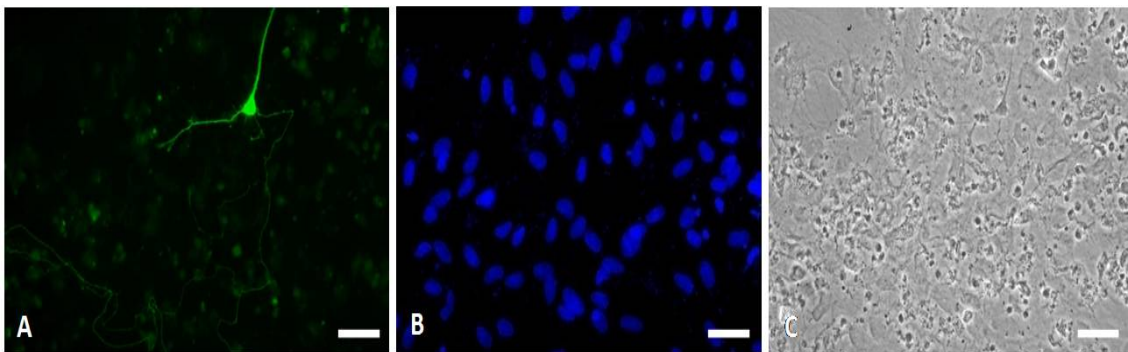


**Fig. 7.** EPC transfected by the calcium phosphate precipitation method on DIV 6. The amount of EGFP vector encoding green fluorescent protein as a marker was 2  $\mu\text{g}/\text{well}$ . A: Transfected cell showing EGFP fluorescence. B: Nuclei are counterstained with 4',6-diamidino-2-phenylindole. C: A phase contrast micrograph of an EPC transfected by the calcium phosphate precipitation method shows altered culture morphology. For comparison, an intact, unaltered EPC can be seen in Fig. 13 A. Scale bars: 20  $\mu\text{m}$ .

### 2.5.2. Polyethylenimine-mediated gene transfer

Transfection of EPC with the commercially available jetPEI™ transfection reagent using an EGFP vector encoding GFP as a marker did not increase the total number of transfected cells above the one seen with the calcium phosphate method, even though combinations of different jetPEI™ and vector concentrations were tested at different time points starting from DIV 2 to DIV 10 (data not shown except for DIV 6 in Fig. 8). Even though the culture morphology was generally not altered by the transfection, the efficiency was below 1% and

no transfected ciliated cells were observed. Only a few of the long, process-bearing, non-epithelial precursor cells were transfected (Fig. 8), as was the case with the calcium phosphate precipitation method.

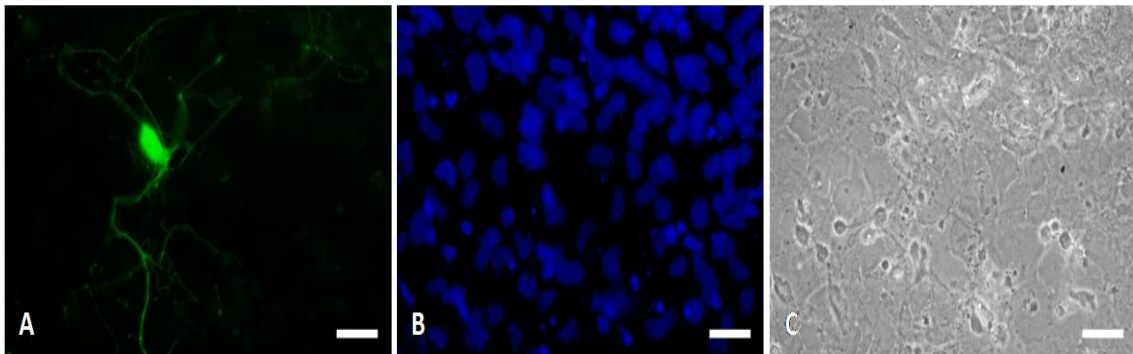


**Fig. 8.** EPC transfected using jetPEI™ transfection reagent on DIV 6. The amount of EGFP vector encoding green fluorescent protein as a marker was 2 µg/well. A: Transfected cell showing EGFP fluorescence. B: Nuclei are counterstained with 4',6-diamidino-2-phenylindole. C: A phase contrast micrograph of an EPC transfected by jetPEI™ transfection reagent is shown in. Scale bars: 20 µm.

## 2.6. Lentiviral vector-mediated gene transfer

The transfection of ependymal cells in primary culture proved difficult with plasmid-based transfection methods. Therefore, it was necessary to find a more efficient alternative for gene transfer to these cells. Since lentiviruses integrate into the genome of their host cells and are capable of infecting a wide variety of dividing and non-dividing cells (Blomer et al., 1997), they were tested for their ability to transfect ependymal cells in primary culture.

### 2.6.1. Production of lentiviral vectors

Lentiviral vectors pseudotyped with vesicular stomatitis virus G-protein (VSV-G) were successfully produced according to the procedure explained in 4.2.2. After virus production, the virus preparation was characterised by titrating it and assaying its p24 concentration (Gelderblom et al., 1987a). This lentivirus (HIV/VSV-G/GFP), in general, encodes GFP under the control of the constitutive promoter of elongation factor 1 alpha (EF1 $\alpha$ ). EF1 $\alpha$  is an essential component of the protein synthetic machinery and expressed abundantly in all kinds of cells (Murray et. al., 1996). Lentiviruses pseudotyped with the envelope



glycoproteins of Rababies, Mokola and Ebola viruses (Cronin et al., 2005), respectively, were also produced.

## 2.6.2. Titration of lentiviral vectors

Titration of lentiviral vector preparations was performed on HEK293T cells (Fig. 9). Transfected cells were identified by their green fluorescence after virally induced GFP expression. Their number increased with increasing number of virus particles applied to the cultured cells (Fig. 9A). Contrary to the expectation (see Methods 4.2.4, and Discussion 3.4) a plot of the volume of viral stock solution applied to the cells ( $V_v$ ) versus the negative natural logarithm of 1 minus the percentage of infected cells ( $-\ln(1-P)$ ) did not yield a straight line (Fig. 9B).

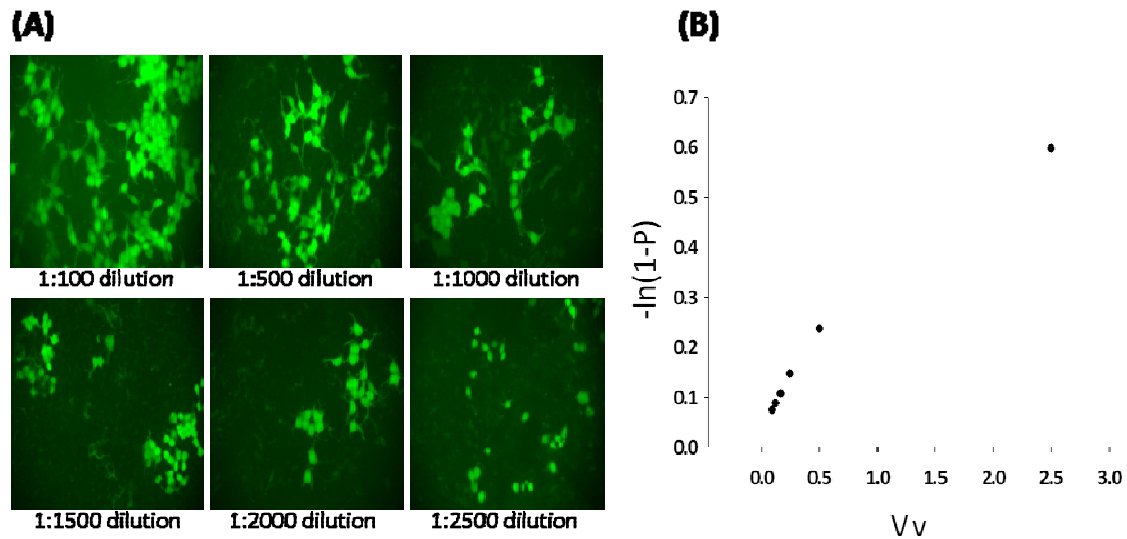


**Fig. 9.** A: Titration of HIV/VSV-G/EF1 $\alpha$ /GFP on HEK293T cells showing the transfected cells after titration with virus suspensions of different serial dilutions. Thirty thousand cells per well were seeded in 24-well plates the day before the titration experiment. Cells were counted on the day of the experiment. Serial dilutions of virus stock solution in media ranging from 1:100 to 1:2,500 were prepared, and the cells were infected with a total volume of 250  $\mu$ l of diluted virus suspension per well. Fresh medium was added the day after, and the cells were fixed 3 days after infection. Approximately 4,000 cells per each dilution were counted manually on photographs taken under the microscope. The titer was calculated from the number of cells expressing GFP after infection with the highest dilution of the series. B: A plot showing the relationship between the volume of the virus stock suspension required in the total medium volume of 250  $\mu$ l ( $V_v$ ) in order to arrive at dilutions varying from 1:100 to 1:2,500 and MOI ( $-\ln(1-P)$ ). P, percentage of infected cells divided by 100.

Nevertheless, the minimal number of infectious viral particles could be calculated from the highest dilution of viral stock solutions (see Methods 4.2.4). The resulting titer values for VSV-G (vesicular stomatitis virus G-protein)-pseudotyped HIV (human immunodeficiency virus) were always significantly higher than those of HIV preparations pseudotyped with Rabbits, Mokola or Ebola envelope glycoprotein. The titers of HIV/VSV-G/spag6-GFP (sperm-associated antigen 6 fused to GFP) were always significantly lower than those of HIV/VSV-G/GFP, HIV/VSV-G/Wdr16-GFP (WD repeat protein 16 fused to GFP) or HIV/VSV-G/pAK7-GFP (putative adenylate kinase 7 fused to GFP). According to the protocols established by Didier Trono at the Trono laboratory (<http://tronolab.epfl.ch/webdav/site/tronolab/shared/protocols/TUvsp24.html>), the relationship between transducing units (TU) and p24 concentration of a well packaged, VSV-G pseudotyped lentiviral vector will be in the range of 10-100 TU/pg of p24. The vectors produced during the project underlying this thesis (HIV/VSV-G/GFP) fell within this range with an infectivity of 61-74 TU/pg of p24. The other vectors had an infectivity rate below 10 TU/pg of p24, indicating possible packaging problems during virus production (Table 2). As the p24 content of the virus preparations stems from both the functional as well as from the non-functional viruses, it is difficult to derive a direct relationship between p24 and functional viral titer. After the concentration of virus by ultracentrifugation, only below 5% of functional virus was recovered. A possible reason for this could be the loss of infectivity of virus due to the applied centrifugal force during ultracentrifugation. Apart from this, infectious viral particles were also observed to be present in the supernatant after ultracentrifugation. This was determined by infecting the HEK293T cells with the viral supernatant and by measuring the p24 content. Obviously, the ultracentrifugation regimen used here was not completely efficient in pelleting all viral particles, even though the applied gXh value was chosen twice as high as stated in several published protocols (Blomer et al., 1997; Kahl et al., 2004; Zhang et al., 2004; Watson et al., 2005). In the case of lentivirus preparations encoding GFP under the control of the cilia-specific FOXJ1 or wdr16 promoters, only the p24 contents of the corresponding virus preparations are shown in Table 2, since the transgene is not expressed in HEK293T cells, and therefore the titer could not be determined independently from transfection experiments on the ependymal cultures.

### 2.6.3. p24 ELISA

After determination of the virus titer as described in 2.6.2, the p24 content of the virus preparation was estimated by a sandwich ELISA for HIV-I gp24 (glycoprotein 24). Briefly, this method involves the attachment of anti HIV-I p24 antibody to the solid phase. This antibody binds the antigen (HIV-I p24) which is then detected by the second, enzyme-labeled specific antibody after the addition of a chromogenic substrate. The p24 content of the individual virus preparations is shown in Table 2.

**Table 2.** Relationship between HIV-1 gp 24 and titers of various lentiviral vector preparations

Designation of virus preparation	p24 (ng/ml)	Titer (TU/ $\mu$ l)	TU/pg of p24	Date of virus harvest (d-m-y)
HIV/VSV-G/GFP-EF1 $\alpha$ concentrated	15,513	537	0.03	30-01-06
HIV/VSV-G/Spag6-GFP concentrated	20,702	174	0.008	16-01-06
HIV/Mokola/GFP concentrated	440	1,070	2.5	13-03-06
HIV/Ebola/GFP concentrated	1,000	1,126	1	20-03-06
HIV/Rabbies/GFP concentrated	520	2,960	5.6	20-03-06
HIV/VSV-G/GFP-EF1 $\alpha$ normal	47	2,907	61	01-08-06
HIV/VSV-G/GFP-EF1 $\alpha$ concentrated	432	32,000	74	01-08-06
HIV/VSV-G/GFP-Wdr16-N1 normal	323	1,800	5.5	01-08-06
HIV/VSV-G/pAK7-GFP normal	40	1,095	27	05-09-06
HIV/VSV-G/GFP-FOXJ1 promoter normal	122	-	-	09-01-07
HIV/VSV-G/GFP-FOXJ1 promoter concentrated	11,900	-	-	09-01-07
HIV/VSV-G/GFP-EF1 $\alpha$ concentrated	13,400	136,000	10	16-01-07
HIV/VSV-G/GFP-wdr16 promoter normal	126	-	-	30-01-07
HIV/VSV-G/GFP-wdr16 promoter concentrated	8,233	-	-	30-01-07

## **2.6.4. Production of pseudotyped lentiviral vectors**

Changing the tropism of lentiviral vectors by pseudotyping permits the transfection of different cell types. Therefore, attempts were made to generate differently pseudotyped lentiviruses. Lentiviral vectors have been generated carrying surface glycoproteins from a variety of different enveloped viruses, including Ebola virus, Mokola virus, Rabies virus and vesicular stomatitis virus. These pseudotyped vectors vary widely in their packaging efficiency and titer (Table 2).

## **2.6.5. Lentiviral vector-mediated transfection of ependymal cells in primary culture**

### **2.6.5.1. Transfection of differentiated ependymal cells in primary culture**

During initial experiments, conducted by Stephan Verleysdonk and Roland Vogel in the laboratory of Jacques Mallet at the Hôpital de la Pitié Salpêtrière, Paris, differentiated EPC were transfected with HIV/VSV-G/GFP and HIV/Mokola/GFP at a multiplicity of infection (MOI) of 100 on DIV 11. This resulted in the expression of transgene only in a few epithelial cells. Even though the number of transgene-expressing cells increased with a switch to HIV/Mokola/GFP virus, polyciliated cells were not observed to express the transgene, but impressed as black blocks in-between the transfected, green-fluorescing non-ciliated cells under the fluorescence microscope (Fig. 10).

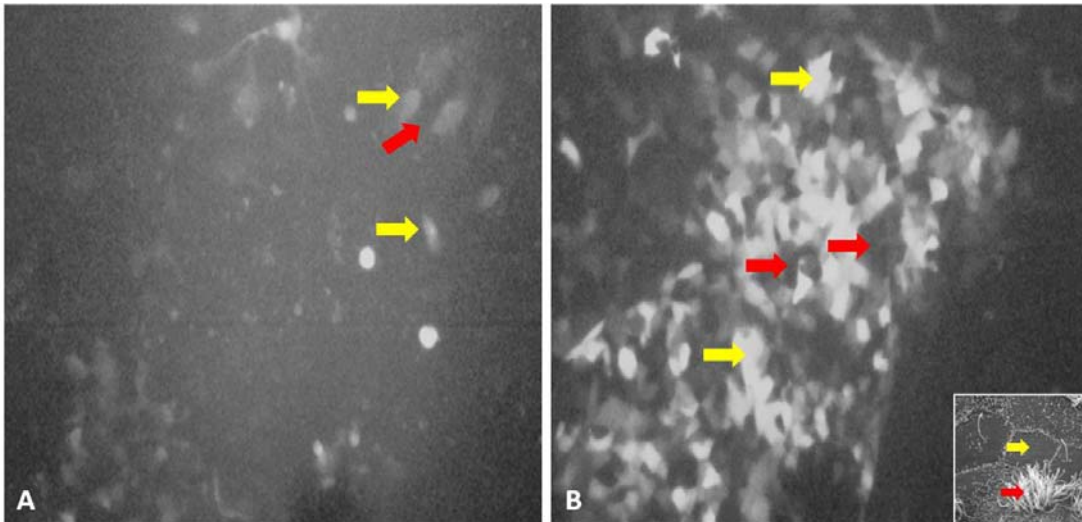


**Fig. 10.** Differentiated EPC transfected on DIV 11 with lentiviral vectors encoding the marker GFP. A: Transfection of EPC with HIV/VSV-G/GFP on DIV 11 (MOI 100) resulted in very few GFP-expressing cells. B: EPC transfected with HIV/Mokola/GFP on DIV 11 (MOI 100) showed transfected non-ciliated cells in between the ciliated epithelial cells. Red arrows indicate polyciliated and yellow arrows indicate non-ciliated epithelial cells. A scanning electron micrograph of EPC showing mono-, poly- and non-ciliated epithelial cells is shown in the inset of B (taken with permission from Prothman et al., 2001). The cilia are unlabeled and thus cannot be seen in these fluorescence images taken from live cells.

### 2.6.5.2. Transfection of undifferentiated ependymal primary cultures

Transfection of undifferentiated EPC with HIV/VSV-G/EF1 $\alpha$ /GFP on DIV 1 increased the transfection efficiencies up to approximately 75-80%, dependent on the MOI applied. In comparison, transfection of primary cultures on DIV 6 at the same virus concentrations resulted in transfection efficiencies of only 15-20%. Most of the kinociliated cells were not transfected in differentiated and in undifferentiated ependymal cells in primary cultures (Fig. 11), although the transfection efficiencies were substantially higher in the latter (Fig. 12).

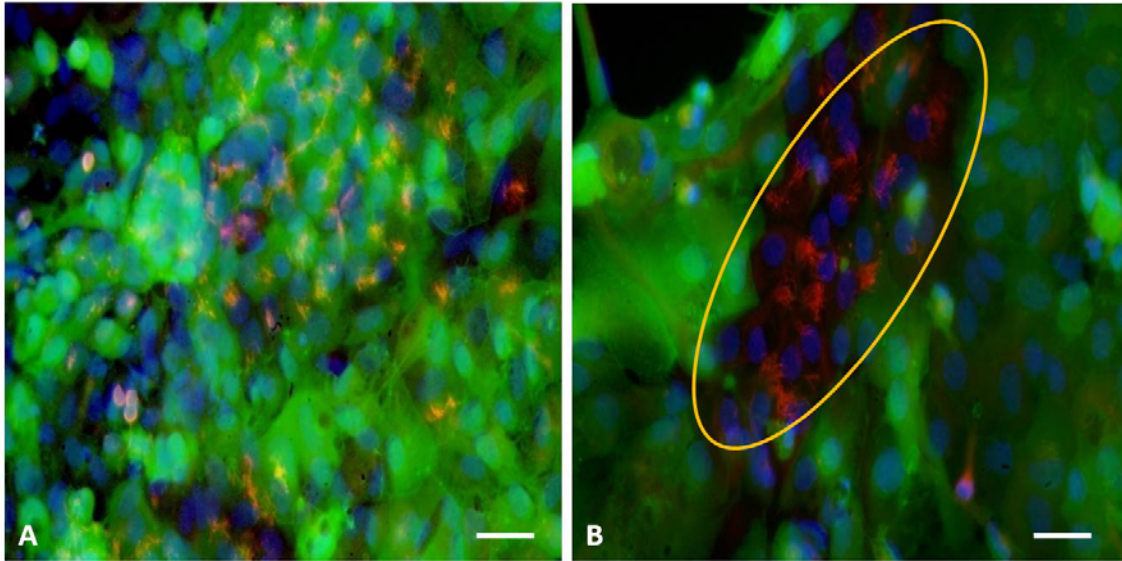


**Fig. 11.** Results of transfection of undifferentiated EPC with lentivirus on DIV 1. EPC were transfected with HIV/VSV-G/EF1 $\alpha$ /GFP on DIV 1 (MOI 10) and inspected after fixation on DIV 13. A: Transfected ciliated as well as non-ciliated cells are visible. B: An area of EPC showing transfected non-ciliated cells and nontransfected kinociliated epithelial cells where all the cells were transfected except the cells bearing kinocilia (ellipse in B). Cilia were stained with an anti-acetylated tubulin antibody (red) and nuclei were counterstained with 4',6-diamidino-2-phenylindole (blue). Scale bars: 20  $\mu$ m.

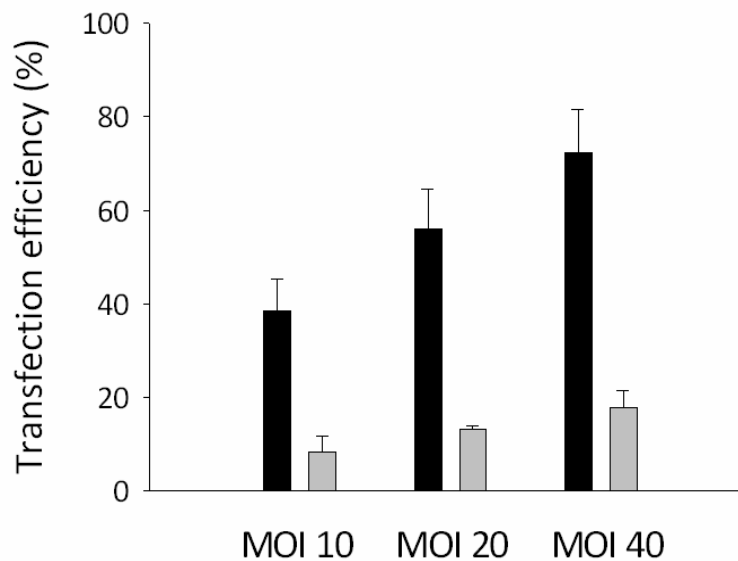


**Fig. 12.** Differences in the efficiencies of transfection of EPCs when transfected with HIV/VSV-G/EF1 $\alpha$ /GFP on DIV 1 or on DIV 6. Cells were grown on coverslips in a 24-well plate. For each condition, cells in 3 wells were transfected with lentivirus at increasing concentrations (MOIs 10, 20, 40 on DIV 1 and on DIV 6), and the cultures were maintained until DIV 13. After fixation and staining with an anti-acetylated tubulin antibody, cilia were counted. Virus-infected cells were identified by their GFP fluorescence. Approximately 1,500 cells were counted per experimental condition. Each bar indicates the mean  $\pm$  standard deviation of the transfection efficiencies measured from three different, independent experiments. Black bars indicate the transfection efficiency after infection on DIV 1 and grey bars that after infection on DIV 6.

### 2.6.6. Transfection of ependymal primary cultures with different pseudotypes

Apart from the VSV-G-pseudotyped lentiviral vectors, lentiviruses pseudotyped with Mokola, Ebola and Rabies envelope proteins were also produced and used to transfect the undifferentiated primary cultures. With none of these viral pseudotypes could satisfactory results be achieved, namely in no case could the successful transfection of a kinocilia-bearing cell be observed (Fig. 13). The major factor that prevented the productive use of these pseudotyped viruses in the primary cultures was their low titers, due to which high amounts of virus (e.g. upto 600 ng of p24/well) had to be applied to infect the cultures. This aggravated the problem already observed with the VSV-G pseudotype of a deleterious effect of the vector on the cultures. Therefore, no further experiments with pseudotypes other than VSV-G were conducted.

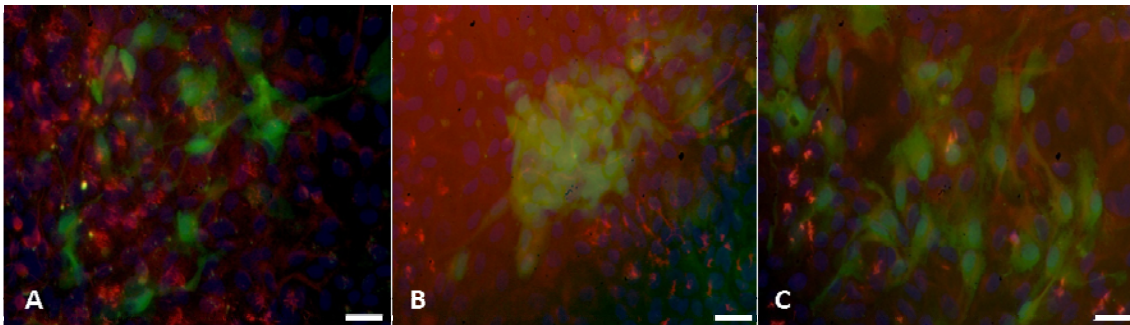


**Fig. 13.** Results of transfection of undifferentiated EPC with differently pseudotyped lentivirus on DIV 1. EPC were transfected with Ebola, Mokola and Rabies envelope-pseudotyped lentiviruses, respectively, on DIV 1 (50 ng of p24/well) and inspected after fixation on DIV 13. A: An area of cells transfected with Ebola pseudotype. B and C depict cultures transfected with Mokola-and Rabies-enveloped pseudotypes. Cilia were stained with an anti-acetylated tubulin antibody (red) and nuclei were counterstained with 4',6-diamidino-2-phenylindole (blue). Scale bars: 20  $\mu$ m.

### 2.6.7. Effect of virus on ependymal primary cultures

Even though the use of lentiviral vectors substantially increased the transfection efficiency in EPC in comparison to plasmids, it also had a deleterious effect on the cultured cells. Consecutive treatment of EPC with virus to the equivalent of 1000 ng of p24/well on DIV 0 and 1 completely destroyed the culture (Fig. 14), while less toxic concentration of virus (10-200 ng of p24/well, or MOI 10-40) still decreased the total number of ciliated cells (i.e. the



sum of monociliated and kinociliated cells) to approximately half in comparison to the control (Fig. 15).

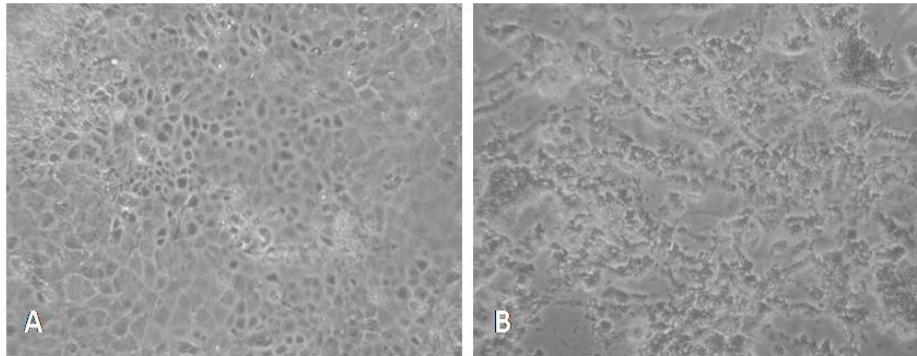


**Fig. 14.** Effect of HIV/VSVG/EF1 $\alpha$ /Spag6 (titer:  $1.7 \times 10^5$  TU/ml, MOI 7) on EPC. A: Normal EPC on DIV 13. B: EPC treated with lentivirus equivalent to  $1 \mu\text{g/ml}$  of p24 on DIV 4 and photographed at DIV 13.

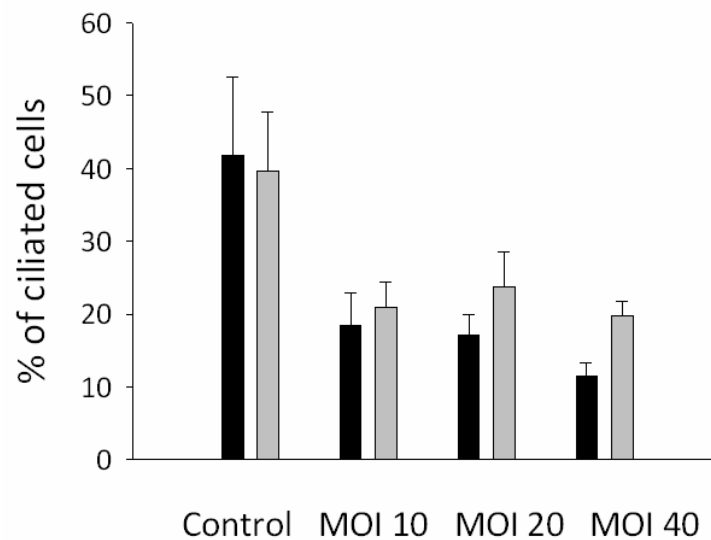


**Fig. 15.** Differences in the percentage of ciliated cells between the control and EPC transfected with lentivirus at different concentrations. Ependymal cells grown on coverslips were transfected with HIV/VSV-G/EF1 $\alpha$ /GFP in a 24-well plate. For each condition, cells in 3 wells were transfected at increasing concentrations of lentivirus (MOI 10, 20, 40 on DIV 1 and on DIV 6) and the cultures were maintained until DIV 13. Cells were fixed on DIV 13 and ciliated cells were counted after staining with an antibody against acetylated tubulin. Approximately 1,500 cells including mono- as well as polyciliated cells were counted per condition. Each bar indicates the mean  $\pm$  standard deviation of the percentage of ciliated cells (i.e. the sum of monociliated and kinociliated cells) counted from three different independent experiments. Black and grey bars indicate the percentages of ciliated cells after infection on DIV 1 and on DIV 6, respectively.



This observation can be linked to the fact that infection of airway epithelial cells with paramyxovirus alters their morphology and causes the loss of cilia during the injury phase (Look et al., 2001). Obviously, viral infection of kinocilia-bearing cells generally tends to entail a loss of cilia. Because of the toxic effects of HIV on EPC, transfection experiments had to be limited to a MOI of maximally 40.

## 2.6.8. Transfection of ependymal primary cultures in the presence of apoptosis inhibitor II (NS3694)

### 2.6.8.1. Transfection in the presence of apoptosis inhibitor II (NS3694)

Viruses can trigger apoptosis of infected cells via a range of mechanisms including direct receptor-mediated activation of cellular signalling pathways, induction of cytokines like interferons, and expression of viral proteins (Hay and Kannourakis, 2002).

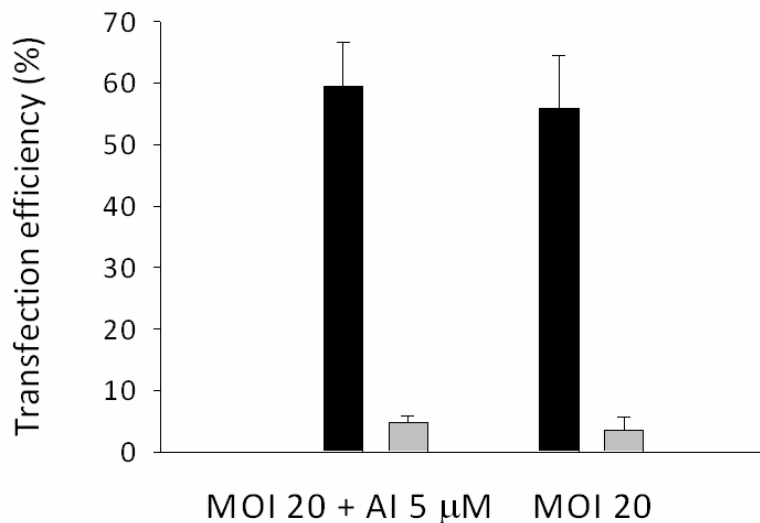


**Fig. 16.** Differences in transfection efficiencies of HIV/VSV-G/EF1 $\alpha$ /GFP toward EPC in the presence or absence of the apoptosis inhibitor AI (NS3694). For each condition, EPC were transfected in triplicates on DIV 1 (MOI 20), and the cultures were maintained in the presence of 5  $\mu$ M of AI from no later than 15 h after first exposure to virus until they were fixed (DIV 13). Cilia were stained with an antibody against acetylated tubulin and the numbers of total transfected cells and transfected ciliated cells were counted manually. Approximately 1,500 cells, including mono- as well as polyciliated cells were counted per condition. Each bar indicates the mean  $\pm$  standard deviation of the percentage of transfected cells counted in three different independent experiments. Black bars indicate the total transfection efficiency and grey bars indicate the transfection efficiency in ciliated cells (i.e. the sum of kinociliated and monociliated cells).

To further analyse whether the decrease in ciliated cells after infection of EPC with HIV/VSV-G was due to virus-mediated apoptosis, virus-infected EPC were maintained in the presence of apoptosis inhibitor II (AI, NS3694), which specifically prevents formation of the active ~700-kDa apoptosome complex triggered by cytochrome *c* release and thereby blocks apoptosome-mediated caspase activation and cell death (Lademann et al., 2003). NS3694 was applied no later than 15 hours after first exposure to virus-containing infection media. The compound was used at a concentration of 5  $\mu$ M in MEM<sub>CT</sub> and kept present until DIV 13. Transfection of EPC with virus corresponding to MOI 20 on DIV 1 resulted in a transfection efficiency of approximately 55%, but only 3-5% of the transfected cells were ciliated (Fig. 16). Treatment of EPC with the apoptosis inhibitor NS3694 did not increase the transfection efficiencies with respect to either total cells or ciliated cells transfected (Fig. 16).

#### **2.6.8.2. Effect of apoptosis inhibitor II (NS3694) on the ependymal primary cultures**

Continuous treatment of the EPC with the AI NS3694 at a concentration of 5  $\mu$ M starting from 48 h after seeding resulted in a decrease of up to 10% in the number of ciliated cells (i.e. the sum of monociliated and kinociliated cells), independently from any exposure to virus (cf. Fig. 17 A: AI, Control). The decrease in the total number of cells after treatment with virus (cf. Fig. 17 B) was not prevented or altered by NS3694 (Fig. 17 B). In summary, the detrimental effect of virus treatment on the total number of cells or of ciliated cells in the EPC was not prevented by application of the AI (Fig. 17).

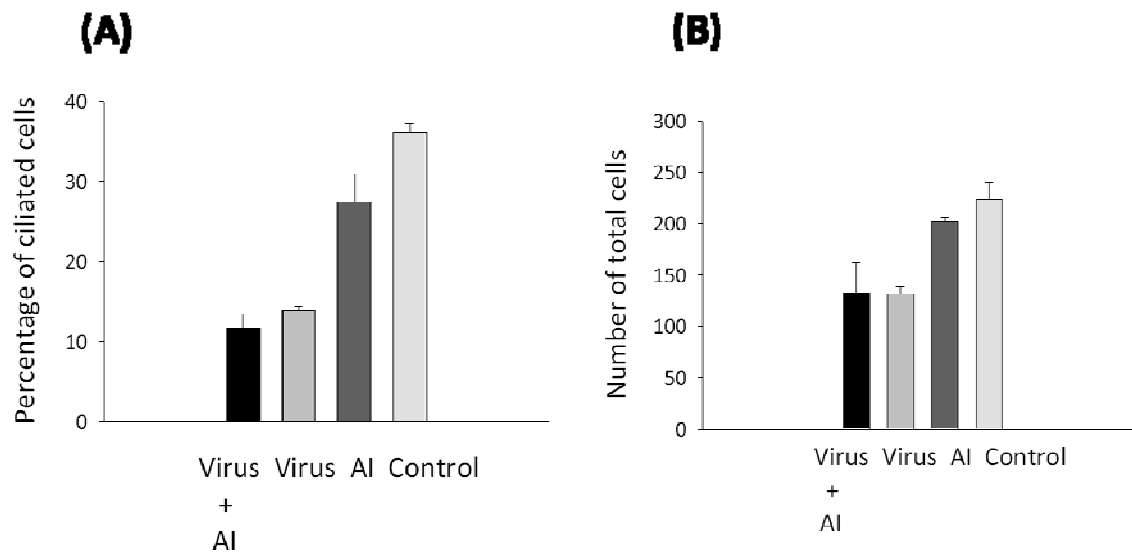


**Fig. 17.** Differences in the percentage of ciliated cells (A) and number of total cells (B) in EPC treated with virus and apoptosis inhibitor II (AI), either alone or in combination. For each condition, 3 wells of an EPC on a 24-well plate were transfected with HIV/VSV-G/EF1 $\alpha$ /GFP (MOI 20) on DIV 1 and the cultures were maintained in the presence of 5  $\mu$ M of the apoptosis inhibitor from DIV 2 until they were fixed on DIV 13. Alternatively, EPC were infected with virus and maintained until DIV 13 without the addition of apoptosis inhibitor, or they were maintained in the presence of apoptosis inhibitors but without virus infection until DIV 13. Cilia were stained with an antibody against acetylated tubulin after fixation on DIV 13, and the total number of ciliated cells was counted manually. Approximately 1,500 cells including mono- as well as polyciliated cells (i.e. the sum of monociliated and kinociliated cells) were counted per experimental condition. Each bar indicates the mean  $\pm$  standard deviation of the percentage of ciliated cells counted from three different independent experiments.

### 2.6.9. Transfection of ependymal primary cultures with virus encoding GFP under the control of kinociliated-cell specific promoters

Even though a total transfection efficiency of 75-80% was achieved in the EPC with virus encoding GFP under the control of the EF1 $\alpha$  promoter, transfection efficiency with respect to ciliated cells was only 5%. This was probably due to a block of cell differentiation induced in ependymal cell precursors by early transgene expression. Therefore, it was decided to put the transgene under the control of a kinocilia-specific promoter in order to restrict its expression to differentiated kinocilia-bearing cells.

### 2.6.9.1. Lentivirus encoding GFP under the control of the FOXJ1 promoter

The forkhead box transcription factor FOXJ1 is required for late stages of ciliogenesis, and the FOXJ1 promoter is able to drive transgene expression in all ciliated cells (Ostrowski et al., 2003). Transfection of EPC with virus encoding GFP under the control of the FOXJ1 promoter drastically decreased the total transfection efficiency from 80% to 25%, but at the same time tripled the specific transfection rate of kinociliated cells from < 5% to 15% (Fig. 18). The transgene under the control of the FOXJ1 promoter is not expressed in HEK293T cells. Therefore it is not possible to titrate the virus preparation on them, and only the p24 content of the virus in terms of equivalence to the known titer of HIV/VSV-G/GFP/EF1 $\alpha$  (200 ng of p24 equivalent to MOI 20 of HIV/VSV-G/GFP/EF1 $\alpha$ ) could be used as a measure for virus load during transfection of EPC.

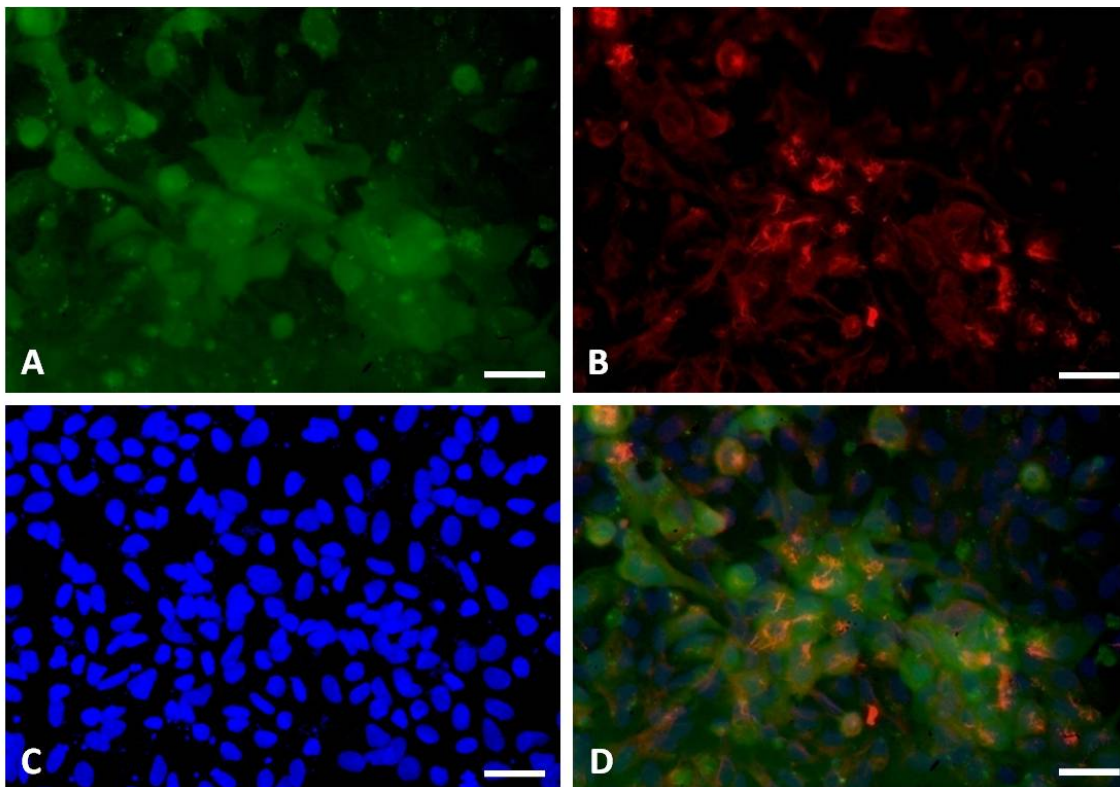


**Fig. 18.** Transfection on DIV 1 of rat EPC with lentivirus encoding GFP under the control of the FOXJ1 promoter. A: EPC were treated with HIV/VSV-G/GFP/FOXJ1 equivalent to 200 ng of p24 (see text) on DIV 1 and inspected for transfected cells on DIV 13. B: Cilia were stained with an antibody against acetylated tubulin. C: Nuclei were counterstained with 4',6-diamidino-2-phenylindole. D: An overlay of the three images identifies the transfected ciliated cells. Scale bars: 20  $\mu$ m.

### 2.6.9.2. Lentivirus encoding GFP under the control of the wdr16 promoter

Wdr16 is up-regulated together with kinocilia formation in testis, ependyma and respiratory epithelium, and therefore the protein is a differentiation marker of kinocilia-bearing cells (Hirschner et al., 2007). Transfection of EPC with virus encoding GFP under the control of the wdr16 promoter gave results similar to the ones obtained with the FOXJ1 promoter. The total transfection efficiency decreased to 25% with respect to the one obtained with the EF1 $\alpha$  promoter, but now the expression of the transgene was restricted to polyciliated cells and the specific transfection rate of kinociliated cells increased to approximately 15% (Fig. 19).

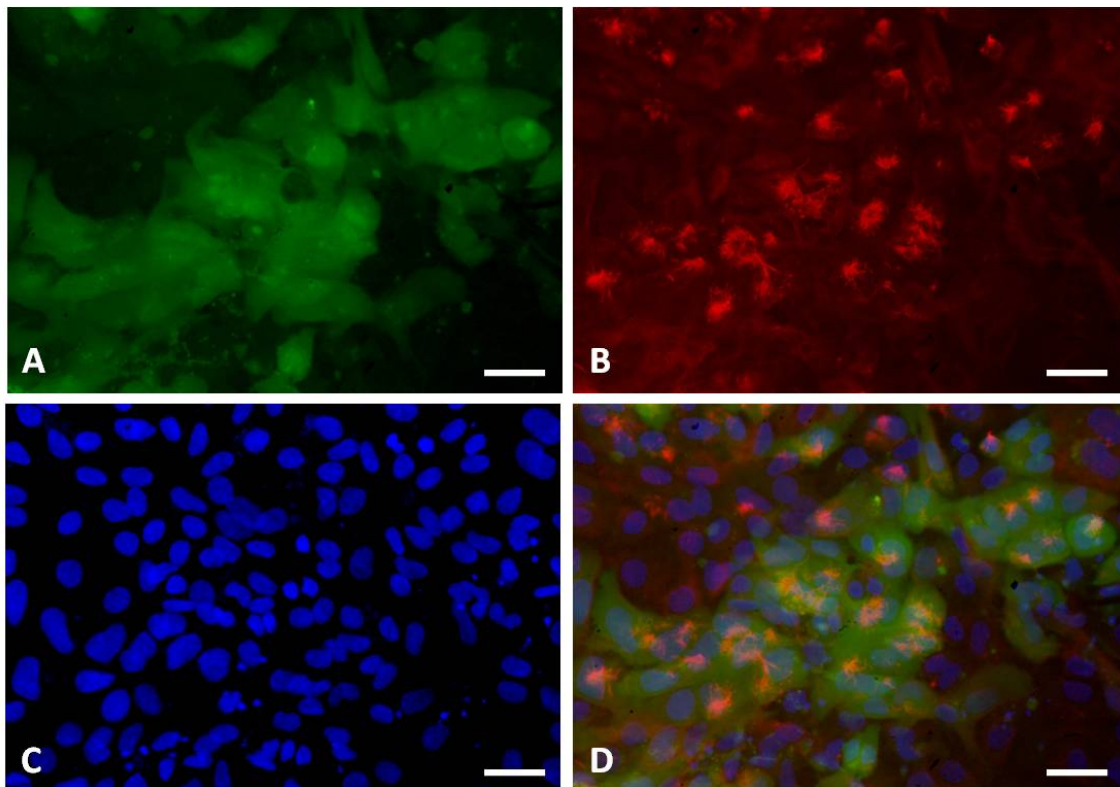


**Fig. 19.** Transfection on DIV 1 of rat EPC with lentivirus encoding GFP under the control of the wdr16 promoter. A: EPC were treated with HIV/VSV-G/GFP/wdr16 promoter equivalent to (see text) 200 ng of p24 on DIV 1 and inspected for transfected cells on DIV 13. B: Cilia were stained with an antibody against acetylated tubulin. C: Nuclei were counterstained with 4',6-diamidino-2-phenylindole. D: An overlay of the three images identifies the transfected ciliated cells. Scale bars: 20  $\mu$ m.

Since the transgene under the control of the *wdr16* promoter is not expressed in HEK293T cells, it is not possible to titer the virus preparation and only the p24 content of the virus in terms of equivalence to the known titer of HIV/VSV-G/GFP/EF1 $\alpha$  (200 ng of p24 equivalent to MOI 20 of HIV/VSV-G/GFP/EF1 $\alpha$ ) is used as a measure for virus load during transfection of EPC.

### 2.6.9.3. Specificity of the FOXJ1 and *wdr16* promoters

Lentiviruses encoding GFP under the control of either the FOXJ1 or the *wdr16* promoter show significantly increased transgene expression in the ciliated cells of EPCs as compared to the unspecific EF1 $\alpha$  promoter. This highlights the importance of kinocilia-specific promoters for achieving the expression of transgenes in kinocilia-bearing cells.

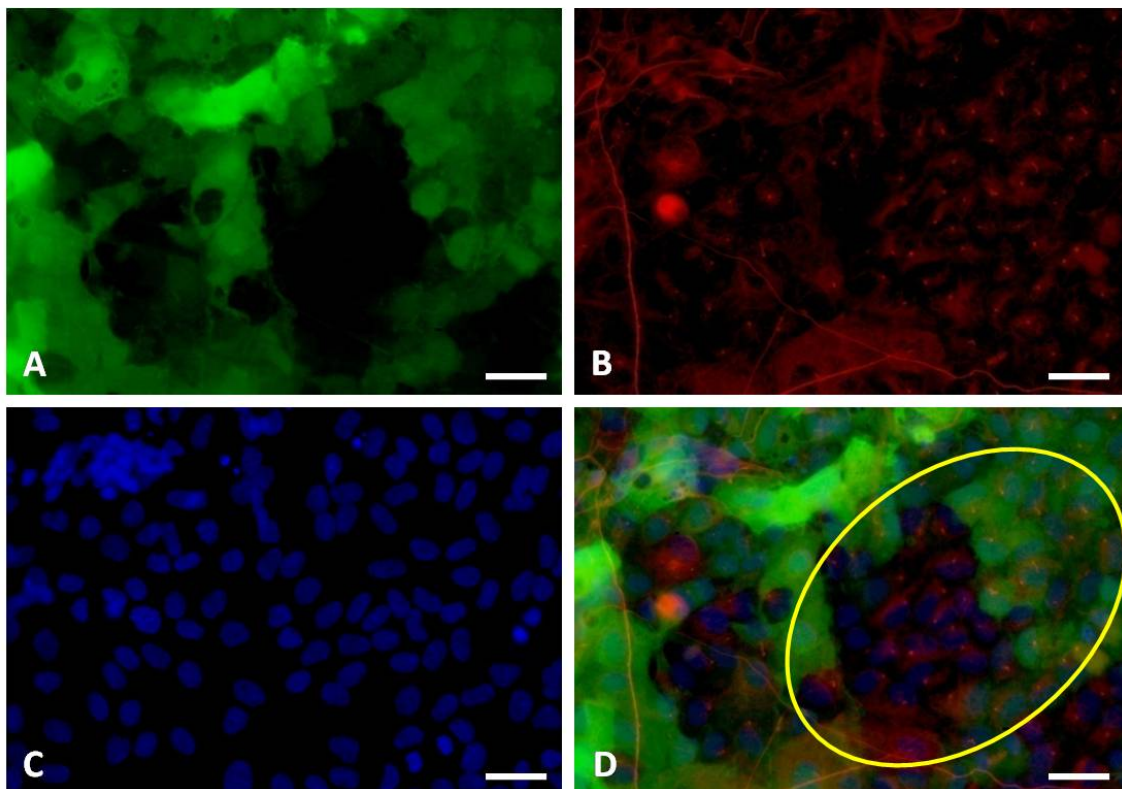


**Fig. 20.** A: Transfection on DIV 1 of rat EPC with lentivirus (HIV/VSV-G/GFP/EF1 $\alpha$ ) encoding GFP under the control of the EF1 $\alpha$  promoter leads to transgene expression in monociliated cells. B: Cilia were counterstained with an antibody against acetylated tubulin. C: Nuclei were visualised with 4',6-diamidino-2-phenylindole. D: The ellipse in the overlay of three images A, B and C delineates an area of the monociliated cells expressing the transgene. Scale bars: 20  $\mu$ m.



Transfection with virus encoding GFP under the control of the promoter of the constitutively expressed elongation factor EF1 $\alpha$  often resulted in the transfection of monociliated cells (Fig. 20). In contrast, virus encoding GFP under the control of the FOXJ1 and wdr16 promoters drives the expression of transgenes specifically in kinociliated cells, and none of the monociliated cells were observed to express the transgene (Figs. 21, 22).

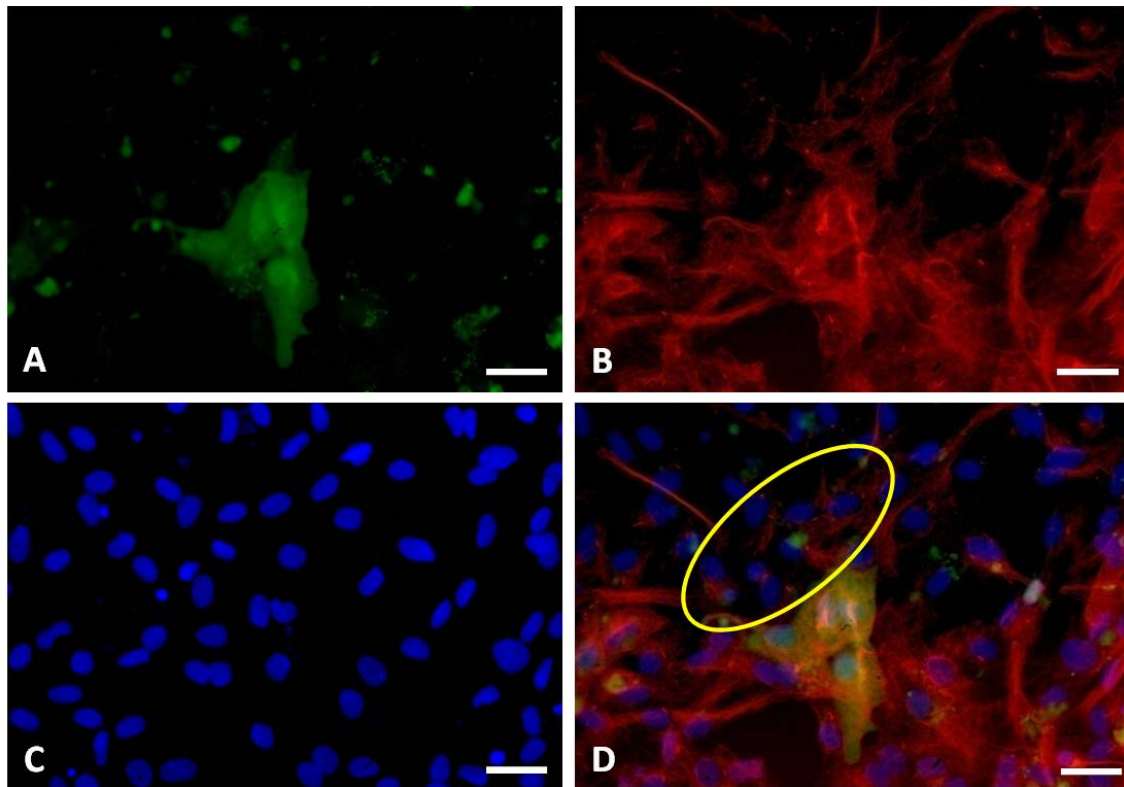


**Fig. 21.** A: Transfection on DIV 1 of rat EPC with lentivirus (HIV/VSV-G/GFP/FOXJ1) encoding GFP under the control of the FOXJ1 promoter shows the specificity of the promoter for cells with multiple kinocilia. Monociliated cells do not express the transgene. All images were taken on DIV 13. B: Cilia were counterstained with an antibody against acetylated tubulin. C: Nuclei were visualised with 4',6-diamidino-2-phenylindole. D: An overlay of the three images A, B and C emphasises the specificity of this promoter for kinociliated cells only. The ellipse in D shows an area of monociliated cells not expressing the transgene. Scale bars: 20  $\mu$ m.

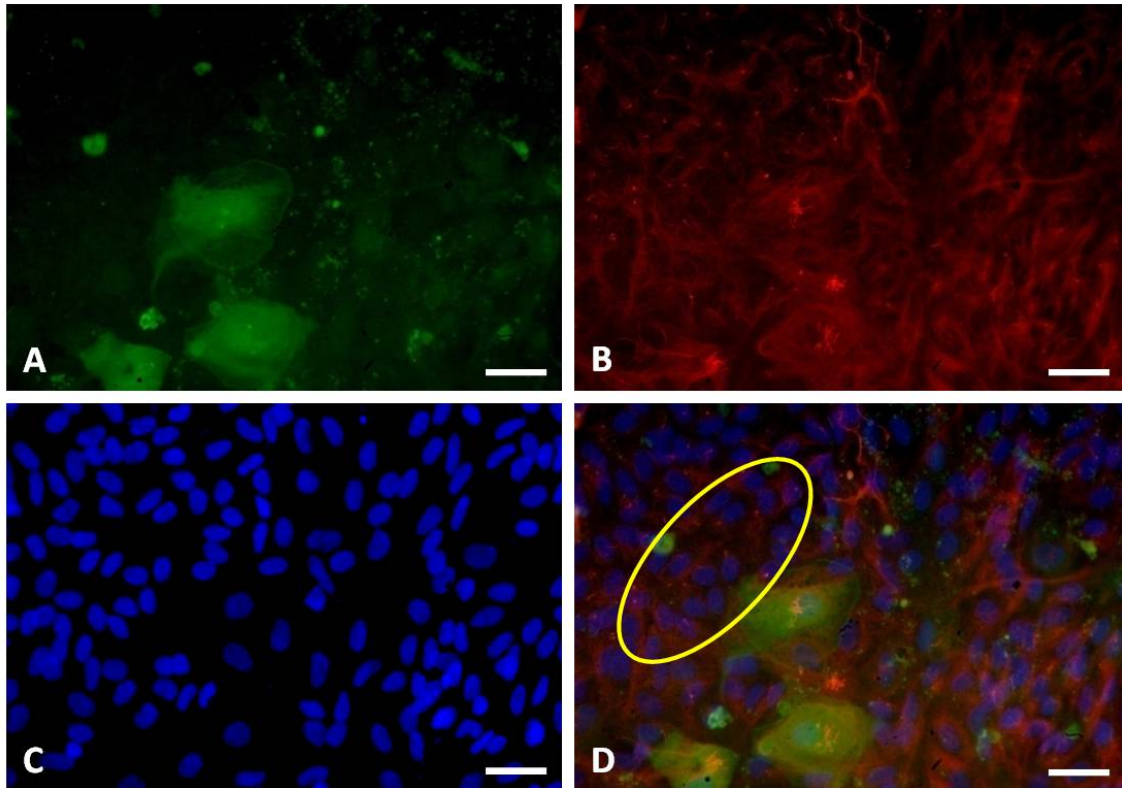


**Fig. 22.** A: Transfection on DIV 1 of rat EPC with lentivirus (HIV/VSV-G/GFP/wdr16 promoter) encoding GFP under the control of the wdr16 promoter shows the specificity of the promoter for cells with multiple kinocilia. Monociliated cells do not express the transgene. All the images were taken on DIV 13. B: Cilia were counterstained with an antibody against acetylated tubulin. C: Nuclei were visualised with 4',6-diamidino-2-phenylindole. D: An overlay of the three images A, B and C emphasises the specificity of this promoter for kinociliated cells only. The ellipse in D shows an area of monociliated cells not expressing the transgene. Scale bars: 20  $\mu$ m.

#### 2.6.9.4. Transfection efficiencies in ciliated cells under the control of different promoters

Transfection of the EPC with a virus encoding GFP under the control of the EF1 $\alpha$  promoter (Fig. 20) resulted in the transfection of 55-60% of the total cells in culture, but only < 5% of them bore kinocilia. Transfection with a virus encoding GFP under the control of either the FOXJ1 (Fig. 21) or the wdr16 promoter (Fig. 22) resulted in the transfection of only 25-30% of all cells, but 15% were kinociliated cells (Fig. 23 A). Usage of promoters specific for kinocilia-related genes may prevent the deleterious effects of transgene expression too early in the development of ciliated cells. This impression arises, because the total number of ciliated cells present after infection with a virus encoding GFP under the control of the



EF1 $\alpha$  promoter was significantly lower than that present after infection with virus encoding GFP under the control of the FOXJ1 or the wdr16 promoter (Fig. 23 B).

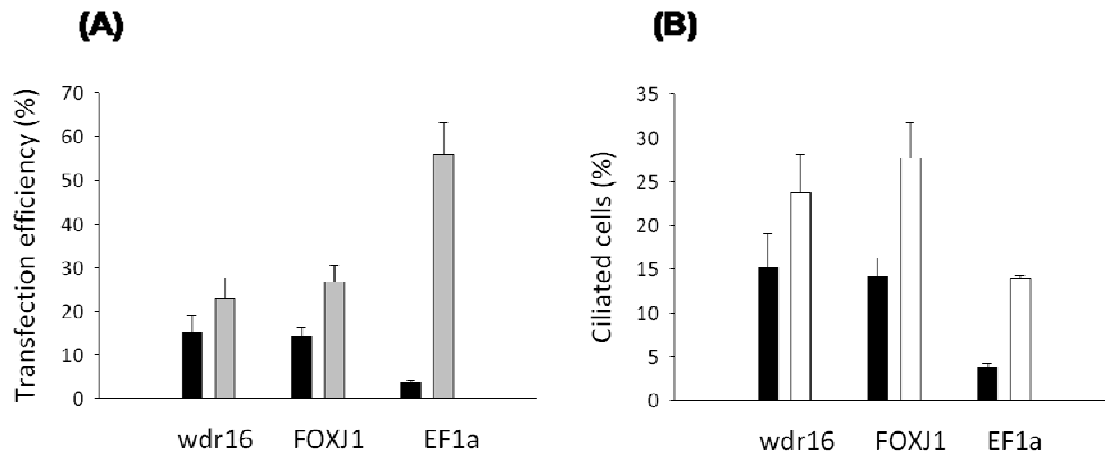


**Fig. 23.** Quantitative analysis of the situation depicted in Figs 20-22. A: Differences in transfection efficiencies after infecting EPC with virus encoding GFP under the control of different promoters. B: Differences in the percentage of ciliated cells in relation to the total number of cells present in EPC after infecting with virus encoding GFP under the control of different promoters. For each condition, 3 wells of an EPC on coverslips in a 24-well plate were transfected on DIV 1 (200 ng of p24) and the cultures were maintained until they were fixed on DIV 13. Cilia were counterstained with an antibody against acetylated tubulin. Virus-infected cells were identified by their GFP fluorescence. Approximately 1,500 cells were counted per experimental condition. Each bar indicates the mean  $\pm$  standard deviation of the percentage of transgene-expressing or ciliated cells counted from three different, independent experiments. In (A) black bars indicate the percentage of transfected ciliated cells (i.e. the sum of kinociliated and monociliated cells in the case of the EF1 $\alpha$  promoter and only kinociliated cells in the cases of the FOXJ1 and wdr16 promoters) and grey bars indicate the total percentage of transfected cells. In (B) black bars indicate the percentage of transgene-expressing ciliated cells and white bars indicate the percentage of ciliated cells (i.e. the sum of monociliated and kinociliated cells in the case of the EF1 $\alpha$  promoter and only kinociliated cells in the cases of the FOXJ1 and wdr16 promoters).

#### 2.6.9.5. FOXJ1 and wdr16 promoters drive the expression of transgenes in different species

The FOXJ1 promoter was cloned from human genomic DNA and shown to be able to drive transgene expression in EPC from both mice (Fig. 24) and rats. In order to find out whether the wdr16 promoter is also able to drive expression in another species, mouse EPC (see section 4.2.1.2) were transfected with virus encoding GFP under the control of the rat wdr16 promoter. The rat wdr16 promoter was found to be indeed able to drive transgene expression in mice EPC (Fig. 25).

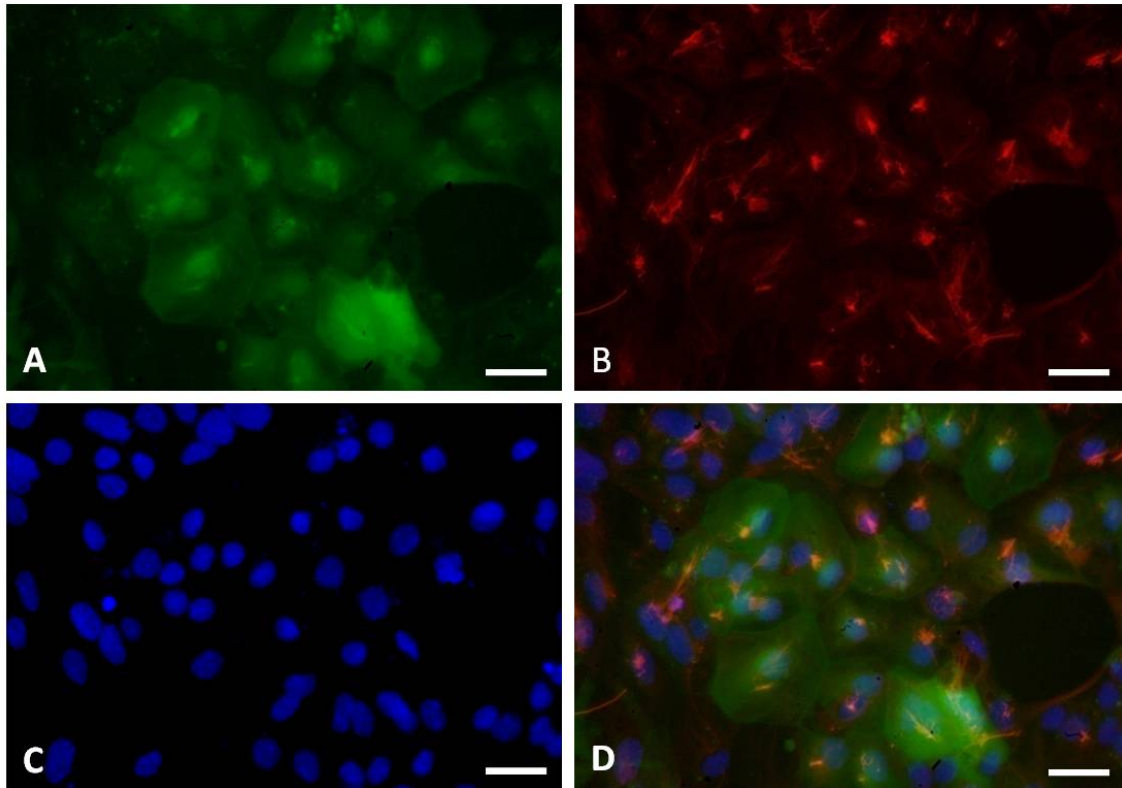


**Fig. 24.** A: Transfection on DIV 1 of mouse EPC with lentivirus (HIV/VSV-G/GFP/FOXJ1) encoding GFP under the control of the FOXJ1 promoter leads to transgene-expressing cells. B: Cilia were counterstained with an antibody against acetylated tubulin. C: Nuclei were visualised with 4',6-diamidino-2-phenylindole. D: An overlay of the three images A, B and C shows the transfected ciliated cells. Scale bars: 20  $\mu$ m.

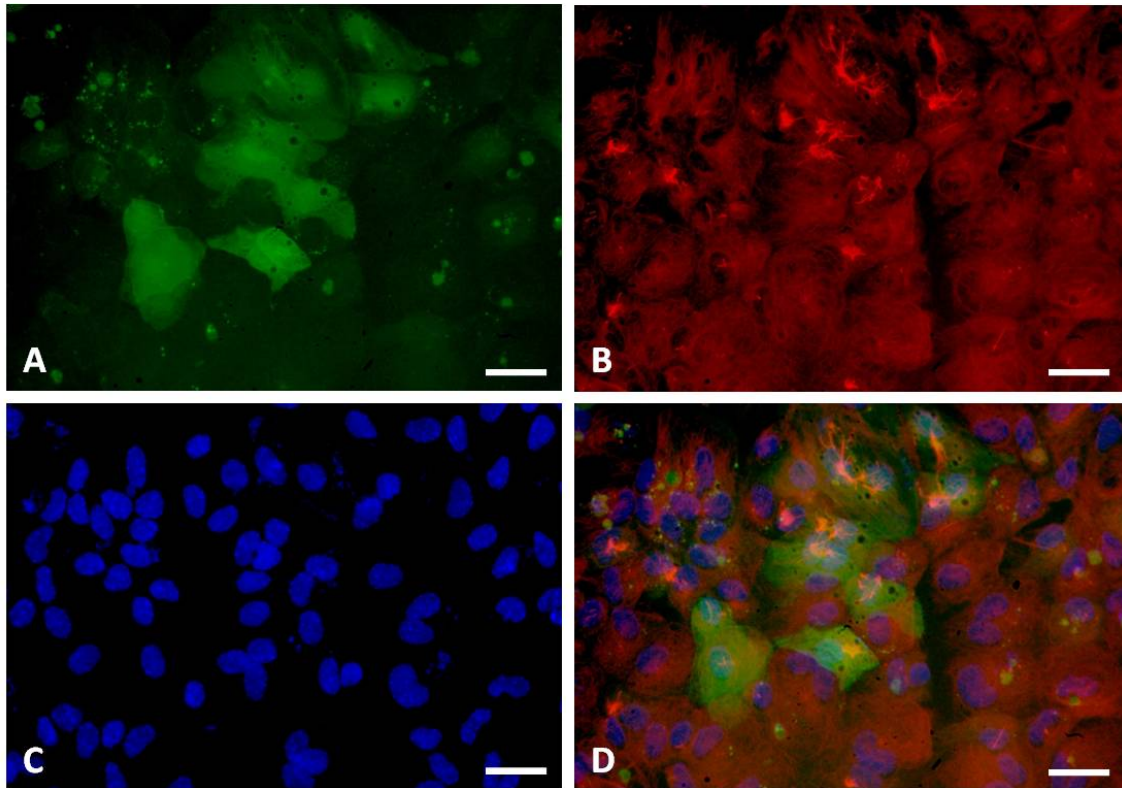


**Fig. 25.** A: Transfection on DIV 1 of mouse EPC with lentivirus (HIV/VSV-G/GFP/wdr16 promoter) encoding GFP under the control of the rat wdr16 promoter leads to transgene-expressing cells. B: Cilia were counterstained with an antibody against acetylated tubulin. C: Nuclei were visualised with 4',6-diamidino-2-phenylindole. D: An overlay of the three images A, B and C shows the transfected ciliated cells. Scale bars: 20  $\mu$ m.

### 2.6.10. Analysis of proviral DNA integration

Early steps of HIV-1 infection involve entry of the viral core into the cells, reverse transcription of the RNA genome to form a linear proviral DNA and its subsequent integration into the host genome. In order to verify genomic integration of the lentiviral vectors and thus successful transfection of EPC, a nested PCR (Roux 1995) was carried out on ependymal culture DNA isolated after virus treatment (see section 4.2.7). The primers for the first round of amplification were designed against the long interspersed nuclear elements (LINE1) of the rat genome and the long terminal repeats (LTR) of the proviral DNA, respectively. The primers of the second set were targeted to the HIV sequence exclusively. The nested PCR procedure was carried out with genomic DNA of cultures infected on DIV 1 and DIV 6. It amplified the expected fragment of 333 bp length (Fig. 26). This was not seen

with DNA from control cultures never exposed to virus, confirming the integration of proviral DNA in the host genome after infection.

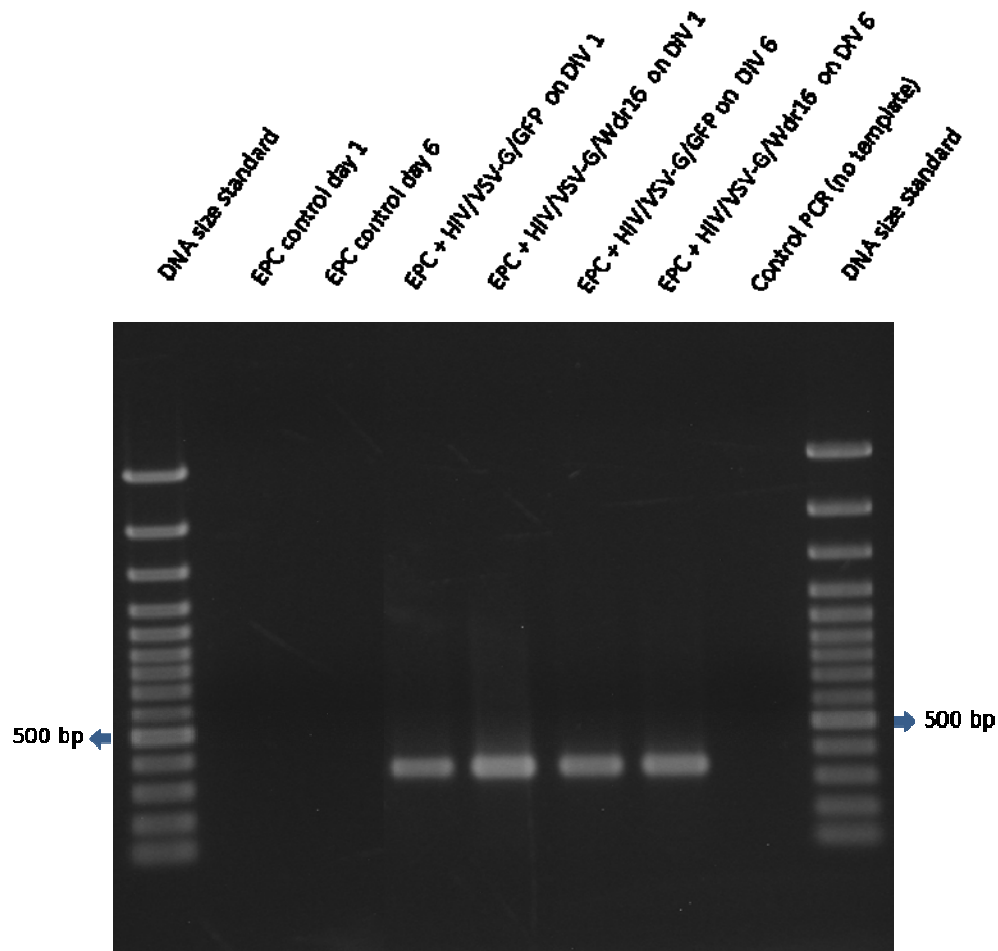


**Fig. 26.** Agarose gel stained with ethidium bromide showing the presence or absence of the integrated viral genome in the cellular genome of EPC. EPC were transfected with virus on DIV 1 or 6, and then maintained until DIV 13. Genomic DNA was isolated from the EPC and a nested PCR was performed to show the presence of the integrated viral genome. 200 ng of genomic DNA was used in the first round of PCR (35 cycles) with the first set of primers directed against rat LINE1 and the LTRs of the proviral DNA. The product of the first PCR was diluted 10-fold and used as a template in the second PCR (25 cycles) with internal primers directed against an internal sequence of the proviral DNA, which allowed the amplification of a fragment of 333 bp in length. As a control, nested PCR was carried out using the genomic DNA isolated from EPC never exposed to virus. Nested PCR of genomic DNA from EPC, infected with lentivirus (HIV/VSV-G/GFP or Wdr16-GFP) on DIV 1 and 6, respectively, yields the expected fragment of 333 bp length. In contrast, no PCR product was obtained for the negative control without template DNA and for control cultures without virus infection. The DNA size standard is a 100 bp ladder.

### 2.6.11. Transfection of EPC with lentiviruses bearing transgenes tagged with GFP

The ependyma-specific proteins Wdr16 and pAK7 had previously been identified by the screening of subtractive ependymal cDNA libraries. While it was already known that these proteins are specifically expressed in ependymal cells, it was still desirable to subcellularly localise these proteins.

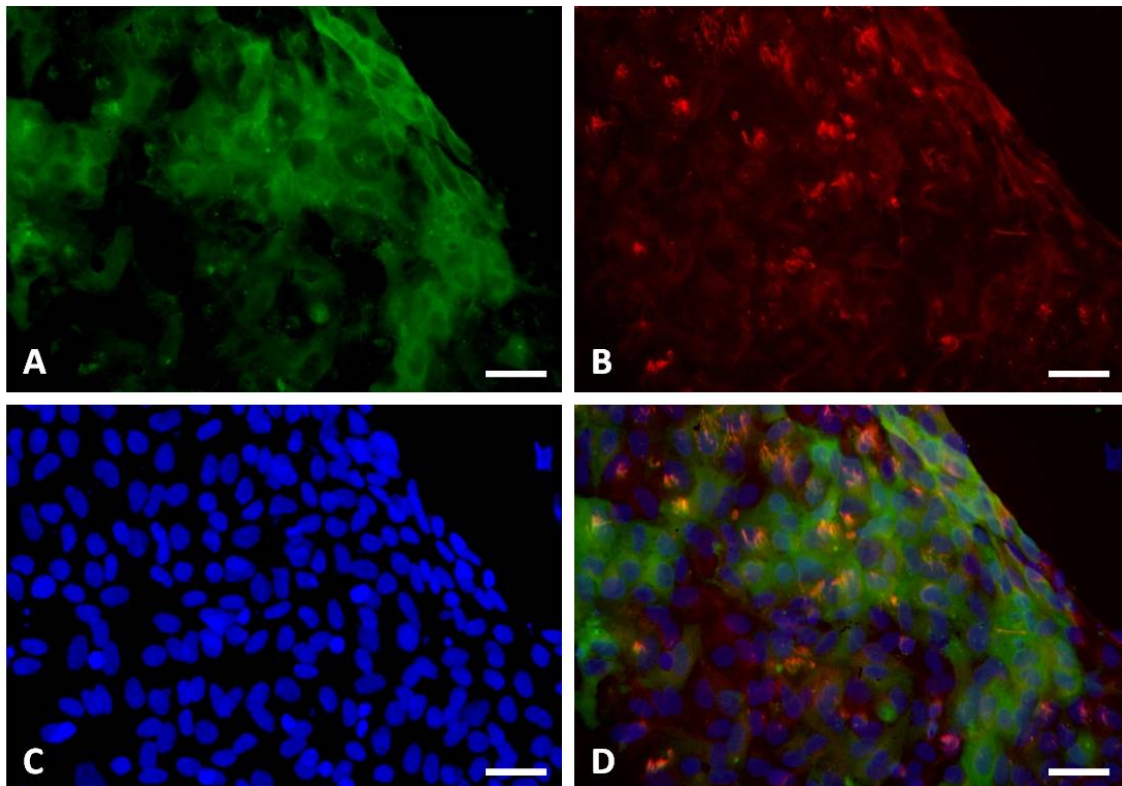


**Fig. 27.** A: Transfection on DIV 1 of rat EPC with lentivirus (HIV/VSV-G/EF1 $\alpha$ /Wdr16-GFP) encoding Wdr16 fused to the C-terminus of GFP shows transgene-expressing cells. B: Cilia were counterstained with an antibody against acetylated tubulin. C: Nuclei were visualised with 4',6-diamidino-2-phenylindole. D: An overlay of the three images A, B and C shows the cytoplasmic location of the Wdr16-GFP fusion protein in kinociliated cells. Scale bars: 20  $\mu$ m.

The C-termini of wdr16 and pAK-7 ORFs were therefore respectively fused to the coding sequence of GFP and the cassettes were inserted into the virus production plasmid pWPXL. For comparison and control purposes, a GFP fusion construct with the known kinocilia-specific protein spag6 was also generated. As the kinocilia-specific FOXJ1 and wdr16 promoters were not in use at the time of these experiments, the transgenes were expressed



under the control of the EF1 $\alpha$  promoter. Transfection of EPC with the corresponding constructs revealed a cytosolic location of the ependyma-specific proteins Wdr16 and pAK7 in ciliated cells (Figs. 27, 28).

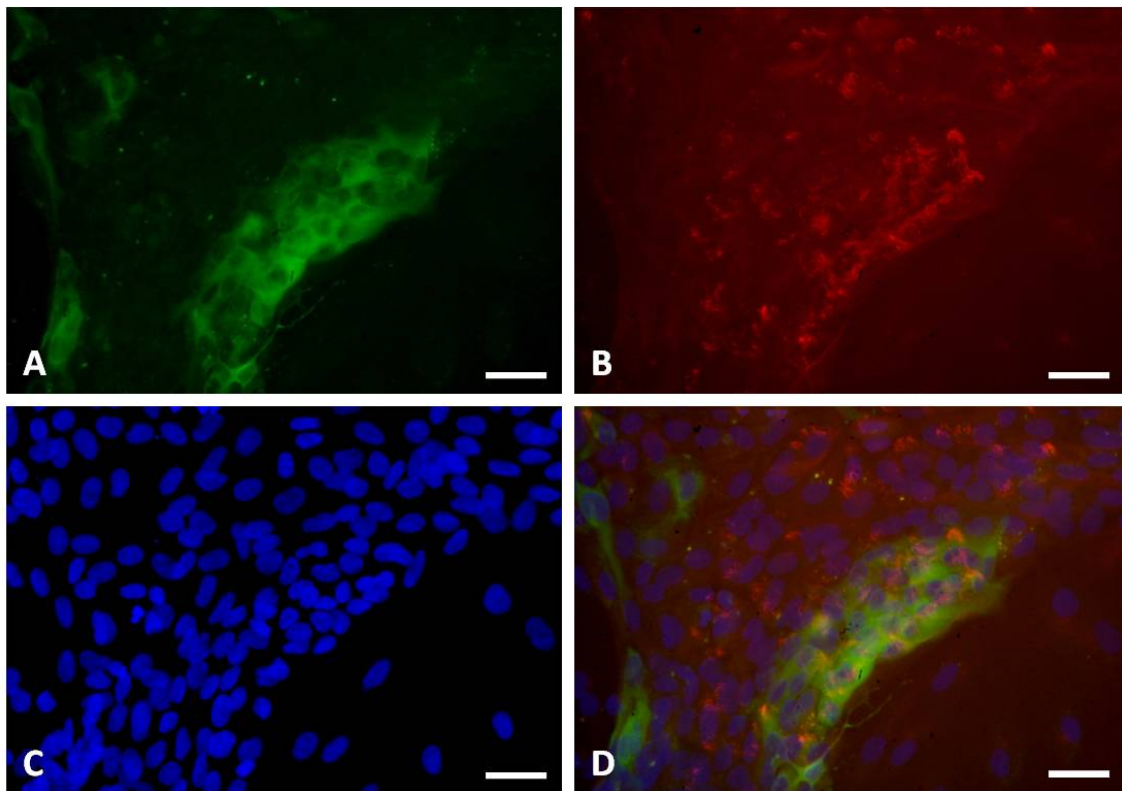


**Fig. 28.** A: Transfection on DIV 1 of rat EPC with lentivirus (HIV/VSV-G/EF1 $\alpha$ /pAK7-GFP) encoding pAK7 fused to the C-terminus of GFP shows transgene-expressing cells. B: Cilia were counterstained with an antibody against acetylated tubulin. C: Nuclei were visualised with 4',6-diamidino-2-phenylindole. D: An overlay of the three images A, B and C shows the cytoplasmic location of the pAK7-GFP fusion protein in kinociliated cells. Scale bars: 20  $\mu$ m.

#### 2.6.11.1. Localisation of the Spag6-GFP fusion protein

Transfection of kinocilia-free HEK293T cells with lentivirus encoding –under the control of the EF1 $\alpha$  promoter– Spag6 fused to the N-terminus of the coding sequence of GFP led to GFP fluorescence localised to the microtubule cytoskeleton, as already reported by Simpson et al. (2000). It is important to note that transfection of EPC with HIV/VSV-G/Spag6-GFP also localised this GFP fusion protein to the microtubule cytoskeleton of the cytosol, but not to the cilia (Fig. 29). This could be because no kinocilia-specific promoter was used and in such

a case the expression of Spag6-GFP starts from the day of infection, i.e. much before the onset of ciliogenesis in culture.

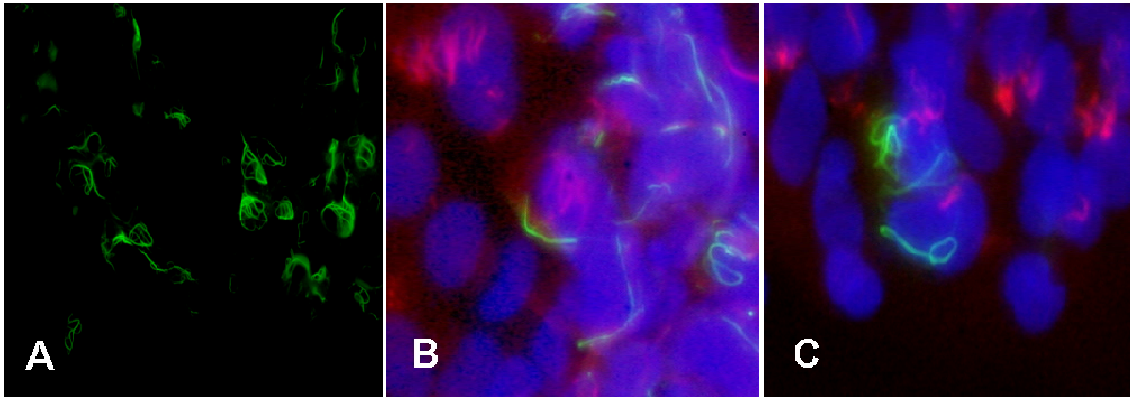


**Fig. 29.** Location of a Spag6-GFP fusion protein in non-ciliated cells and ciliated cells. A: HEK293T cells transfected with HIV/VSV-G/EF1 $\alpha$ /Spag6-GFP show a microtubular cytoskeletal location. B, C: Ependymal cells in different areas of a primary culture transfected with HIV/VSV-G/Spag6-GFP also show a microtubular cytoskeletal location of Spag6 (green). In B and C, the cilia are stained with an antibody against acetylated tubulin (red) and nuclei were visualised with 4',6-diamidino-2-phenylindole (blue).

## 2.6.12. Analysis of different small hairpin RNAs targeting Wdr16

Wdr16, a WD repeat protein identified by screening of an ependymal cDNA library, had previously been shown to be specific to kinocilia, and a gene knockdown to cause severe hydrocephalus in zebrafish (Hirschner et al., 2007). Transfection of EPC with lentivirus encoding a GFP fusion construct of Wdr16 located it to the cytoplasm of ciliated ependymal cells (Fig. 27). In order to study the function of Wdr16 by RNAi-based gene knockdown experiments (Downward, 2004), different short hairpin RNA (shRNA) constructs targeting wdr16 mRNA were designed and cloned into the lentiviral vector, pLVTHM.

### 2.6.12.1. HEK-wdr16 cell line

Different anti-wdr16 shRNAs needed to be tested for their ability to facilitate a gene knockdown of wdr16. For this purpose, the ability of the lentiviruses to integrate into the genome of a host cell was exploited to produce a stable HEK293T cell line expressing wdr16

fused to the ORF of GFP (Fig. 30). This HEK-wdr16 cell line was then used as a tool to test different anti-wdr16 shRNA constructs in wdr16 gene knockdown studies.

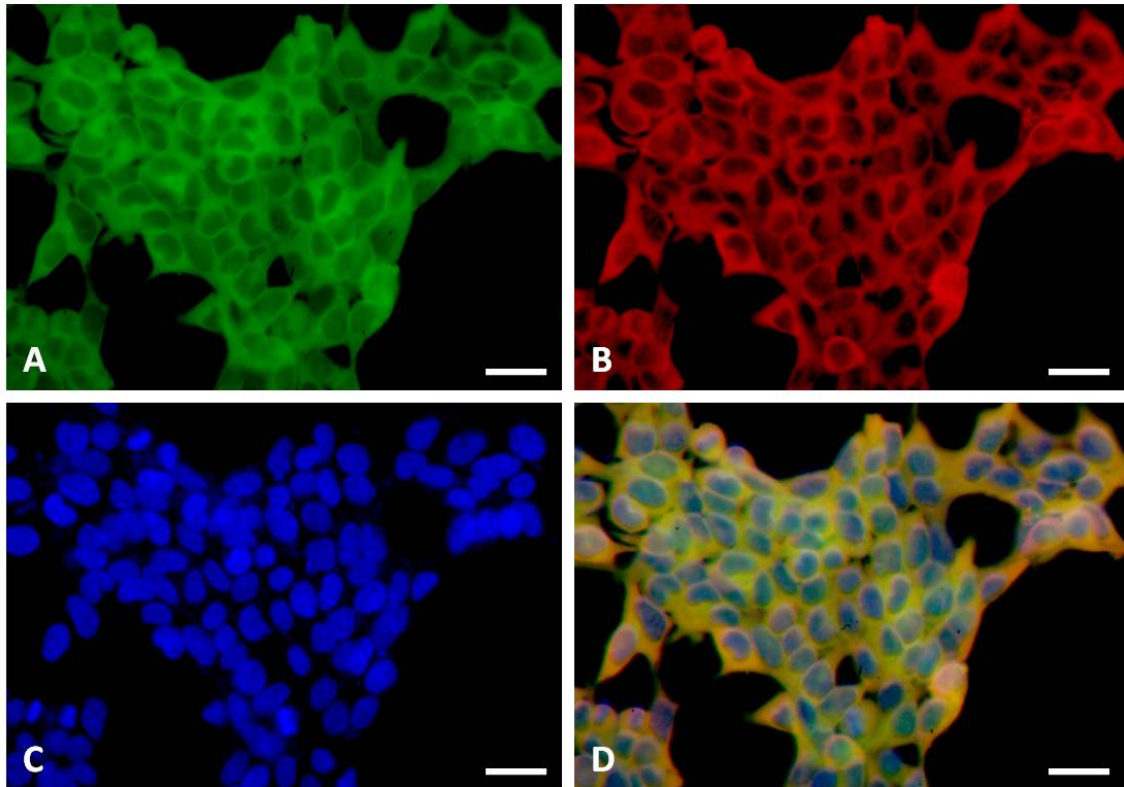


**Fig. 30.** Stable HEK-wdr16 cell line showing the cytoplasmic location of the Wdr16-GFP fusion protein. A: HEK293T cells were transfected with HIV/VSV-G/wdr16-GFP and cells producing the Wdr16-GFP fusion protein were cloned to yield the HEK-wdr16 cell line. B: Immunostaining with guinea pig Wdr16 antiserum shows cytoplasmic location of the Wdr16-GFP fusion protein in the HEK-wdr16 cell line. C: Nuclei were counterstained with 4',6-diamidino-2-phenylindole. D: The overlay of the three images A, B and C is depicted in (D). Scale bars: 20  $\mu$ m.

#### 2.6.12.2. Analysis of different anti-wdr16 shRNAs with the HEK-wdr16 cell line

In order to identify the shRNA construct causing the maximum silencing of wdr16 expression, lentiviruses harbouring three different constructs designed for that purpose were successfully produced. A control virus harbouring a scrambled sequence not present in the EST database at the NCBI, Bethesda, USA was also obtained. Cells from the HEK-wdr16 line were transfected with the respective viruses (equivalent to 30 ng of HIV-I p24), and the cells were collected for Western blotting at different time points. Anti-wdr16 shRNA



construct 1 was shown to be the most efficient one for silencing of wdr16 in the HEK-wdr16 cell line (Fig. 31).

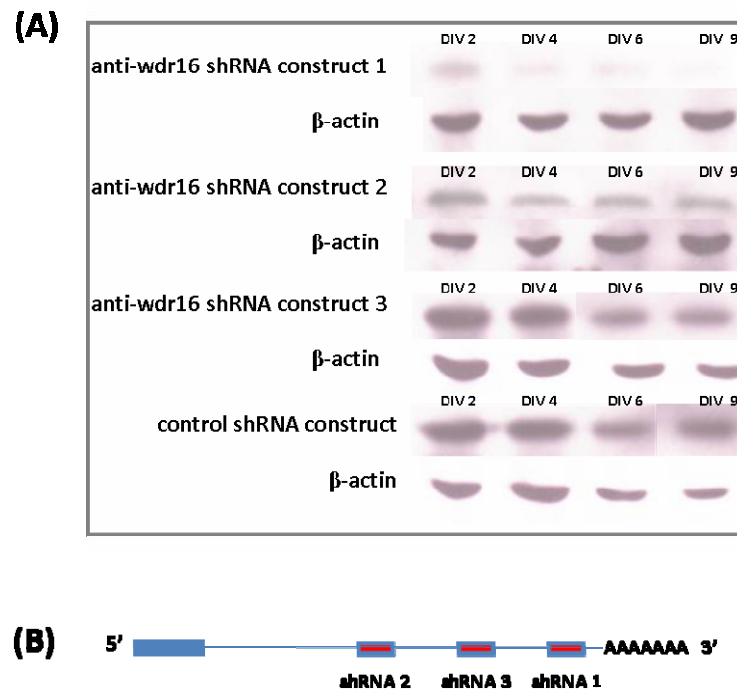


**Fig. 31.** A: Western blot analysis of the effect of different lentiviral anti-wdr16 shRNA constructs, shRNA 1, shRNA 2 and shRNA 3, on wdr16 expression in the HEK-wdr16 cell line. Three constructs targeting Wdr16 and a control shRNA (the sequence of which is not present in the EST database at the NCBI, Bethesda, USA) were tested. Transfected HEK-wdr16 cells were collected on DIV 2, 4, 6 and 9, washed once with phosphate buffered saline (PBS), lysed in cold dH<sub>2</sub>O and stored frozen at -20°C. Each lane of the denaturing 10% polyacrylamide gel was loaded with 20 µg of protein from the different HEK-wdr16 cell homogenates. The proteins from each sample were separated by SDS-PAGE and transferred to a nitrocellulose membrane by electroblotting. The blotting membrane was then probed for 1 hour with guinea pig Wdr16 antiserum diluted 1:10,000. The secondary antibody was donkey-anti guinea pig IgG-peroxidase conjugate diluted 1:120,000 (incubation time 1 h). Detection was performed with an enhanced chemiluminescence system. B visualises the positions of the different shRNA targets in the wdr16 mRNA.

### 2.6.12.3. Analysis of the effect of different anti-wdr16 shRNAs on ependymal primary cultures

Application of different anti-wdr16 shRNAs to the cells of the HEK-wdr16 line showed that the anti-wdr16 shRNA construct 1 is efficient in silencing wdr16 (Fig. 31). In order to confirm the efficiency of this shRNA construct on kinociliated cells, EPC were virally transfected with it on DIV 1 (30 ng of HIV-I p24/well) and the cultures were maintained until

they were collected on DIV 13. Western blot analysis indeed confirmed that also in EPC the anti-wdr16 shRNA construct 1 downregulates wdr16 expression (Fig. 32 A).

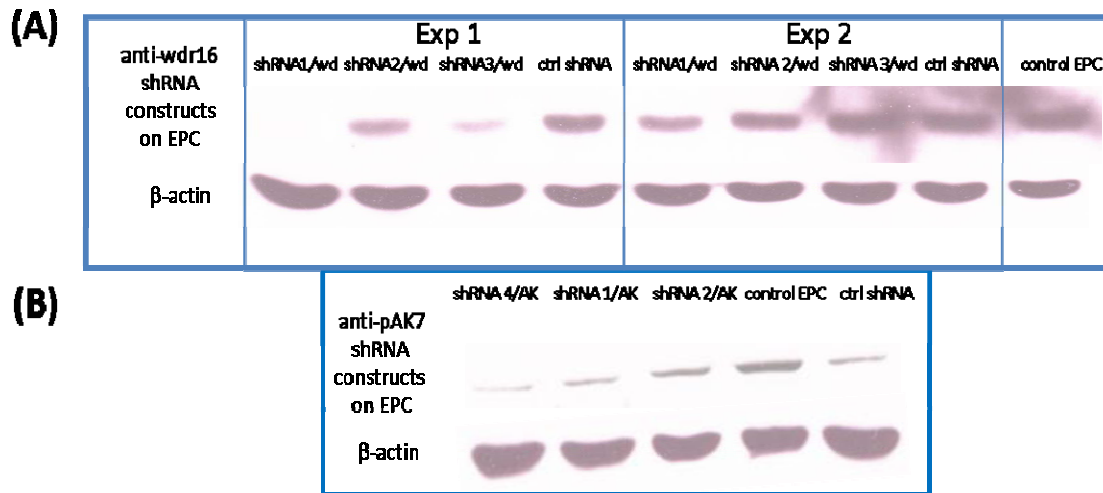


**Fig. 32.** Western blot analysis of the effect of different lentiviral anti-wdr16 and anti-pAK7 shRNA constructs, shRNA 1, shRNA 2, shRNA 3, shRNA 4 and control shRNA on wdr16 and pAK7 expression in EPCs. The shRNAs shRNA1/wd, shRNA2/wd and shRNA3/wd denote the shRNAs targeting wdr16 mRNA where as shRNA1/AK, shRNA2/AK and shRNA4/AK denote the shRNAs targeting pAK7 mRNA. Three constructs each targeting wdr16 or pAK7 (another novel kinocilia-related protein), respectively, and a control shRNA (the sequence of which is not present in the EST database at the NCBI, Bethesda, USA) were tested. On DIV 1, EPCs were infected with the respective viruses (30 ng of HIV-1 p24/well) and maintained until DIV 13. On DIV 13, the cells were collected by trypsinisation, washed once with PBS, lysed in cold ddH<sub>2</sub>O and stored frozen at -20°C. The proteins from each sample were separated by SDS-PAGE and transferred to a nitrocellulose membrane by electroblotting. Each lane of the denaturing 10% polyacrylamide gel was loaded with 20 µg of protein from the different cell homogenates. In the case of Wdr16, the blotting membrane was probed for 1 h with guinea pig Wdr16 antiserum diluted 1:10,000. The secondary antibody was donkey-anti guinea pig IgG-peroxidase conjugate diluted 1:120,000 (incubation time 1 h). In the case of pAK7, the blotting membrane was probed overnight at 4°C with rabbit antiserum diluted 1:5,000. The secondary antibody was anti-rabbit IgG-peroxidase conjugate diluted 1:120,000 (incubation time 1 h). Detection was performed with an enhanced chemiluminescence system. For Exp 2 in A and in the experiment depicted in B, dishes from one and the same EPC were used on the same day. One and the same control (ctrl) shRNA virus preparation was used in all cases. However, Exp 1 in A was conducted 2 weeks after Exp 2 in A and the experiment depicted in B. At the time Exp 1 in A was performed, the experiment depicted in B was also repeated. The result was exactly the same as shown in B and is therefore not shown.

However, the degree of gene knockdown varies considerably between individual experiments (cf. Exp 1 and Exp 2 in Fig. 32 A). Additionally, there is evidence that even the control shRNA virus may be deleterious to EPC, as shown in Fig 32 B, in which such a control virus is compared with other viruses bearing shRNA constructs targeted toward the knockdown of another kinocilia-specific gene, pAK7 (Frommer, 2003). Inexplicably, no such

deleterious effect was observed in two independent experiments with the very same control virus (Exp 1 and Exp 2 in Fig. 32 A), though one of those experiments (Exp 2 in Fig. 32 A) was even performed on the same day the experiment demonstrating the deleterious effect (Fig. 32 B) was done, and culture dishes from the same EPC were used.

### 2.6.13. Transfection of HepG2 cells with HIV/VSV-G/GFP under the control of the *wdr16* promoter

The human ortholog of *wdr16* has previously been shown to be present in the hepatocellular carcinoma cell line, HepG2 (Silva et al., 2005). This was also confirmed at the protein level by Hirschner (2007), who successfully used a Wdr16 antiserum in Western blot analysis of HepG2 homogenates.

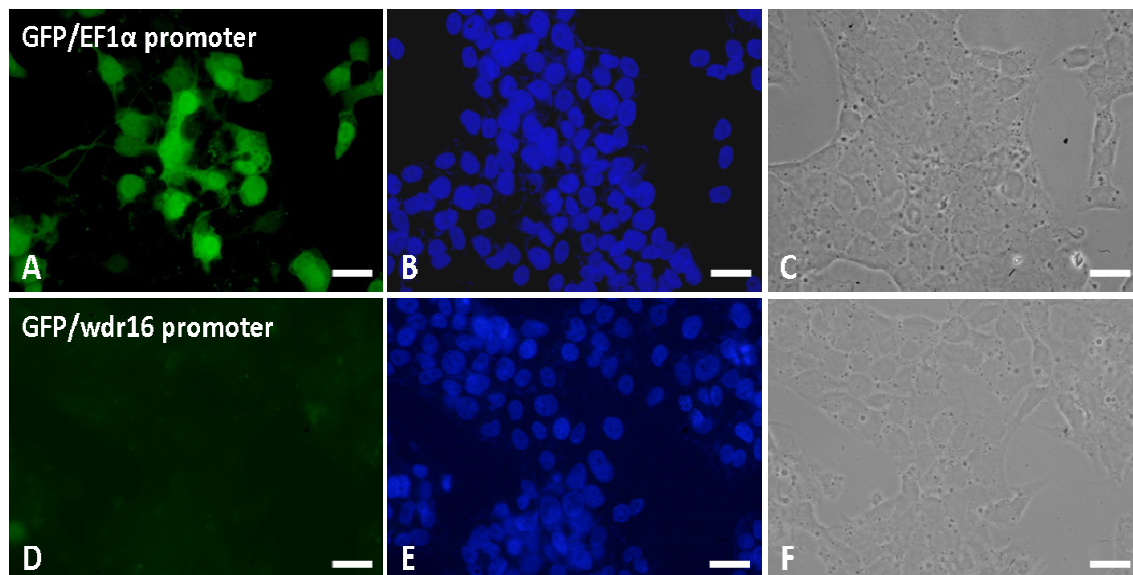


**Fig. 33.** HepG2 cells transfected with lentiviruses bearing the GFP ORF as a marker under the control of the EF1 $\alpha$  promoter or the *wdr16* promoter. A: HepG2 cells transfected with HIV/VSV-G/EF1 $\alpha$ /GFP show expression of GFP. B: Nuclei are counterstained with 4',6-diamidino-2-phenylindole. C: A phase contrast view of the transfected area. D: HepG2 cells transfected with HIV/VSV-G/GFP-*wdr16* promoter do not express GFP. E: The nuclei are counterstained with 4',6-diamidino-2-phenylindole. F: A phase contrast view of HepG2 cells. Scale bars: 20  $\mu$ m.

In the present study, transfection of HepG2 cells with lentivirus encoding GFP under the control of the EF1 $\alpha$  promoter resulted in the expression of GFP in these cells. In contrast,

transfection of HepG2 cells with lentivirus encoding GFP under the control of the wdr16 promoter failed to result in GFP expression (Fig. 33), indicating that the Wdr16 protein present in HepG2 cells does not arise from the wdr16 gene under the control of its own promoter. Instead, a genetic recombination event connected to the transformation of these cells into a cancerous cell line may have put wdr16 behind a completely different promoter.

## **3. Discussion**

### **3.1. Quality of the employed subtractive ependymal cDNA libraries**

Screening of the subtractive ependymal and SCO cDNA libraries that had been prepared for the identification of ependyma-specific transcripts by exploiting the principle of suppression subtractive hybridization (Diatchenko et al., 1996) yielded, among others, clones encoding previously known kinocilia-related transcripts like those for axonemal dynein intermediate chain 1, Spag6 and wdr16. Axonemal dyneins are the motors of eukaryotic kinocilia and flagella, and mutations in their genes may cause situs inversus and primary ciliary dyskinesia (Guichard et al., 2001). Spag6 is a constituent of the kinocilia central apparatus and can therefore be regarded as a kinocilia marker (Sapiro et al., 2000). Wdr16 is a marker protein for kinocilia-bearing cells and abundantly expressed in testis and cultured ependymal cells (Hirschner et al., 2007). Since ependymal cells are the only kinocilia-bearing cell type of the brain, the finding of transcripts specifically related to kinocilia confirms the high quality of the employed subtractive cDNA libraries and suggests them as effective tools for finding genes that are specifically expressed in ependymal cells.

### **3.2. E71 and the occurrence of coiled-coil proteins in ciliated cells**

Coiled-coil domains are characterised by heptad repeats forming an amphipathic alpha helix and are present in a number of functionally diverse proteins. Hydrophobic interactions between coiled-coil domains result in stable protein-protein interactions (Beck and Brodsky, 1998) and may lead to the formation of stable polymers, as exemplified by intermediate filaments, collagen fibers, and the tail domain of myosin heavy chains. Most commonly, coiled-coil domains mediate homodimer and heterodimer formation (Lupas, 1996). The striated ciliary rootlet is a prominent cytoskeletal element originating from the basal body at

the proximal end of a cilium. Rootletin, the structural component of the ciliary rootlet, is a large protein composed almost entirely of coiled-coil domains (Yang et al., 2002). For another example, the *Chlamydomonas reinhardtii* ODA3 gene encodes a protein which is essential for the assembly of both the outer dynein arm (ODA) and the ODA docking complex (ODA-DC) onto flagellar doublet microtubules. The secondary structure of the ODA3 gene product is predicted to contain regions of extended  $\alpha$ -helix with a strong propensity to form coiled-coil structures (Koutoulis et al., 1997). Furthermore, in *Chlamydomonas*, the MBO2 locus encodes a conserved coiled-coil protein important for flagellar waveform conversion that plays a role in the regulation of the force-generation machinery during the ciliary beat (Tam and Lefebvre, 2002). These examples emphasise the structural and functional importance of coiled-coil proteins in kinocilia. The identification of clones corresponding to the novel putative coiled-coil protein of approximately 110 kDa, E71, in the present screening and the high transcription rate of its gene in testes and cultured ependymal cells are consistent with a specific role of E71 in ciliated cells.

### **3.3. Transfection of ciliated epithelial cells**

#### **3.3.1. Nonviral vector-mediated gene transfer**

The author is not aware of any previous attempts to facilitate gene transfer to ependymal cells in primary culture. In the absence from the literature of information about gene transfer to cultured ependymal cells, something may be learned from kinociliated airway epithelial cells as a model for the difficulty of transfecting kinociliated cells in culture. The failure of different transfection methods involving naked plasmid DNA to work on differentiated or undifferentiated EPC was not completely unexpected in view of the following literature reports about attempted transfections of cultured airway epithelial cells. The complete resistance of the ependymal cells toward gene transfer with nonviral vector-mediated methods may have several reasons. Cationic lipids are known to deliver genes quite efficiently into some cell lines and primary culture cells of certain tissues. Nevertheless, their *in vitro* transfection efficiency is low in well-differentiated airway cells (Fajac et al., 2003). This is partially explainable by the absence of membrane lectins known

to be required for the uptake of plasmid DNA in complex with cationic polymers like polyethylenimine (PEI, brand name “jetPEI”). In addition, impaired intracellular trafficking of the plasmid DNA / polymer complexes has also been suggested as an explanation for the poor transfection efficiency in differentiated airway epithelial cells (Fajac et al., 2003). Likewise, treatment of differentiated primary cultures of human ciliated airway epithelial cells with DNA-lipid complexes generated only low levels of transgene expression. In comparison, immature human airway epithelial cells immediately after seeding exhibited a significantly improved transfectability (Fasbender et al., 1997), suggesting a role of mitosis in cationic or lipid-mediated gene transfer (Oudrhiri et al., 1997). Indeed, it has been reported that the epithelia of intact rabbit trachea and of ciliated human airways *in vitro* are always resistant to cationic lipid-mediated gene transfer, emphasising that the transfected DNA does not easily enter the nuclear compartment during interphase (Fasbender et al., 1997). Also during liposome-mediated gene transfer, liposome-DNA complexes enter the cell via phagocytosis, and entry across the nuclear membrane rather than across the plasma membrane is one of the rate-limiting steps and accounts for the poor transfectability of undifferentiated cells (Zabner et al., 1995). In contrast, absence of the phagocytosis internalization pathway mainly decreases the transfection efficiency in differentiated epithelial cells (Matsui et al., 1997). PEI is a cationic polymer that enters the cell through nonspecific endocytosis and is able to disrupt endosomal membranes to release plasmid DNA into the cytosol (Boussif et al., 1995). It also promotes transgene delivery from the cytoplasm to the nucleus in mammalian cells (Pollard et al., 1998). However, gene transfer efficiency is reportedly lower in differentiated cells than in poorly differentiated cells (Fajac et al., 2003). This would explain the difficulties of gene transfer to differentiated, kinocilia-bearing ependymocytes and warranting the use of more efficient gene transfer methods.

### **3.3.2. Lentiviral vector-mediated gene transfer**

Vectors derived from human immunodeficiency virus (HIV) infect dividing and non-dividing cells, including neurons (Blomer et al., 1997). The ability of HIV-1 to replicate in non-dividing cells is partly accounted for by the karyophilic properties of the viral preintegration complex which, after virus infection, is actively transported to the host cell nucleus. The gag-derived

matrix protein of HIV-1 contains a nuclear localisation sequence which directs its nuclear import (Bukrinsky et al., 1993). Lentiviral vectors produce long-term transgene expression when introduced into the brain parenchyma or ventricles (Davidson and Breakefield, 2003). Lentiviral vectors pseudotyped with the Ebola-Zaire (Ebola-Z) glycoprotein efficiently transduce lung epithelial cells (Kobinger et al., 2001). This prompted the attempt to optimize the lentiviral transduction of ependymal cells in primary culture by using an Ebola-Z pseudotype. This approach did not lead to the desired improvement. On the contrary, almost no transfection of cells in the EPC was observed even when virus to the equivalent of very high p24 concentrations (6 µg p24/ml) was employed. The major factor preventing the successful employment of an Ebola-Z pseudotype was most probably the low titer of the corresponding virus preparations. This titer could not be increased by adjusting the conditions of virus production, e.g. by variation of the amounts of the various plasmids transfected into the production cells. The low titers of the Ebola-Z pseudotypes required the application of excessive amounts of p24 to the target EPC in order to achieve the necessary number of TU. Perhaps, the considerable number of defective viral particles indicated by this high amount of p24 had an additional detrimental effect on the cultures on top of the one already to be expected by the presence of the Ebola-Z envelope protein with its known cytotoxicity. Furthermore, the analogy between ependymal cells and airway epithelial cells may not go as far as originally anticipated when the decision was made to use Ebola-Z pseudotypes. Ependymal cells are neural cells, and it is well known that certain cell types of the mouse CNS are not permissive for Ebola-Z-mediated lentiviral transduction. This includes cells of the thalamus, hippocampus, and corpus callosum, as well as primary cultures of hippocampal neurons, astrocytes and oligodendrocytes at either the precursor or differentiated stages of maturation (Watson et al., 2002).

In contrast, lentiviral vectors pseudotyped with VSV-G envelope transduce airway epithelia efficiently, with the majority of the cells transduced being respiratory ciliated cells (Kremer et al., 2007). Similarly, transduction of the neonatal ventricular system of mouse with lentivirus pseudotyped with VSV-G glycoprotein mediates long-term gene expression and mostly affects the ependymal layer and the choroid plexus, indicating that VSV-G-pseudotyped lentiviral vectors are not principally unsuitable for gene delivery to ependymal cells (Watson et al., 2005). In view of the results obtained with the Ebola-Z pseudotype



which were by no means superior to those achievable by the employment of VSV-G pseudotypes, further experiments with the Filovirus envelope protein were discouraged.

The experiments conducted with lentiviral vectors pseudotyped by the Rabies or the Mokola virus envelope protein, respectively, yielded results as unsatisfactory as those from the Ebola-Z pseudotype. Again the problem was to obtain significant titers at a given amount of p24 in the respective viral preparations. It must be assumed that the viral envelope proteins of Ebola-Z, Rabies and Mokola all interfere with the production of infectious viral particles. A high percentage of those viral particles which are indeed produced appear to be defective. At least the Ebola-Z envelope glycoprotein is known to be highly toxic to cells (Yang et al., 2000). Therefore, it is conceivable that its expression is somehow downregulated in the virus-producing cells of the HEK293T line, possibly preventing proper membrane enclosure and budding of viral particles. Alternatively, viral particles with too few envelope proteins in their membrane may be produced, leading to the inability of such particles to properly bind to the cells they are supposed to infect.

### **3.4. Titration of lentiviral vectors**

A plot of the amount of virus added to the cell cultures in terms different volumes of viral stock solution ( $V_v$ ) against the MOI ( $-\ln(1-P)$ ) did not yield a straight line (see Results 2.6.2. and Methods 4.2.4.). One possible explanation for this would be a positive effect of viral infection on the proliferation rate of the HEK293T cells employed for the titration. If the proliferation rate of the virally infected cells and the non-infected cells were the same, then there should not be any difference in the ratio between GFP expressing cells and non-infected cells after several cell divisions, as all cells multiply at the same rate. An increase in the proliferation rate of the virus-infected cells above that of the uninfected cells would cause a deviation from linearity. Another possible explanation would be that there is a concentration-dependent progressive aggregation of viral particles causing a deviation from linearity.

### 3.5. Lentiviral vector-mediated gene transfer to ependymal cells in primary culture

Transfection of undifferentiated as well as differentiated EPC with lentiviral vectors produced by a second-generation packaging system (Zufferey et al., 1997), pseudotyped with the VSV-G envelope protein (Burns et al., 1993) and bearing GFP as a marker, resulted in a tremendous increase in transfection efficiencies compared to the use of plasmid. The enhancement amounted to a factor of 75 with respect to undifferentiated primary cultures and by a factor of 20 with respect to differentiated primary cultures. This difference in the transfection efficiency is similar to the one reported in a study about usage of VSV-G-pseudotyped lentiviral vectors on airway epithelial cells. Undifferentiated airway epithelia were efficiently transduced, but the well-differentiated pseudostratified columnar epithelium of mature human bronchial xenografts was largely resistant (Goldman et al., 1997). The reduction in transfection efficiencies accompanying the differentiation of EPC may be attributable to the inaccessibility to the virus of the basolateral surface of the differentiated ependymal cells in their epithelial formation. This idea derives support from the observation that apical application of vector to polarized, well differentiated human airway epithelial cells in culture leads to minimal levels of transgene expression, whereas basolateral application of vector enhances the levels of transduction approximately 30-fold (Johnson et al., 2000). According to the literature, direct *in vivo* delivery of HIV vectors to the nasal epithelium and trachea of mice failed to mediate gene transfer, but pretreatment with sulphur dioxide before vector delivery enhanced gene transfer efficiency to the nasal epithelium of both mice and rats, suggesting that injury-increased access of vector to the basolateral membrane of airway surface epithelial cells boosts transfection rates (Johnson et al., 2000).

Even though the use of lentiviral vectors in the present project increased the transfection efficiencies with respect to undifferentiated EPC to a level of 75%, the transfection efficiency with respect to ciliated cells generally was < 5%, and it was even below 1% when differentiated primary cultures were used for the transfection. This decrease in the efficiency of transfection of ciliated cells concomitant with their differentiation could be due to the inaccessibility of their basolateral surface to the viral particles. Alternatively, *cis-*

acting elements within the vector, i.e. the chosen promoter and other vector sequences, might negatively affect the level of *in vitro* persistence of transgene expression (Johnson et al., 2000). One possibility here would be promoter attenuation through poorly defined mechanisms (Gill et al., 2001). Treatment of cells with gene transfer vectors may induce cytokine production, and these cytokines, possibly including interferon gamma (IFN- $\gamma$ ) and tumour necrosis factor alpha (TNF- $\alpha$ ), could inhibit transgene expression from certain widely used viral promoters/enhancers and may also inhibit total cellular protein synthesis (Qin et al., 1997). The elimination/killing of transfected ciliated cells, possibly by cytokines that may be released upon viral infection in the EPC, is likely, since the total number of ciliated cells decreases significantly after exposure to virus.

### 3.6. Effect of lentivirus on the ependymal primary cultures

Transfection of EPC with lentiviral vectors generally resulted not only in higher transfection efficiencies as compared to plasmid-based methods, but also in the loss of ciliated cells from the primary cultures. In the case of two shRNA virus preparations (Fig. 32, ctrl shRNA and shRNA 3), contradictory results were obtained. One and the same virus preparation, applied in the same amount, had a deleterious effect on one EPC, whereas another EPC was not negatively affected, as judged from a Western blot that shows the same levels of the kinocilia-related protein, Wdr16, in the lanes of virus-treated and untreated cultures (Fig. 32, cf. lanes ctrl shRNA and shRNA 3/wd). As described in 2.6.12.3., two independent experiments with the shRNA control virus preparation resulted in deleterious effects on the respective EPC, which is in accord with the observations concerning virus preparations bearing the ORF of GFP under the control of the EF1 $\alpha$  promoter (see Figs. 14, 15). It is difficult to conceive why this harmful effect was not detected in the two experiments depicted in Fig. 32 A. All that can be said presently is that more experiments point to a deleterious effect of lentiviruses encoding genes under the control of the EF1 $\alpha$  promoter than to the lack of such a negative effect. In those normal cases of an adverse effect of virus, transfection of undifferentiated or differentiated EPC with HIV/VSV-G decreased the total number of ciliated cells to 50% of the control values, irrespective of the concentration of virus applied.

A negative effect of virus treatment on kinocilia-bearing cells has also been described in other systems. For example, kinociliated airway epithelial cells are lost upon exposure toward certain respiratory viruses like paramyxoviruses (eg, parainfluenza and respiratory syncytial virus) in domestic animals and rodents (Bryson et al., 1983; Massion et al., 1993). Furthermore, influenza A virus infection has been shown to result in loss of kinociliated cells from the eustachian tube of guinea pigs (Ohashi et al., 1991), as well as in the loss of characteristic cuboidal shape and cilia in ependymal organ cultures (Kohn et al., 1981). Infection of primary human bronchial epithelial cell cultures with respiratory syncytial virus entails a marked loss of cilia and ciliated cells, suggesting a direct virus effect (Tristram et al., 1998). The forkhead transcription factor (hepatocyte nuclear factor-3/forkhead homologue 4; HFH-4) HFH-4/FOXJ1, expressed in later stages of epithelial cell differentiation, is a known regulator of ciliogenesis (Blatt et al., 1999; Brody et al., 2000). In mice, inflammatory bronchitis induced by Sendai virus (SdV), is associated with a decrease in FOXJ1 expression, showing the susceptibility of kinocilia and kinociliated cells to direct viral injury (Look et al., 2001). In the case of the ependyma, SdV infection leads to partial or complete necrosis of the ependymal layer (Mims and Murphy, 1973). The decrease in the number of cilia after virus infection may thus in principle be due to either impaired ciliogenesis, perhaps due to a direct effect of virus on FOXJ1 expression, direct cilia loss due to the virus interfering with cellular mechanisms needed for cilia maintenance, or death of ciliated cells (Look et al., 2001). In mice, intracerebroventricular injection of lentiviral tat protein in low nanomolar quantities is sufficient to induce an inflammation and kill ependymal cells (Philippon et al., 1994; Carbonell et al., 2005). The cytotoxicity of the VSV-G protein and the envelope of VSV-G-pseudotyped HIV has been shown in different mammalian cells (Burns et al., 1993; Beyer et al., 2002; Zhang et al., 2004; Qiao et al., 2006). Accordingly, necrosis of ependymal cells has been described in deer mice infected with VSV (Cornish et al., 2001). Therefore, the direct killing of ciliated cells by HIV/VSV-G has to be considered an important mechanism of cilia loss in the EPC paradigm.

Nevertheless, the situation may be further aggravated by cytokines released after viral infection, which are known to potentially alter epithelial cell differentiation and change the phenotype of epithelial cells (Saunders et al., 1994; Tristram et al., 1998; Thomas et al., 2000). Furthermore, virus-infected cells may be subject to changes in gene expression

connected to the random genomic integration of lentivirus. This may interrupt biochemical pathways of cell differentiation, possibly resulting in impaired ciliogenesis or loss of cilia. Alternatively, this effect could result from transgenes overexpressed in ciliated cells after viral infection. Perhaps virus-infected ependymal cells can also undergo transdifferentiation as observed for ciliated respiratory epithelial cells in models of diseases such as acute asthma or viral infection (Reader et al., 2003; Tyner et al., 2006).

### **3.7. Expression of transgenes in ciliated cells using ciliated cell-specific promoters**

Even though lentiviral vector-mediated gene transfer to ependymal cells in primary culture was shown to be quite efficient, only < 5% of the ciliated cells were transfected by HIV/VSV-G bearing the EF1 $\alpha$  promoter, and especially kinociliated cells in clusters of transfected cells were often observed to be devoid of transgene expression, raising questions about the viability of the method for achieving high levels of gene transfer to ependymal cells. The use of cell-specific transcription regulatory elements appeared as a venue to possibly increase the strength and persistence of transgene expression, since it is well known that some viral promoters are inactivated in transduced cells after a certain time (Loser et al., 1998). This, in combination with the possible deleterious effect of early transgene expression on the differentiation of ependymal cells (see above), prompted the use of promoters specific for kinocilia-bearing cells.

#### **3.7.1. The FOXJ1 promoter**

FOXJ1 is a member of the forkhead/winged helix family of transcription factors the expression of which is tightly restricted to cells possessing motile cilia or flagella (Hackett et al., 1995; Lim et al., 1997; Blatt et al., 1999). A 5' fragment of the human FOXJ1 gene was reportedly capable of driving expression of a reporter gene specifically in the ciliated cells of well-differentiated human bronchial epithelial cultures. Transgenic mice with this 1.0-kb fragment of the FOXJ1 promoter region inserted in front of an EGFP expression cassette demonstrated strong EGFP expression in the ciliated cells of the tracheal, bronchial and

nasal epithelium of the respiratory tract. EGFP fluorescence was also observed in ciliated ependymal cells lining the ventricles of the brain, the ciliated epithelium of the oviduct and the developing sperm in the testis (Ostrowski et al., 2003), showing the specificity of the FOXJ1 promoter for kinociliated cells. Transfection of the EPC with lentivirus encoding GFP under the control of the FOXJ1 promoter resulted in the productive transfection of 15% of the kinociliated cells, which was at least a 3-fold increase over the percentage obtained with the EF1 $\alpha$  promoter. The remaining nonciliated transgene-expressing cells in the primary cultures may have been ependymal precursor cells yet without surface cilia, as it is known from the literature that the FOXJ1 promoter is able to drive transgene expression not only in ciliated cells, but also in their precursors (Rawlins et al., 2007).

### **3.7.2. The wdr16 promoter, a novel ciliated cell-specific promoter**

Wdr16, a differentiation marker of kinocilia-bearing cells, is up-regulated concomitantly with kinocilia formation in testis, ependyma and respiratory epithelium. In different species, the genes orthologous to wdr16 are always found in “head to head” orientation with respect to the syntaxin 8 genes on their respective chromosomes (Hirschner et al., 2007). In the rat genome, the distance between syntaxin 8 and wdr16 is only 0.7 kb, and the wdr16 core promoter region can be assumed to be present in this 0.7 kb stretch. In order to probe the possibility of using it for driving transgene expression specifically in kinocilia-bearing cells, a lentiviral vector was generated with the 0.7 kb fragment in front of the GFP ORF. Transfection of the EPC with this lentivirus resulted in the expression of GFP in a pattern similar to that observed with the FOXJ1 promoter, i.e., almost exclusively in kinociliated cells. The total transfection efficiency in the EPCs was 25%, where 15% fell on kinociliated cells and 10% on cells without kinocilia. Thus, the specificity of the wdr16 promoter for kinociliated cells is comparable to that of the FOXJ1 promoter.

### **3.7.3. Specificity of the FOXJ1 and wdr16 promoters**

The loss of ciliated cells observed in EPC upon treatment with lentiviral vectors encoding GFP under the control of the EF1 $\alpha$  promoter was not observed after transfection with lentivirus containing either the FOXJ1 or the wdr16 promoter. It may be concluded that the EF1 $\alpha$  promoter-driven overexpression of transgenes in undifferentiated EPC may interfere with the process of ciliogenesis. The use of the FOXJ1 or the wdr16 promoter appears to preclude this.

Transfection of EPCs with lentivirus encoding GFP under the control of the EF1 $\alpha$  promoter resulted in the transfection of some monociliated cells. This was not observed when either the FOXJ1 or the wdr16 promoter was used. FOXJ1 is expressed in tissues containing kinocilia, such as testis, oviduct, lung, brain (Gurok et al., 2004), and in the embryonic node with its unique 9+0 kinocilia, but not in tissues that contain only primary cilia (Brody et al., 2000). FOXJ1 (Hfh-4)-null mice have randomized left/right asymmetry of the body axis due to an unresolved defect connected to the embryonal node and completely lack 9+2 kinocilia (Brody et al., 2000). This shows the specific importance of FOXJ1 for the generation, and maybe the maintenance of kinocilia. Wdr16 expression is specifically restricted to kinocilia-bearing cells (Hirschner et al., 2007), and the results obtained with the wdr16 promoter in the present study are highly similar to those reported here and by others (Brody et al., 2000), with the FOXJ1 promoter further demonstrating that Wdr16 is a protein only present in kinocilia-bearing cells. Although the specificity of the human FOXJ1 and the rat wdr16 promoters in driving transgene expression in kinocilia-bearing cells of EPC from mice and rat is shown in this thesis, the ability of the wdr16 promoter to direct transgene expression in human kinociliated cells remain to be studied.

### **3.8. Integration of proviral DNA**

In the EPCs, transfection efficiency in kinociliated cells decreases by a factor of four with the differentiation of the cultures. Nevertheless, the integrated proviral DNA was found, by nested PCR, in the genomic DNA of both the DIV 1 infected undifferentiated as well as the

DIV 6 infected cultures after viral treatment. The very low number of transfected kinocilia-bearing cells in EPC that were treated with virus after their differentiation (Fig. 12) indicates a predominant genomic establishment of the provirus in non-ciliated cells. Unfortunately, the nested PCR protocol employed for provirus detection did not allow the quantitation of HIV in the genome of the EPC. It is therefore not possible to judge whether all integrated proviruses were able to drive reporter gene (GFP) expression, or if GFP transcription was attenuated in kinociliated cells (see 1.8).

### **3.9. Expression of Wdr16 in the hepatocarcinoma cell line HepG2**

Wdr16 has been reported to be present in and to increase the proliferation rates of cells from the hepatocellular carcinoma line HepG2 (Silva et al., 2005). This appears to be at odds with the known specificity of Wdr16 for differentiated kinocilia-bearing cells. While a Western blot analysis has confirmed the expression of Wdr16 in HepG2 cells, their transfection with lentivirus encoding GFP under the control of the wdr16 promoter failed to result in GFP expression, warranting the assumption that the wdr16 gene has come under the control of a different regulator of transcription during the tumorigenic transformation event or thereafter.

### **3.10. Effect of apoptosis inhibitors on virus-infected EPC**

Apoptosis is an important physiological process for host defence against viral infection (Evan and Littlewood, 1998). A virus infection may thus result in apoptosis (Thompson, 1995), and this effect is likely to contribute to viral pathology (Young et al., 1997). HIV-1 encodes proteins that function to both promote and inhibit apoptotic cell death (Hay and Kannourakis, 2002). Even though many of these proteins are absent from the lentiviral particles used for gene transfer, there still remains the possibility that other viral proteins present in the vector particles (p24, viral protease, integrase) may be causally related to the negative effect of virus treatment on the EPC.



Alternatively, expression of vector-encoded transgenes at inappropriate times during cellular differentiation might also result in apoptotic cell death. Therefore, experiments with an inhibitor of apoptosis were conducted in hopes of improving the results of lentiviral transfection of EPC. In accord with the already discussed sensitivity of kinocilia-bearing cells, treatment of the EPC with the AI, NS3694, resulted in a clear decrease in the total number of ciliated cells, even in the absence of virus. This could be explained by an increase in the proportion of other contaminating cells during the differentiation of the culture, caused by the presence of the AI. Since during the experimental work for this thesis the impression had developed that the vulnerability of the cultures toward detrimental agents was highest immediately after seeding, NS3694 was applied no sooner than 48 h after seeding and up to 15 h after first exposure to virus. Based on reports from the literature (Cooray et al., 2003), it was assumed that this timing of the application of the AI would be adequate to still prevent virally induced apoptosis, should it be triggered. The cytopathic effect of HIV infection has been shown to occur no earlier than 24 h after infection (Lenardo et al., 2002) and to not be dependent on the VSV-G envelope protein frequently used for pseudotyping (Lenardo et al., 2002). Furthermore, there is evidence that virally induced apoptosis does not commence until 48 h after infection (Cooray et al., 2003). Unfortunately, NS3694 was not capable of preventing the decrease in the total number of ciliated cells routinely observed upon treatment of EPC with HIV/VSV-G. There was no significant difference in the transfection efficiencies between the EPC infected with virus and those infected and treated with the AI. These results are consistent with the assumption that cell death and decrease in total number of ciliated cells in virus-infected EPC is not due to apoptosis, or, specifically to apoptosome-mediated caspase activation. They are further in accord with reports that point to a necrotic, rather than an apoptotic mechanism of viral cytopathogeny (Cooray et al., 2003).

### **3.11. Wdr16 silencing in ependymal primary culture**

Lentiviruses encoding different anti-wdr16 shRNAs were tested on the wdr16-HEK cell line and on EPC. It was shown that anti-wdr16 shRNA construct 1 is most efficient in silencing wdr16. At the same time, the control shRNA was observed to cause a significant decrease in

the expression of the kinocilia marker, pAK7. This decrease in pAK7 protein may be attributed to either the continuous expression of control shRNA from the H1 promoter or the continuous expression of GFP under the control of the EF1 $\alpha$  promoter. In the present lentivirus-based shRNA system, shRNAs were expressed under the control of the H1 RNA polymerase-III (Pol III) promoter, which is active in all tissues and efficiently directs synthesis of hairpin RNA with a 21 nucleotide long double stranded stretch in cultured mammalian cells (Brummelkamp et al., 2002). However, overexpression of shRNA in mammalian cells may be toxic, as it may lead to degradation of partially complementary off-target mRNAs and also induce interferon responses (Sledz et al., 2003; Jackson and Linsley, 2004; Grimm et al., 2006). Since the shRNA vector constructs also encode GFP under the control of the EF1 $\alpha$  promoter, overexpression of this transgene, which is normally not present in the ependymal cells, may also interfere with their differentiation process. Therefore, in future research, it may be worthwhile to employ cell type-specific Pol II promoters in front of the shRNA cassette. This may provide the opportunity for conditional synthesis of shRNAs (Shinagawa and Ishii, 2003; Rao et al., 2006; Rao and Wilkinson, 2006; Wiznerowicz et al., 2006). It may further be necessary to replace the EF1 $\alpha$  promoter by kinocilia-specific promoters like the ones of FOXJ1 or wdr16 to prevent the expression of GFP until the onset of differentiation of primary cultures.

### **3.12. Localisation of cilia-specific, GFP-tagged proteins**

Transfection of EPC with HIV/VSV-G/EF1 $\alpha$ /Wdr16-GFP resulted in the localisation of the GFP fusion protein to the cytoplasm of ciliated cells, which is in agreement with the localisation of Wdr16 in kinocilia-bearing cells visualised by immunostaining (Hirschner et al., 2007). Transfection of EPC with HIV/VSV-G/EF1 $\alpha$ /pAK7-GFP also resulted in a cytoplasmic localisation of the fusion protein, also in accordance with corresponding immunostaining results (D. Scheible, unpublished results). Transfection of CHO cells with cDNA encoding Spag6, a protein which these cells do not normally contain, resulted in colocalisation of the expressed protein with microtubules surrounding the nucleus (Zhang et al., 2005). Similarly, transfection of HEK293T cells and EPC with HIV/VSV-G/EF1 $\alpha$ /Spag6-GFP also resulted in the

localisation of Spag6 to the microtubule cytoskeleton. Spag6 is known to be located in the axoneme of 9+2 kinocilia. Its appearance in the cytoplasm of the transfected cells, no matter whether they were ciliated or not, is likely to be due to the overexpression of the fusion protein. The failure of the fusion protein to enter the kinocilia may be ascribed to the increased spatial requirements due to the GFP moiety, which are apparently incompatible with the spatial restrictions inside the axoneme. This failure of a known axonemal protein to enter its native compartment when tagged with GFP is noteworthy and should be considered in subsequent localisation studies employing similar strategies.

### 3.13. Outlook

The present work has shown the difficulties of transfecting ependymal cells in primary culture by conventional methods. Even though transfection efficiencies up to 75% were achieved by employing HIV as the vector, the number of transfected kinociliated cells was low and the loss of ciliated cells after virus infection quite substantial. Lentiviral vectors encoding transgenes under the control of promoters specific for kinocilia-bearing cells significantly increased the transfection efficiency.

The characterisation of the *wdr16* promoter region will yield a novel kinocilia cell-specific promoter with a potentially much smaller size than that of the *FOXJ1* promoter.

Studies to identify the transcription factors binding to the *wdr16* promoter region will be useful to further investigate the role of *wdr16* in kinociliated cells.

As it was shown in the HEK-*wdr16* cell line that the anti-*wdr16* shRNA construct 1 resulted in an efficient knockdown of *wdr16* expression, lentiviral vectors bearing the anti-*wdr16* shRNA construct 1 should be tested *in vivo* to analyse the effects of *wdr16* silencing.

Studies on the expression of shRNAs under the control of Pol II promoter would be another approach to further investigate the silencing of *Wdr16* *in vitro* as well as *in vivo*.

Producing a specific antibody against E71 will be useful to show the exclusive synthesis of the E71 protein in kinociliated cells via Western blotting and immunostaining experiments.

## 4. Materials and methods

### 4.1. Materials

#### 4.1.1. Devices

Autoclave	Type 669, Aigner, München Fedegari, Spain Type 5075 ELV, Tuttnauer, Systec
Cameras	Coolpix 995, Nikon, Düsseldorf Canon EOS 350D, Canon, Krefeld
Cell incubator	Type B 5060 EC CO <sub>2</sub> , Heraeus, Hanau Function LINE, Heraeus
Centrifuge	Varifuge K, Heraeus, Hanau Biofuge fresco, Heraeus Multifuge 3 S-R, Heraeus
Containment hood	Lamin Air HLB 2448, TL 2448, Heraeus, Hanau Technoflow 3F150-11GS, Integra Biosciences
Cryosystem	Chronos 80 and liquid N <sub>2</sub> tank Jupiter Colora E-80 Siegtal Cryotherm, Siegen
Drying oven	Type U-30, Memmert, Schwabach
Electroblotting chamber	Bio-Rad, München
Electrophoresis chamber	For agarose gels: Model B1 (110 mm x 90 mm), Owl separation systems, USA For polyacrylamide gels: Bio-Rad, München
Gel documentation system	Mitsubishi, Japan
Heating block	Grant QBT, CLF Laborgeräte, Emersacker
Hybridisation oven	Biometra, Göttingen

LightCycler®	Roche, Mannheim
Magnetic stirrer	IKAMAG RCT, Bachofer, Reutlingen
Microplate reader	Titertec Plus MS 212, connected to a PC running the EIA3 software by ICN, Meckenheim
Microscopes	Model IM, IM 35 and Axiovision 2, Zeiss, Oberkochen Axiovert 25, Nikon, Jena
Microwave oven	Micro-Chef FM 3915 Q, Moulinex
Osmometer	Osmometer Automatic, Knauer, Eppelheim
PCR Thermocycler	Primus 96 plus, MWG AG Biotech, Ebersberg
pH-meter	PHM 92, Radiometer, Copenhagen, Denmark
Pipettors	Finn pipettors (5-40 µl, 40-200 µl, 200-1000 µl), Labsystems, Finland Eppendorf pipettors (0.5-10 µl, 10-100 µl, 200-1000 µl), Eppendorf, Hamburg Multichannel pipettor Titerman, Eppendorf, Hamburg
Power supply	Consort E 132, BioBlock Scientific, Illkirch, France 2301 Macrodrive 1, LKB Bromma, Vienna, Austria Power Supply Model 200, Bethesda Research Laboratories, Life Technologies, Inc., USA Computer Controlled Electrophoresis Power Supply Model 3000 X, Bio Rad, München
Rotor for Ultracentrifugation	Type 70 Ti, Beckman-Coulter
Scales	Type 1403 and L2205, Sartorius, Göttingen

SDS-PAGE device	Ready Gel Cell, Bio-Rad, München
Shaker	Vortex Genie, Bender & Hobein, München
Shaking platform	Horizontal-Schüttelplattform KL2, Bühler, Tübingen
Sonifier	Branson B-30 with microtip, Heinemann, Schwäbisch Gmünd
Spectrophotometers	Uvikon 860 with Plotter 800, Kontron, Eching
Table top centrifuge	Centrifuge 5415 C, Eppendorf, Hamburg
Tissue homogeniser	Potter-Elvehjem homogeniser, Braun, Melsungen
Ultracentrifuge	Optima L-80, Beckman-Coulter
UV transilluminator	UVP from San Gabriel, CA, USA
Vacuum filter device	Sterile filtration apparatus, Millipore, Eschborn
Water bath	Julabo Standard, Julabo PC Thermostat, Labora, Mannheim GFL-1083 shaking water bath, Helago laboratory equipment, Medingen
Water Purification unit	USF Elga (0.22 µm-filter), Purelabs, USA
Welding apparatus for preparing mesh bags	Super Poly 281, Audion Elektron, Kleve
X-ray film developing machine	Röntgenfilm Entwicklungsmaschine SRX-101, Konica Europe, Hohenbrunn
X-ray film exposure cassette	Hypercassette, Amersham Buchler, Braunschweig

#### **4.1.2. General material**

Coverslips 12 mm (round), 18 mm x 18 mm (square)	Roth, Karlsruhe
Cryo tubes, 2 ml	Greiner, Frickenhausen

Culture dishes, (35 mm diameter)	Becton Dickinson, Heidelberg
Culture dishes, (90 mm diameter)	Nunc, Wiesbaden
Culture flasks, 80 cm <sup>2</sup>	Nunc, Wiesbaden
Filter paper (Whatman 3MM)	Whatman, Göttingen
Filtration units (sterile Millex units)	Millipore, Eschborn
Glass pipettes, 1 ml, 5 ml, 10 ml	Hirschmann, Eberstadt
Glass ware	Schott, Mainz ; Brand, Wertheim
Hybridisation container	Fisher Scientific, Schwerte
Syringes, 20 ml, sterile	Braun, Melsungen
Microscope slides (26 mm x 76 mm x 1 mm)	Menzel via Roth, Karlsruhe
Microscope slides "Superfrost" (26 mm x 76 mm x 1 mm)	Menzel via Roth, Karlsruhe
Microtiter plates (Maxisorp Immuno plate F96)	Nunc, Wiesbaden
MultiGuard™ barrier tips	Sorenson Biosciences, Inc., via Roth, Karlsruhe
Nitrocellulose membrane (Trans-Blot, 0.45 µm)	Bio-Rad, München
Nylon cloth (132, 210 µm mesh size)	Sefar GmbH, Wasserburg/Inn
Nylon membrane, positively charged	QBIOgene, Heidelberg
PCR tubes (0.2 ml)	PeqLab, Erlangen
Petri dishes (AD94/H16mm)	Roth, Karlsruhe
Pipette tips	Braun, Melsungen
Plastic tubes, 14 ml	Greiner, Frickenhausen
Plastic tubes, 50 ml	Nunc, Wiesbaden
Plastic reaction tubes, 1.5 ml	Brand, Wertheim
Pursept®-A disinfectant solution	Merz via Fischer, Frankfurt
Safe Skin Satin Plus powder-free latex gloves	Kimberly Clark, Koblenz-Rheinhafen
Sterile filters (0.2 µm and 0.45 µm)	Renner GmbH, Dannstadt
Sterile single use serological pipets (10 ml)	Falcon via Multimed, Kirchheim u. Teck
X-ray film	Amersham, Freiburg



### 4.1.3. Chemicals

Ammonium peroxodisulfate (APS)	Fluka, Steinheim
Apoptosis Inhibitor II, NS3694	Calbiochem, Darmstadt
Bradford assay dye reagent	Bio-Rad, München
Bromophenol blue	Fluka, Steinheim
BSA	Sigma-Aldrich, Steinheim
Calcium chloride dihydrate	E. Merck, Darmstadt
“CDP-Star” chemiluminescence substrate	Roche, Mannheim
Coomassie brilliant blue R 250	Sigma-Aldrich, Steinheim
D-glucose	Fluka, Steinheim
Dimethylsulfoxide (DMSO)	Sigma-Aldrich, Steinheim
EDTA	Roth, Karlsruhe
“Empigen” detergent 30% solution (w/w)	Calbiochem, Darmstadt
FuGENE®6	Roche, Mannheim
Glycerol	Roth, Karlsruhe
Glycine	Roth, Karlsruhe
“Immu-mount” mounting medium	Thermo Shadon, Pittsburgh, USA, via Thermo Electron, Bremen, Germany.
JetPEI™ transfection reagent	QBIogene, Heidelberg
Mercaptoethanol	Roth, Karlsruhe
MnCl <sub>2</sub>	Fluka, Steinheim
3-(N-Morpholino)propanesulfonic acid (MOPS)	Fluka, Steinheim
NaCl	Roth, Karlsruhe
NaHCO <sub>3</sub>	Roth, Karlsruhe
p-Nitrophenylphosphate	Roche, Mannheim
PageRuler™ prestained protein ladder	MBI Fermentas
Paraformaldehyde	Fluka, Steinheim
Potassium chloride	E. Merck, Darmstadt
RbCl	Sigma-Aldrich, Steinheim
Roti®-Block 10x Concentrate	Roth, Karlsruhe
Roti®-ImmunoBlock 10x Concentrate	Roth, Karlsruhe
Rotiphorese® Gel 30	Roth, Karlsruhe
Sodium hypochlorite solution	Roth, Karlsruhe
SDS	Fluka, Steinheim
Sucrose	Roth, Karlsruhe

N,N,N',N'-Tetramethylethylenediamine (TEMED)	Sigma-Aldrich, Steinheim
Tris	Roth, Karlsruhe
Tween <sup>®</sup> 20	Fluka, Steinheim
Vectashield mounting medium with DAPI (1.5 µg/ml)	Vector via Alexis (Axxora), Grünberg

#### 4.1.4. Kits

Advantage <sup>®</sup> 2 PCR kit	Clontech (now Takara Bio), Heidelberg
DNeasy <sup>®</sup> Tissue kit	Qiagen, Hilden
Enhanced chemiluminescence (ECL) detection reagent	Amersham, Freiburg
E.Z.N.A. Plasmid Miniprep Kit I (classic line)	Peq lab, Erlangen
HotStarTaq Master Mix kit	Qiagen, Hilden
Imject <sup>®</sup> Conjugation kit	Pierce via PerbioScience, Bonn
NucleoSpin <sup>®</sup> Extract II kit	Macherey-Nagel, Düren
NucleoSpin <sup>®</sup> Plasmid kit	Macherey-Nagel, Düren
NucleoSpin <sup>®</sup> Xtra Midi Plus kit	Macherey-Nagel, Düren
Omniscript Reverse Transcriptase kit	Qiagen, Hilden
PCR digoxigenin (DIG) probe synthesis kit	Roche, Mannheim
PCR Select <sup>™</sup> cDNA subtraction kit	Clontech (now Takara Bio), Heidelberg
PCR Select <sup>™</sup> differential screening kit	Clontech (now Takara Bio), Heidelberg
QIAGEN PCR Cloning <sup>plus</sup> kit	Qiagen, Hilden
QIAprep spin miniprep kit	Qiagen, Hilden
QIAquick gel extraction kit	Qiagen, Hilden
QIAquick PCR purification kit	Qiagen, Hilden
RNeasy RNA isolation kit	Qiagen, Hilden
SMART <sup>™</sup> PCR cDNA synthesis kit	Clontech (now Takara Bio), Heidelberg
SulfoLink <sup>®</sup> Coupling gel	Pierce via PerbioScience, Bonn
TripleMaster <sup>®</sup> PCR System	Eppendorf, Hamburg

#### 4.1.5. Reagents for molecular biology

Agarose	PeqLab, Erlangen
Anti-DIG-alkaline phosphatase (AP), Fab-fragments	Roche, Penzberg
BSA (100x)	New England Biolabs, Frankfurt a.M.
Dithiothreitol (DTT), 0.1 M	Gibco BRL, Karlsruhe
GeneRuler 1 kb DNA ladder	MBI Fermentas, St. Leon-Rot
GeneRuler 100 bp DNA ladder plus	MBI Fermentas, St. Leon-Rot
Deoxyribonucleoside triphosphate (dNTP; 10 mM each)	PeqLab, Erlangen
Ethidium bromide	Fluka, Steinheim
Oligo(dT <sub>15</sub> ) primer	Invitrogen, Karlsruhe
PCR primers	Invitrogen, Karlsruhe
	Biomers, Ulm
Phenol/chlorophorm/isoamylalcohol (25 :24 :1) (v/v/v)	Appllichem, Darmstadt
RNAsin ribonuclease inhibitor (40 U/μl)	Promega, Mannheim
T4 DNA Ligation Buffer (10x)	MBI Fermentas, St. Leon-Rot

#### 4.1.6. Enzymes for molecular biology

BamHI	New England Biolabs, Frankfurt a.M.
Calf intestine alkaline phosphatase (1U/μl)	MBI Fermentas, St. Leon-Rot
Clal	New England Biolabs, Frankfurt a.M.
EcoRI	New England Biolabs, Frankfurt a.M.
EcoRV	New England Biolabs, Frankfurt a.M.
HindIII	New England Biolabs, Frankfurt a.M.
HotStart Taq DNA polymerase	Qiagen, Hilden
Mfel	New England Biolabs, Frankfurt a.M.
Mlul	MBI Fermentas, St. Leon-Rot

Omniscript Reverse Transcriptase	Qiagen, Hilden
Pacl	New England Biolabs, Frankfurt a.M.
<i>PfuUltra</i> <sup>™</sup> Hotstart High-Fidelity DNA polymerase	Stratagene, Amsterdam
Polynucleotide kinase	MBI Fermentas, St. Leon-Rot
PstI	New England Biolabs, Frankfurt a.M.
PvuII	New England Biolabs, Frankfurt a.M.
Pwo polymerase	Peq lab, Erlangen
RNase A	Qiagen, Hilden
Sall	MBI Fermentas, St. Leon-Rot
SmaI	New England Biolabs, Frankfurt a.M.
Taq polymerase	Eppendorf, Hamburg
T4 DNA ligase	MBI Fermentas, St. Leon-Rot
“TripleMaster” polymerase mix (5U/μl)	Eppendorf, Hamburg
XhoI	New England Biolabs, Frankfurt a.M.

#### 4.1.7. Constituents and reagents for bacterial and mammalian cell cultures

Antimycotic/antibiotic	Sigma-Aldrich, Steinheim
Carbenicillin, disodium salt	Roth, Karlsruhe
Dulbecco’s modified Eagle’s medium (DMEM) powder lacking pyruvate and NaHCO <sub>3</sub>	GibcoBRL, Karlsruhe
Fetal calf serum (FCS)	Biochrome, Berlin
Hank’s balanced salt solution (HBSS)	GibcoBRL, Karlsruhe
Insulin	Sigma-Aldrich, Steinheim
Kanamycin	Applichem, Darmstadt
LB-agar powder	Fluka, Steinheim
LB-broth powder	Fluka, Steinheim
Minimal Essential Medium (MEM) powder	GibcoBRL, Karlsruhe

Penicillin G, potassium salt	Serva, Heidelberg
Superoptimal broth, catabolite repression (SOC) medium	Novagen, Schwalbach/Ts
Streptomycin sulfate	Serva, Heidelberg
Thrombin (human)	Provided by Mirna Rapp, Aventis Behring, Marburg
Transferrin	Roche, Mannheim
Trypsin	ICN, Eschwege

## 4.1.8. Antibodies

### 4.1.8.1. Primary antibodies

Monoclonal anti-acetylated $\alpha$ -tubulin antibody	Sigma-Aldrich, Steinheim
Monoclonal anti- $\beta$ -actin antibody	Sigma-Aldrich, Steinheim
Polyclonal antibody to HIV-I p24	Acris, Herford
Polyclonal antibody to HIV-I p24 (biotin)	Acris, Herford
Anti-Wdr16 antiserum	Provided by Wolfgang Hirschner

### 4.1.8.2. Secondary antibodies

Donkey anti-guinea pig IgG Cy3 conjugate	Jackson, via Dianova, Hamburg
Donkey anti-guinea pig IgG peroxidase conjugate	Jackson, via Dianova, Hamburg
Goat anti-mouse IgG Alexa Fluor 568 conjugate	Molecular Probes, via Invitrogen, Karlsruhe
Goat anti-mouse IgG peroxidase conjugate	Jackson, via Dianova, Hamburg
Streptavidin-alkaline phosphatase conjugate	Jackson, via Dianova, Hamburg
Donkey anti-rabbit IgG peroxidase conjugate	Jackson, via Dianova, Hamburg

Goat anti-rabbit IgG alkaline phosphatase conjugate

Jackson, via Dianova, Hamburg

#### **4.1.9. Bacterial strains**

DH5 $\alpha$  E.coli cells

Gift from F. Madeo, IFIB,  
University of Tübingen

NovaBlue Singles<sup>TM</sup> competent cells

Novagen, Schwalbach/Ts.

Qiagen EZ competent cells

Qiagen, Hilden

#### **4.1.10. Mammalian cell lines**

293T Human embryonic kidney cells

Provided by Roland Vogel, Paris

HepG2 cells

American Type Culture Collection (ATCC;  
catalog number HB-8065), via Promochem,  
Wesel

C6-BU-1 rat glioma cell line,  
bromodeoxyuridine resistant

Provided by Bernd Hamprecht

#### **4.1.11. Animals**

Wistar rats

Purchased from Charles River, Kisslegg;  
bred in the animal facility of the institute

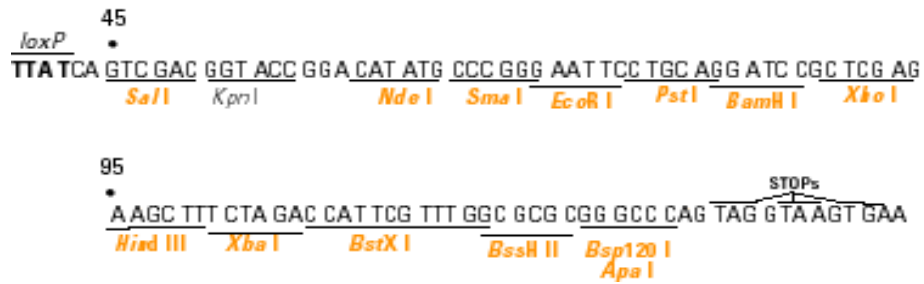
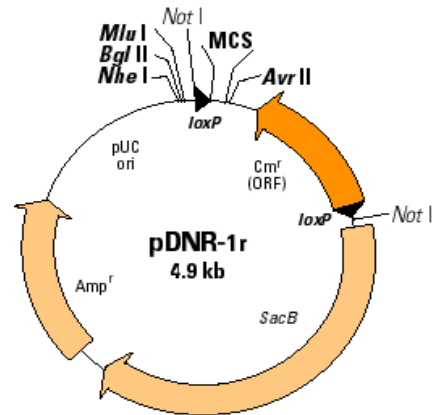
BL 6 mice

Purchased from Charles River, Kisslegg

## 4.1.12. Vectors

### 4.1.12.1. Prokaryotic expression vectors

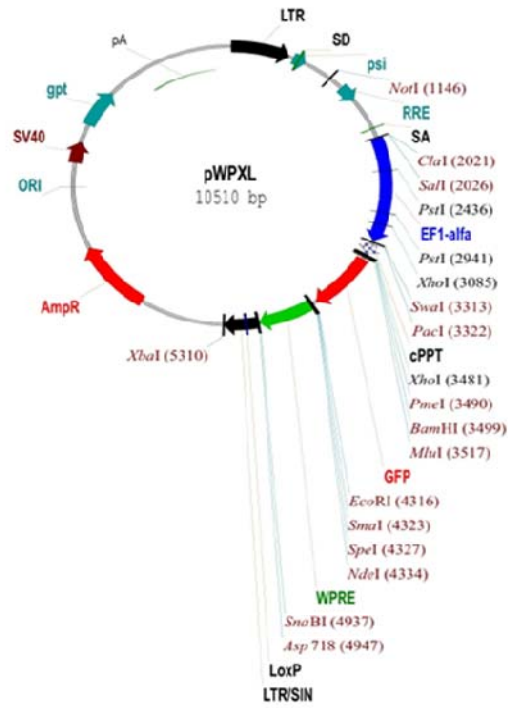
pDNR-1r, Clontech (now Takara Bio), Heidelberg



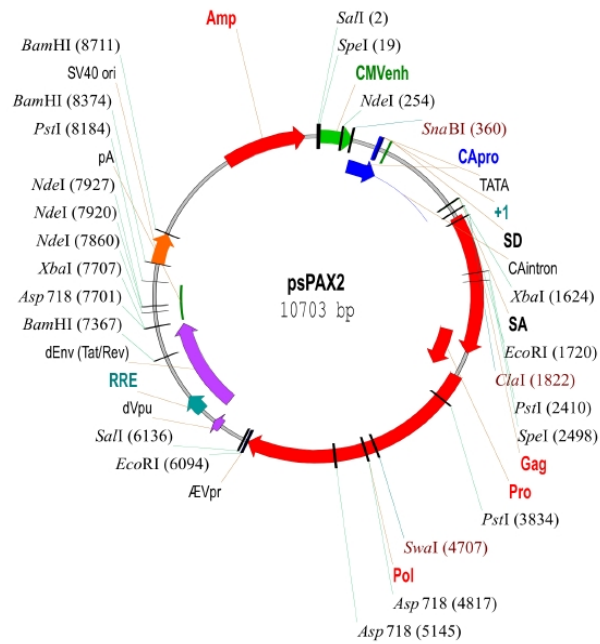
### 4.1.12.2. Lentiviral vectors

(All provided by Didier Trono, Laboratory of Virology and Genetics, EPFL, Lausanne, Switzerland)

pWPXL

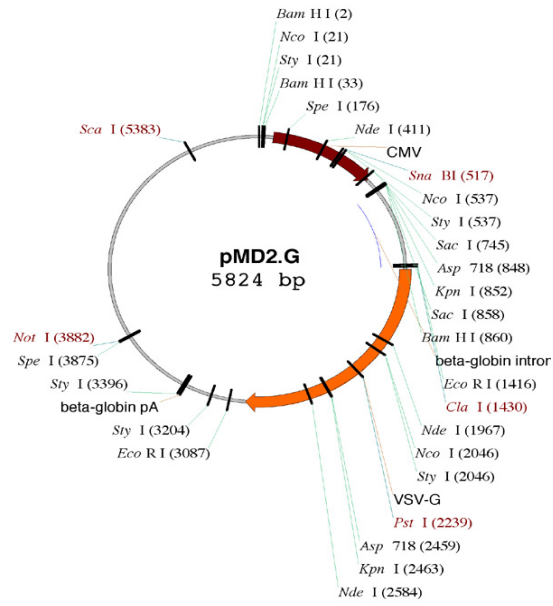


psPAX2

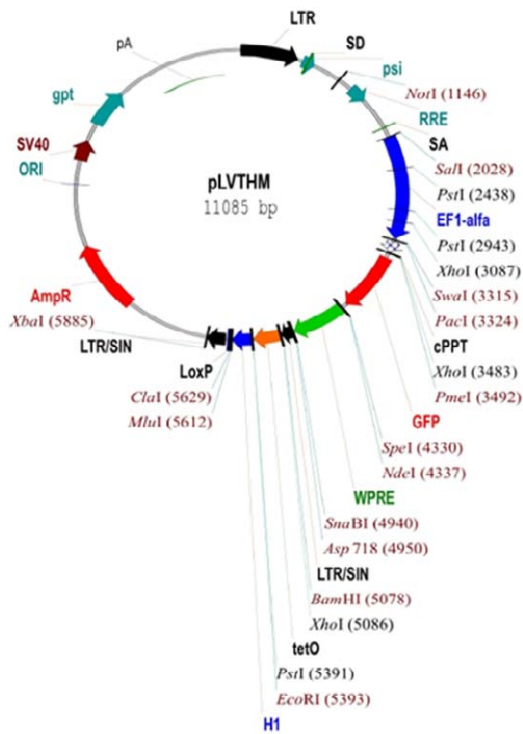




pMD2.G



pLVTHM



## 4.2.Methods

### 4.2.1. Cell culture

#### 4.2.1.1. Media and solutions for cell culture

##### **Penicillin/streptomycin (PS) stock solution**

651 mg penicillin G, potassium salt (1536 U/mg) and 1 g streptomycin sulfate (750 U/mg), dissolved in 50 ml ddH<sub>2</sub>O

##### **Puck's D1 solution**

137 mM NaCl, 5.4 mM KCl, 0.22 mM KH<sub>2</sub>PO<sub>4</sub>, 0.17 mM Na<sub>2</sub>HPO<sub>4</sub>; pH 7.4

##### **Puck's D1 / Gluc / Suc solution**

5 mM D-glucose, 58.4 mM sucrose, in Puck's D1 solution

##### **Trypsin solution 0.05 % (w/v)**

Puck's D1 / Gluc / Suc solution supplemented with 0.2% (v/v) phenol red and 0.05% (w/v) trypsin

##### **MEM<sub>Wash</sub>**

9.65 g MEM powder and 2.2 g NaHCO<sub>3</sub>, dissolved in 1 l ddH<sub>2</sub>O. The medium was gassed with CO<sub>2</sub> until the colour became orange.

##### **MEM<sub>C</sub>**

MEM<sub>Wash</sub> medium supplemented with 0.5 g/l BSA, 5 mg/l insulin, 10 mg/l transferrin and 1 ml PS stock solution per liter of medium

##### **MEM<sub>CT</sub>**

MEM<sub>C</sub> supplemented with 500 U/l thrombin

### **DMEM**

133.75 g DMEM powder lacking pyruvate and NaHCO<sub>3</sub>, 2.2 g sodium pyruvate and 74 g NaHCO<sub>3</sub> were dissolved in 20 l ddH<sub>2</sub>O. The medium was gassed with CO<sub>2</sub> until the colour became orange. The osmolarity was 320-340 mOsmol/l.

### **90% DMEM / 10% FCS**

900 ml DMEM plus 100 ml FCS

### **90% DMEM / 10% FCS / PS**

1 ml PS stock solution was added to 1 l 90% DMEM / 10% FCS

### **90% DMEM / 10% FCS / antimycotic**

1 ml 1000-fold concentrated antimycotic stock solution was added to 1 l 90% DMEM / 10% FCS

## **4.2.1.2. Ependymal primary cultures**

EPC were prepared from the brains of newborn Wistar rats or BL6 mice not older than 24 h according to the method of Weibel et al. (1986) as modified by Prothmann et al. (2001).

### **Coating of culture dishes with fibronectin**

Fibronectin was isolated according to Miekka et al. (1982) with modifications described by Prothmann (1995).

Culture dishes either 35 mm in diameter or 24-well plates with round coverslips 12 mm in diameter were incubated at 37°C with 0.7 ml or 200 µl of sterile-filtered fibronectin solution (200 µg/ml), respectively, for 2 h. Afterwards, the fibronectin solution was recollected and the culture dishes were refilled with 2 ml MEM<sub>wash</sub>. Coated culture dishes were stored in a cell incubator at 37°C in an atmosphere of 95% air and 5% CO<sub>2</sub> until cells were seeded.

### **Preparation of rat / mice brains**

Newborn rats / mice were decapitated with a pair of scissors. The brains were squeezed through the foramen magnum by application of pressure to the skull roof and transferred to a sterile Petri dish containing 10 ml ice-cold Puck's D1 / Gluc / Suc solution.

### **Dissociation into single cells**

Prior to the procedure, nylon gauze bags were created from nylon cloth (132  $\mu\text{m}$  and 210  $\mu\text{m}$  mesh size) with a welding apparatus. These nylon bags were autoclaved before they were used in the preparation of the cultures. The brains were packed into a 210  $\mu\text{m}$  mesh size nylon gauze bag and dissociated by massaging them through the mesh with sterile forceps. The suspension was collected in a Petri dish filled with 10 ml ice cold Puck's D1 / Gluc / Suc solution, where it was triturated to apparent homogeneity with a 10 ml glass pipette. Removal of the remaining large aggregates was further achieved by passing the cell suspension through a 132  $\mu\text{m}$  mesh size gauze bag, and the cell suspension was collected into a 50 ml plastic tube. After 5 min of centrifugation in a Heraeus/Christ Varifuge K at 1500 revolutions per minute (rpm) and 4°C, the supernatant was sucked off and the pellet was resuspended in 10 ml of MEM<sub>C</sub>. The suspension was passed through a 132  $\mu\text{m}$  mesh size gauze bag into an appropriate volume of MEM<sub>C</sub> to yield the seeding suspension. For each dissociated brain, 30 ml of MEM<sub>C</sub> were used as described in Weibel et al. (1986).

### **Seeding of dissociated brain cells**

MEM<sub>wash</sub> was removed from fibronectin-coated dishes and replaced by either 2 ml of cell suspension when dishes in 35 mm diameter were used, or by 0.5 ml of cell suspension for 24-well plates. Seeded cells were cultivated at 37°C in an atmosphere of 95% air and 5% CO<sub>2</sub>. After 2 days, MEM<sub>C</sub> was replaced by MEM<sub>CT</sub>. The culture medium was renewed every 2 days. The state of the cultures was regularly monitored under a light microscope.

### **4.2.1.3. Cultures of the human embryonic kidney cell line HEK293T**

#### **Starting of the culture**

The HEK293T cell line was kindly provided by Roland Vogel as a cryo stock at passage number 5. To take the cells into culture, the cryo stock was rapidly thawed at 37°C in a pre-warmed circulating water bath. Afterwards, the cell suspension was transferred to an 80 cm<sup>2</sup> culture flask containing 20 ml DMEM /10% FCS supplemented with antimycotic solution and subsequently incubated at 37°C in an atmosphere of 95% air and 5% CO<sub>2</sub> for 4 h. After attachment of the cells to the culture dish (approximately 4 hours after seeding), the medium was renewed by fresh DMEM / FCS supplemented with antimycotic and antibiotic.

#### **Maintenance of the cell culture**

The HEK293T cell line was cultured in 75 cm<sup>2</sup> culture dishes using DMEM / FCS at 37°C in humidified atmosphere containing 5% CO<sub>2</sub>. The medium was renewed every 3<sup>rd</sup> day. The state of the cultures was routinely monitored under a microscope.

#### **Passaging of the cells**

When the cells became confluent in the 75 cm<sup>2</sup> flask (after approximately 4-5 days), the culture medium was removed and adherent cells were washed with 1 ml 0.05% trypsin solution. Subsequently, the washing solution was discarded, replaced by 2 ml 0.05% trypsin solution and the flask was incubated at 37°C in a cell incubator until cells started to detach (approximately 2-3 min). To inhibit trypsin activity, detached cells were resuspended in 10 ml DMEM/FCS/PS and subsequently transferred to a 50 ml plastic tube. After centrifugation (1,000 rpm / 4°C / 5 min) in a Heraeus/ Multifuge 3 S-R, the supernatant was discarded and the cell pellet was triturated with 15 ml DMEM / FCS. To start a new passage, 500 µl of this cell suspension was added to a new culture flask containing 10 ml DMEM / FCS.

#### **Preparation of cryo stocks**

Freezing medium: DMEM + 15% FCS + 5% DMSO; filter-sterilized and stored at -20°C

For the preparation of cryo stocks, 80-90% confluent cell cultures were trypsinised with 0.05% trypsin, and the cells were collected by centrifugation (1,000 rpm / 5 min / 4°C). The cells were then resuspended in 3 ml of freezing medium, stored in 1 ml cryo vials and immediately frozen at -80°C after wrapping with paper towels. Later the cryo stocks were transferred to a cell bank and stored over liquid nitrogen.

## **4.2.2. Production of lentiviral vectors in HEK293T cells**

### **Solutions**

Calcium chloride: 2.5 M solution in ddH<sub>2</sub>O, sterile-filtered

2x HEPES-buffered saline (HBS): (for 500 ml) 8 g NaCl, 0.38 g KCl, 0.1 g Na<sub>2</sub>HPO<sub>4</sub>, 5 g HEPES, 1 g glucose; pH 7.05, sterile-filtered

MEM<sub>c</sub> supplemented with 25 mM glucose

### **Experimental procedure**

#### **Day 1: Plating**

The day before transfection, HEK293T cells suspended in 90% DMEM / 10% FCS (v/v) were seeded into cell-culture dishes of 10 cm in diameter at a density of 2.5 - 3 million cells per plate.

#### **Day 2: Transfection**

Transfection was carried out by the calcium phosphate method (Jordan et al., 1996). Calcium phosphate precipitate (1 ml / 90 mm culture dish) was prepared in the following way: 20 µg of transfer vector (pWPXL), 15 µg of packaging plasmid (psPAX2) and 6 µg of envelope plasmid (pMD2.G) were put into a sterile reaction tube. The volume was approximately 150 - 200 µl. To this plasmid solution, 50 µl of 2.5 M calcium chloride solution was added. The solution was brought to a volume of 500 µl with autoclaved ddH<sub>2</sub>O and was mixed thoroughly with the aid of a “Vortex” mixer. After transferring 500 µl of double-concentrated HBS solution to another reaction tube, the calcium chloride solution was added to the HBS solution very slowly (dropwise), and the solution was mixed thoroughly

with the aid of a “Vortex” mixer. Incubation at room temperature for 1 min was followed by dropwise addition of the precipitate to the cells under gentle shaking of the plate. The plate was then incubated at 37°C in a humidified atmosphere of 95% air and 5% CO<sub>2</sub>. After 6-8 hours of transfection, the calcium phosphate precipitate-containing medium was removed and the cells were washed briefly with 5 ml of 90% DMEM / 10% FCS (v/v), before 6 ml of fresh MEM<sub>C</sub> supplemented with 25 mM glucose were added and the plate was incubated at 37°C in a humidified atmosphere of 95% air and 5% CO<sub>2</sub>.

#### **Day 3, 4 and 5: Collection of virus**

The virus-containing supernatant was harvested into a sterile tube, centrifuged (3000 rpm, 5 min, RT), filtered through a 0.45 µm mesh filter and stored at 4°C. Further supernatant was harvested on days 2, 3 and 4 after transfection, pooled with the first sample and stored frozen at -80°C for future use. Alternatively, the virus was concentrated by ultracentrifugation (see below, 4.2.3.).

For the large scale production of lentivirus, 24 cell cultures in dishes 90 mm in diameter were transfected and the virus supernatant was harvested as described above.

#### **4.2.3. Concentration of lentiviral vectors**

Virus solution was transferred into sterile Beckman 25 mm X 89 mm centrifuge tubes and centrifuged (100,000 g, 2 h, 4°C) in an Optima L-80 Ultracentrifuge (Beckman-Coulter) using the Type 70 Ti rotor. After the spin, the supernatant was discarded and the virus pellet was resuspended in 1 ml of MEM<sub>C</sub> medium. Aliquots of 40 µl were prepared and stored frozen at -80°C for future use.

#### **4.2.4. Titration of lentiviral vectors**

Lentivirus titration was carried out according to the protocol from the Trono laboratory, at [http://tronolab.epfl.ch/webdav/site/tronolab/shared/protocols/protocols\\_LVtitration.html](http://tronolab.epfl.ch/webdav/site/tronolab/shared/protocols/protocols_LVtitration.html). HEK293T cells were used for the titration of the lentiviral vectors. HEK293T cells were

seeded at a density of 30,000 cells into each well of a 24-well plate. On the following day, the cells were counted in one well before infecting the cells in the other wells at different serial dilutions of the virus, respectively. Six different serial dilutions of virus (250  $\mu$ l total volume per well) were normally used. In case of non-concentrated virus, 150  $\mu$ l of virus solution, and in case of concentrated virus, 15  $\mu$ l of virus stock was used to prepare the serial dilutions. The non-concentrated virus was serially diluted 10, 50, 100, 150, 200 and 250 times, the concentrated virus 100, 500, 1,000, 1,500, 2,000 and 2,500 times. On day 3, the medium was removed and fresh 90% DMEM / 10% FCS (v/v) was added. The cells were fixed on DIV 5, and those expressing the green fluorescent protein were counted manually from pictures taken with a Nikon Coolpix 995 digital camera. The percentage of cells that are infected by a given amount of viral particles can normally be calculated by the equation,  $P = 1 - e^{-MOI}$ , which, in turn, is derived from the Poisson distribution. Thus, the MOI can be calculated according to the formula  $MOI = -\ln(1-P)$ , where P is the percentage of infected cells. MOI can be substituted by  $V_v([V]/N_c)$ , where  $V_v$  is the volume of stock virus suspension that had to be added to the total media volume above the cultured cells to arrive at the required dilution step of the series, [V] is the concentration of infectious particles and  $N_c$  is the number of cells. A plot of  $V_v$  versus  $-\ln(1-P)$  should yield a straight line with a slope of  $[V]/N_c$ . However, the titration data obtained in the present thesis do not obey this relationship (see Discussion). Therefore, the MOI was calculated from the number of GFP expressing cells after infection with the highest dilution of the series according to the equation  $MOI = -\ln(1-P)$ .

## **4.2.5. Transfection of ependymal primary cultures**

### **4.2.5.1. Calcium phosphate precipitation method**

For transfection of EPCs with plasmids by the calcium phosphate precipitation method, 4  $\mu$ g of DNA were dissolved in 90  $\mu$ l autoclaved ddH<sub>2</sub>O, and 10  $\mu$ l of 2.5 M CaCl<sub>2</sub> solution were added to make a final volume of 100  $\mu$ l. The solution of DNA and CaCl<sub>2</sub> was then added to 100  $\mu$ l of 2x HBS solution in a new reaction tube. After thorough mixing, the liquid was collected by brief centrifugation and incubated at room temperature for 1 minute. To each



well of a 24-well plate containing an EPC, 50  $\mu$ l of this reaction mixture were then added and the cells were incubated at 37°C in a humidified atmosphere of 95% air and 5% CO<sub>2</sub>. After 6 hours, the medium was replaced with fresh medium, and the primary culture was maintained until DIV 13 with regular media changes.

#### **4.2.5.2. Polyethylenimine-mediated gene transfer**

EPCs were transfected with commercially available jetPEI™ transfection reagent at an N / P ratio (measure of the ionic balance of the complexes, which refers to the number of nitrogen residues of jetPEI™ per DNA phosphate) of 5 using 2  $\mu$ g of plasmid DNA and 4  $\mu$ l of jetPEI™ transfection reagent. Briefly, 2  $\mu$ g of plasmid DNA were dissolved in 50  $\mu$ l of 150 mM NaCl solution, mixed gently and centrifuged briefly. In another tube, 4  $\mu$ l of jetPEI™ solution were filled up to 50  $\mu$ l with 150 mM NaCl and centrifuged briefly after mixing. The jetPEI™ and DNA solutions were combined, immediately mixed on a “Vortex” mixer and centrifuged briefly to collect the fluid at the bottom of the tube. The mixture was then incubated at room temperature for 15-30 min. It was then added drop-wise to the media above an EPC grown in a 24-well plate, and the culture was incubated at 37°C in a humidified atmosphere of 95% air and 5% CO<sub>2</sub>. The medium was changed after 6 hours and the cultures were maintained until DIV 13 with regular media changes.

#### **4.2.5.3. Lentiviral vector-mediated gene transfer**

EPCs were transfected with lentiviral vectors either on DIV 1 or on DIV 6. During the infection on DIV 1, MEM<sub>C</sub> was used for dilution of the viral stock, while it was MEM<sub>CT</sub> on DIV 6. During the transfection, care was taken not to exceed 50% of virus stock while infecting with the non-concentrated virus. In case of the concentrated viral stocks, 200 ng of HIV-I p24 per well 15 mm in diameter or an MOI of 40 was used as a maximum virus load. The total volume of media per well during infection was 250  $\mu$ l, which was doubled to 500  $\mu$ l when the virus-containing medium was replaced by fresh medium after an overnight incubation. The transfected EPCs were maintained with regular media changes at 37°C in a water vapour-saturated atmosphere of 5% CO<sub>2</sub> and 95% air until they were fixed on DIV 13.

#### **4.2.6. Isolation of genomic DNA from the transfected ependymal primary cell cultures**

EPCs were transfected with virus either on DIV 1 or on DIV 6, and the genomic DNA was isolated on DIV 13. The medium was removed from the wells and the cells were washed with 250 µl of 0.05% trypsin solution. After washing, 500 µl of fresh trypsin solution was added per well and the cells were incubated at 37°C for 5 min. The detached cells were collected by repeated pipetting and transferred into 10 ml of 90% DMEM / 10% FCS (v/v), which was then centrifuged (1000 rpm, 5 min, 4°C). The cell pellet was suspended in 200 µl of PBS and stored frozen at -20°C for further use. Alternatively, it was immediately processed for the genomic DNA isolation using the DNeasy<sup>®</sup> Tissue kit from Qiagen according to the manufacturer's instructions (see 4.2.14.7.). The concentration of the isolated genomic DNA was measured photometrically.

#### **4.2.7. Analysis of proviral DNA integration**

In the transfected EPCs, genomic integration of lentivirus was analysed by nested PCR using two sets of primers designed against rat LINES and LTRs of the proviral DNA. The HotStarTaq Master Mix kit from Qiagen was used for the PCR amplification. In the first round of PCR in a final volume of 25 µl, 12.5 µl of HotStarTaq Master Mix and 200 ng of genomic DNA were used. The primers used were 5'- GCTGTCTCTTTATGAGGAGTTGTG-3' and 5'- CAAGACGGATGATCAAATGTG-3'. The cycling parameters were: 94°C, 30 s; 52°C, 30 s; 72°C, 3 min (35 cycles); final elongation (72°C, 10 min). Before thermal cycling, the samples were heated to 95°C for 15 min. For the second round of nested PCR, the reaction mix from the first PCR was diluted 1:10, and 1 µl was used as the template. The total reaction volume was 25 µl and the primers were 5'- TCCTTCTGCTACGCCCTTC-3' and 5'- ATGCTGCTTTTTGCTTGTACTG-3'. The cycling parameters were: 94°C, 30 s; 52°C, 30 s; 72°C, 30 s (25 cycles); final elongation (72°C, 10 min). Before thermal cycling, the samples were heated to 95°C for 15 min. After the second PCR, the products were analysed by agarose gel electrophoresis using 1% agarose gels. A band of 333 bp length was expected in the presence of genomically integrated provirus.

## 4.2.8. Immunostaining of the transfected ependymal primary cultures

### Solutions

Fixing solution: 4% (v/v) paraformaldehyde in PBS

Blocking solution: 10% goat serum in PBS; pH 7.4

Washing buffer: 0.1% (v/v) and 0.3% (v/v) Triton X-100 / PBS; pH 7.4

### Experimental procedure

After removal of the culture medium, the cells grown on 12 mm round coverslips placed in 24-well culture dishes were washed once with 0.5 ml PBS for 5 min and fixed with 0.5 ml 4% PFA / PBS at RT for 10 min. After washing three times with 0.5 ml PBS for 5 min, the remaining PFA was inactivated by washing with 0.5 ml 0.1% glycine / PBS for 5 min. The coverslips were then washed again with 0.5 ml PBS (three times for 5 min), followed by incubation with 0.5 ml 0.3% Triton X-100 / PBS for 10 min. Subsequently, the cells were incubated with 100  $\mu$ l of anti-acetylated tubulin primary antibody diluted 1:1,000 in blocking solution at room temperature for 2 h. The coverslips were then washed three times with 0.5 ml of 0.1% Triton X-100 washing buffer for 5 min each, followed by an incubation with 100  $\mu$ l of anti-mouse IgG Alexa fluor 568 diluted 1:1,000 at room temperature for 1 h. Finally, the coverslips were washed three times with 0.5 ml of 0.1% Triton X-100 washing buffer (5 min each) and briefly rinsed in PBS. After the staining procedure, a drop of "Vectashield" mounting medium containing DAPI was placed on the coverslip, which was then transferred onto a microscope slide for inspection. Alternatively, the nuclei of the cells on the coverslip were stained with 10  $\mu$ g/ml of DAPI in PBS for 5 min and mounted cells down on microscope slides using "Immu-mount" mounting medium.

## 4.2.9. Production of cell lines

Freshly harvested viral supernatant (see 4.2.2.) was used for the stable transfection of HEK293T cells to produce cell lines. HEK293T cells were stably transfected with the respective virus and the cells were seeded into the wells of a 96-well plate after

trypsinisation. The cell suspension had previously been diluted to a final concentration of approximately one cell per well. The single colonies growing in 90% DMEM / 10% FCS (v/v) in the 96-well plates were analysed for expression of the GFP fusion protein under a fluorescence microscope. These cell lines were further tested for their expression of fusion proteins by adequate methods including Western blot.

#### **4.2.10. Analysis of the efficiency of different shRNA constructs**

The efficacies of different wdr16-directed shRNA constructs were tested on the cell line HEK-wdr16 and EPC. HEK-wdr16 cells were seeded at 30,000 cells per 60 mm dish and transfected with HIV/VSV-G (30 ng of HIV-I p24) encoding different shRNA targeting constructs. The cells were collected by trypsinisation for Western blot analysis on DIV 2, 4, 6 and 9, respectively. The cell pellets were lysed with ddH<sub>2</sub>O after washing with PBS and stored frozen at -20°C until they were analysed by Western blotting.

#### **4.2.11. Cultures of the human hepatocarcinoma cell line HepG2**

##### **Starting of the culture**

Frozen HepG2 cells, provided by Wolfgang Hirschner, were thawed at 37°C in a pre-warmed water bath. The cells were then transferred to a 75 cm<sup>2</sup> culture flask filled with 20 ml 90% DMEM / 10% FCS (v/v) and incubated at 37°C in an atmosphere containing 5% CO<sub>2</sub> for 6 h. After that time the cells had attached to the culture flask and the medium was renewed.

##### **Maintenance of the cell culture**

HepG2 cells were cultured in 80 cm<sup>2</sup> culture flasks using 90% DMEM / 10% FCS (v/v) as the culture medium in an atmosphere containing 5% CO<sub>2</sub>. The medium was renewed every fourth day.

### **Passaging of the cells**

The cells were passaged as described for HEK293T cells. However, the trypsin solution contained 0.25% trypsin and 0.53 mM EDTA in PBS at pH 7.4.

### **4.2.12. Harvesting of cells from culture dishes for Western blotting**

Depending on the experimental requirements, 6-12 culture dishes of either 35 mm or 60 mm in diameter were used. After removal of the culture medium, the cells were washed once with 1 ml 0.05% trypsin before 2 ml of 0.05% trypsin solution was added to each dish and incubated at 37°C for not more than 5 min. The cells were collected by trituration and pipetting into 50 ml plastic tubes with 10 ml of 90% DMEM / 10% FCS. After centrifugation (1,000 rpm, 4°C, 5 min) in a Heraeus Multifuge 3 S-R, the supernatant was discarded and the cell pellet was resuspended in 1 ml PBS, transferred to 1.5 ml microfuge tubes. After centrifugation at 3,000 rpm and 4°C for 5 min in a Heraeus Biofuge table top centrifuge, the supernatant was discarded and the cell pellet lysed with 50-100 µl of distilled water at 4°C. The lysate was stored at -20°C.

### **4.2.13. Screening of subtracted ependymal cDNA libraries**

Subtracted libraries were screened with a dot blot array, following the protocol supplied with the PCR-Select differential screening kit. Putative differentially expressed sequences were sent to SeqLab Laboratories, Göttingen, for commercial sequencing.

### **4.2.14. Other molecular biology techniques**

#### **4.2.14.1. Preparation of medium for bacterial cultures**

##### **Solution**

1000-fold concentrated carbenicillin stock solution: 50 mg/ml

LB broth powder (20 g) was dissolved in 1000 ml ddH<sub>2</sub>O with the aid of a magnetic stirrer and subsequently autoclaved at 121°C for 15 min. After the liquid had cooled down to approximately 50°C, 1 ml of a 1000-fold concentrated antibiotic stock solution was added to the medium and stored at 4°C.

#### **4.2.14.2. Preparation of agar plates**

Preparation of selection plates was performed according to 4.2.14.1, but 30 g LB agar were used instead of LB broth. After autoclaving and addition of the required antibiotic stock solution (50 mg/ml of 1000-fold carbenicillin), the liquid was distributed among Petri dishes under sterile conditions. When the agar had solidified, the plates were stored at 4°C.

#### **4.2.14.3. Bacterial liquid cultures**

In order to amplify bacterial clones for plasmid isolation, bacterial liquid cultures were prepared. For this, bacterial single colonies from a fresh agar streak plate were transferred to 4 ml of antibiotic-containing LB medium via a sterile toothpick. Subsequently, liquid bacterial cultures were incubated overnight at 37°C on a shaker platform.

#### **4.2.14.4. Preparation of bacterial glycerol stocks**

For preparing bacterial glycerol stocks, 0.5 ml of a bacterial overnight culture and 0.5 ml of glycerol were mixed in cryotubes and stored at -80°C.

#### **4.2.14.5. “Mini” scale preparation of plasmid DNA from bacterial liquid cultures**

Bacterial liquid overnight cultures were centrifuged in a Heraeus/Christ Varifuge K (3,000 rpm, 4°C, 5 min). The supernatant was discarded and plasmid DNA was isolated from the

bacterial pellet with the NucleoSpin® Plasmid miniprep kit from Macherey-Nagel according to the manufacturer's instructions, as explained below.

Briefly, the bacterial pellet was resuspended in 250 µl of buffer A1 supplemented with RNaseA. The same volume of buffer A2 was also added to the above solution and, after mixing gently by inverting the tube 6-8 times, incubated at RT for not more than 5 min. After the incubation, 300 µl of buffer A3 was added and mixed by inverting the tube 6-8 times. The lysate was centrifuged at 13,000 rpm for 10 min at RT in a table top centrifuge. The supernatant of the lysate was transferred to the NucleoSpin® Plasmid column supplied with the collection tube and centrifuged (13,000 rpm, RT, 1 min). The flow-through was discarded and the silica membrane of the column was washed with 600 µl of buffer A4 (with ethanol) by centrifugation for 1 min as mentioned before. After washing with buffer A4 the silica membrane of the column was dried again by brief centrifugation (13,000 rpm, RT, 1 min). The column was placed in a 1.5 ml sterile microfuge tube and the plasmid DNA was eluted with 50 µl of buffer AE by centrifugation (13,000 rpm, RT, 1 min). The concentration of isolated DNA was measured photometrically (see below, 4.2.14.10.).

#### **4.2.14.6. Isolation of total cellular RNA from cultured cells**

Total cellular RNA was isolated using RNeasy RNA isolation kit from Qiagen. The cells (approximately  $10^7$  cells) were collected by trypsinisation and pelleted by brief centrifugation. The cell pellet was disrupted by adding 600 µl of buffer RLT and repeated pipetting. Then 1 volume of 70% ethanol was added to the lysate, and the solution was mixed well by pipetting. The sample was transferred to an RNeasy spin column supplied with the collection tube and centrifuged (13,000 rpm, RT, 15 s). The flow-through was discarded and the membrane of the column was washed by adding 700 µl of buffer RW1 and a brief centrifugation (13,000 rpm, RT, 15 s). The flow-through was discarded and the membrane of the column again washed with buffer RPE (with ethanol) by centrifugation (13,000 rpm, RT, 1 min). After this step, the column was again briefly centrifuged (13,000 rpm, RT, 1 min) to prevent ethanol carry-over and to dry the column. The column was subsequently placed in a 1.5 ml sterile microfuge tube, and the total RNA was eluted with

50 µl of RNase-free water by centrifugation (13,000 rpm, RT, 1 min). The concentration of isolated RNA was measured photometrically (see below, 4.2.14.10.).

#### **4.2.14.7. Isolation of genomic DNA from cultured cells**

Genomic DNA was isolated using the DNeasy tissue kit from Qiagen. HEK293T cells (approximately  $5 \times 10^6$  cells) were collected by trypsinisation and pelleted by brief centrifugation. The cell pellet was resuspended in 200 µl of PBS. The resuspended cells were disrupted by adding 200 µl buffer AL and 20 µl of proteinase K during an incubation at 56°C for 10 min. After the incubation, 200 µl of ethanol were added, and the solution was mixed by repeated pipetting. The mixture was transferred into a DNeasy mini spin column with collection tube and centrifuged (8000 rpm, RT, 1 min). The flow-through was discarded, and 500 µl of buffer AW1 was added to the column. After centrifugation (8000 rpm, RT, 1 min), the flow-through was discarded and 500 µl of buffer AW2 were added. The column was again centrifuged (13,000 rpm, RT, 3 min) and the flow-through was discarded. After another brief centrifugation to dry the column, the genomic DNA was eluted into a sterile 1.5 ml microfuge tube by addition of 200 µl buffer AE (10 mM Tris-Cl, 0.5 mM EDTA, pH 9.0) and centrifugation (8,000 rpm, RT, 1 min). The concentration of isolated genomic DNA was measured photometrically (see below, 4.2.14.10.).

#### **4.2.14.8. Extraction of DNA from agarose gels**

DNA from one sample was loaded into two adjacent lanes of an agarose gel. The lane placed next to a DNA standard, named the analytical lane, contained a lower volume than the preparative lane from which the DNA was to be extracted later on. After gel electrophoresis, the part of the gel containing the marker lane together with the analytical lane was cut off with a scalpel and stained with 0.005% ethidium bromide / TAE for 10 min. The desired band in the analytical lane was marked by cutting it out under UV illumination. Afterwards, the analytical lane was again aligned precisely to the preparative lane of the gel in order to facilitate the cutting out of the desired band from the preparative lane. Isolation of DNA



from the agarose fragment was accomplished by the QIAquick gel extraction kit according to the manufacturer's protocol.

The gel fragment from which DNA had to be extracted was excised based on the position of the respective DNA size standards in a reference lane stained with ethidium bromide. After weighing the gel slice, 3  $\mu$ l of buffer QG were added per mg of gel slice mass and the mixture was incubated at 50°C until the gel slice was completely dissolved in buffer QG. To this solution, isopropanol was added (1  $\mu$ l per mg of gel slice mass) and mixed thoroughly. This solution was transferred to a QIAquick column with collection tube and centrifuged (13,000 rpm, RT, 1 min). The flow-through was discarded and the column was washed with 750  $\mu$ l of buffer PE by centrifugation as mentioned above. The flow-through was discarded and the column was centrifuged for an additional 1 min to remove all traces of residual ethanol. The column was placed in a 1.5 ml sterile microfuge tube and the DNA was eluted with buffer EB (10 mM Tris-Cl, pH 8.5) after a brief centrifugation. The concentration of extracted DNA was measured photometrically (see below, 4.2.14.10.).

#### **4.2.14.9. Direct purification of PCR products**

The NucleoSpin® Extract II kit from Macherey-Nagel was used to purify PCR products. Briefly, 2 volumes of buffer NT were mixed with 1 volume of sample and transferred to a NucleoSpin®Extract II column with collection tube. After centrifugation (13,000 rpm, RT, 1 min), the flow-through was discarded and the column silica membrane was washed once with 600  $\mu$ l of buffer NT3. After centrifugation (13,000 rpm, RT, 1 min), to dry the silica membrane, the PCR products were extracted into a sterile 1.5 ml microfuge tube by addition of 15-20  $\mu$ l of elution buffer NE (5 mM Tris-Cl, pH 8.5) and centrifugation (13,000 rpm, RT, 1 min). The concentration of extracted DNA was measured photometrically (see below, 4.2.14.10.).

#### **4.2.14.10. Photometric determination of nucleic acid concentration**

The concentration of DNA or RNA solution was determined photometrically. For this, the absorbance (OD) was measured at a wavelength of 260 nm. The solvent in which the sample was diluted was used as a reference (blank). An  $OD_{260}$  value of 1 corresponded to a concentration of 50  $\mu\text{g/ml}$  for double-stranded DNA and to 40  $\mu\text{g/ml}$  for RNA. The diluted solutions were prepared in such a way that the absorbance fell into the range from 0.1 to 1, assuring linear correlation between nucleic acid concentration and absorbance. The sample volume was 10  $\mu\text{l}$ . To estimate the purity of samples, the  $OD_{260}/OD_{280}$  ratio was calculated. A protein-free nucleic acid solution was assumed to display a ratio from 1.8 up to 2.0.

#### **4.2.14.11. Cloning of the E71 PCR products into the pDNR-1r vector**

Total cellular RNA was isolated from EPC and testis with the RNeasy RNA isolation kit according to the manufacturer's protocol (4.2.14.6.). One microgram of total RNA was mixed with 1  $\mu\text{l}$  RNasin (40 U/ $\mu\text{l}$ ) and 1  $\mu\text{l}$  oligo (dT<sub>15</sub>) primer (500  $\mu\text{g/ml}$ ). The reaction volume was filled up to 12  $\mu\text{l}$  with ddH<sub>2</sub>O and incubated at 70°C for 10 min. After brief chilling on ice, the following components were added: 1  $\mu\text{l}$  RNasin (40 U/ $\mu\text{l}$ ), 2  $\mu\text{l}$  10-fold concentrated Omniscript buffer RT, 2  $\mu\text{l}$  DTT (0.1 M), 1  $\mu\text{l}$  dNTP (10 mM each) and 1  $\mu\text{l}$  ddH<sub>2</sub>O. The tube content was incubated at 42°C for 2 min. After addition of 1  $\mu\text{l}$  Omniscript RT (4 U/ $\mu\text{l}$ ), the reaction was further incubated at 42°C for 50 min to facilitate reverse transcription. The enzyme was heat-inactivated at 95°C for 5 min, the reaction tube briefly chilled on ice, and the cDNA was stored at -80°C until further use.

For the PCR amplification of E71 from testis and EPC cDNA, the "High Fidelity TripleMaster" polymerase Mix was used. For this, 3  $\mu\text{l}$  of cDNA was mixed with 10  $\mu\text{l}$  10-fold concentrated "High Fidelity" PCR buffer, 6  $\mu\text{l}$  primer mix (10  $\mu\text{M}$  each), 2  $\mu\text{l}$  dNTPs (2 mM each) and 1  $\mu\text{l}$  "TripleMaster" polymerase Mix (5U/ $\mu\text{l}$ ). The reaction volume was brought to 100  $\mu\text{l}$  with ddH<sub>2</sub>O. The PCR primers were designed with the recognition sequences for BamHI and EcoRI, respectively, and had the nucleotide sequences as shown below.

5'-GGGAATCCATGAGCAGTGAGTTCCTGTCAGAACTG-3'

5'- GTGGATCCGCTTTGTTGAGCTTTTTTCCTTAGGG -3

The cycling parameters used were: 95°C, 30 s; 56°C, 30 s; 72°C, 3 min (35 cycles); final elongation (72°C, 10 min). Before thermal cycling, the samples were heated to 95°C for 2 min. The PCR product was then purified with the PCR purification kit according to the manufacturer's instructions (4.2.14.9.).

The purified E71 PCR product was double-digested with BamHI and EcoRI according to the protocol supplied by the company, New England Biolabs. The pDNR-1r vector DNA also was double-digested with EcoRI / BamHI under identical conditions and dephosphorylated with calf intestine alkaline phosphatase (CIAP) in order to prevent vector self-ligation in the subsequent ligation reaction.

The digested E71 PCR products as well as the pDNR-1r vector DNA were purified by preparative agarose gel electrophoresis. The desired bands were cut out from the agarose gel, and DNA was isolated with the QIAquick gel extraction kit according to the manufacturer's instructions (4.2.14.8.).

pDNR-1r vector DNA and the amplified E71 PCR products were ligated using T4 ligase, the ligation product was transferred into NovaBlue Singles<sup>TM</sup> competent cells, and transformed cells were selected on carbenicillin-containing agar plates (50 mg/ml of 1000-fold carbenicillin). Agar streak plates were prepared from colonies growing after overnight incubation, which were in turn used to start bacterial liquid cultures, from which the recombinant plasmid DNA was isolated with the QIAprep Spin miniprep kit according to the manufacturer's protocol. The isolated recombinant plasmid DNA was subjected to digestion with XhoI and then analysed on an analytical 1% agarose gel. The insert regions of the plasmids showing the expected band pattern were commercially sequenced by SeqLab Laboratories, Göttingen, Germany. One of the bacterial clones bearing the mutation-free recombinant plasmid was used to prepare a bacterial glycerol stock that was stored frozen at -80°C.

#### 4.2.14.12. Cloning of the Spag6 PCR products into the pWPXL vector

For the amplification of Spag6 from EPC cDNA, the “High Fidelity TripleMaster” polymerase Mix was used. For this, 3 µl of cDNA was mixed with 10 µl 10-fold concentrated “High Fidelity” PCR buffer, 6 µl primer mix (10 µM each), 2 µl dNTPs (2 mM each) and 1 µl “TripleMaster” polymerase Mix (5 U/µl). The reaction volume was brought to 100 µl with ddH<sub>2</sub>O. The PCR primers were designed with Mlul recognition sites and had the sequences as shown below.

5'-GGACGCGTATCTGTGGCTGGTAGCTGTCCACCC-3'

5'-GAACGCGTATGAGCCAGCGGCAGGTGCT-3'

The cycling parameters used were: 95°C, 30 s; 56°C, 30 s; 72°C, 1 min 30 s (30 cycles); final elongation (72°C, 10 min). Before thermal cycling, the samples were heated to 95°C for 2 min. The PCR product was then purified with the QIAquick PCR purification kit according to the manufacturer’s instructions. The purified Spag6 PCR products were digested with Mlul. The pWPXL vector DNA was also digested with Mlul under the same conditions that were used to digest the Spag6 PCR products. It was subsequently dephosphorylated with CIAP in order to prevent vector self-ligation in the following ligation reaction. The digested Spag6 PCR products as well as the pWPXL vector DNA were purified by preparative agarose gel electrophoresis. The desired bands were cut out from the agarose gel, and DNA was isolated with the QIAquick gel extraction kit according to the manufacturer’s instructions (4.2.14.8.).

pWPXL vector DNA and the amplified Spag6 PCR product were ligated using T4 ligase, the ligation product was transferred into NovaBlue Singles™ competent cells, and transformed cells were selected on carbenicillin-containing agar plates (50 mg/ml of 1000-fold carbenicillin). Agar streak plates were prepared from colonies growing after overnight incubation, which were in turn used to start bacterial liquid cultures, from which the recombinant plasmid DNA was isolated with the QIAprep Spin miniprep kit according to the manufacturer’s protocol (4.2.14.5.). The isolated recombinant plasmid DNA was subjected to digestion with XhoI and then analysed on an analytical 1% agarose gel. The insert regions of the plasmids showing the expected restriction pattern were commercially sequenced by SeqLab Laboratories, Göttingen, Germany. One of the bacterial clones bearing the mutation-

free recombinant plasmid was used to prepare a bacterial glycerol stock that was stored frozen at -80°C.

#### 4.2.14.13. Cloning of shRNAs into the pLVTHM vector

Annealing buffer: 100 mM potassium acetate, 30 mM HEPES; pH 7.4 and 2 mM magnesium acetate.

The oligonucleotide pairs used to prepare the wdr16 mRNA targeting constructs were:

Position	Oligonucleotide sequence	Length (bases)
shRNA 1 (1787-1805 bp)	5'-CGCGTCCCCGTCCAGGAAACCAGTATATTTCAAGAGAATATACTGGTTTCCTGGACTTTTTGGAAAT-3' 5'-CGATTTCCAAAAGTCCAGGAAACCAGTATATTTCTTGAATATACTGGTTTCCTGGACGGGGA-3'	67 65
shRNA 2 (871-889 bp)	5'-CGCGTCCCCGGTGGCATCACTTCTATCATTCAAGAGATGATAGAAGTGATGCCACCTTTTTGGAAAT-3' 5'-CGATTTCCAAAAGGTGGCATCACTTCTATCATCTTGAATGATAGAAGTGATGCCACCGGGGA-3'	67 65
shRNA 3 (1535-1553 bp)	5'-CGCGTCCCCATGATCTGGAATCTCCG TTGATATCCG CGGAAGAATCCAGATCAT TTTTTGGAAAT-3' 5'-CGATTTCCAAAAGATGATCTGGAATCTCCGCGGATATCAACGGAAGAATCCAGATCATGGGGA-3'	67 65

The oligonucleotides were dissolved in autoclaved distilled water to a final concentration of 100 pmol/μl. To anneal the oligonucleotides, 2 μl each of solutions of the forward and reverse oligonucleotide were added to 46 μl of oligonucleotide annealing buffer. The mixture was subsequently incubated at 95°C for 4 min and then at 70°C for 10 min, cooled down and stored at -20°C. These annealed oligonucleotides were phosphorylated before ligation into pLVTHM. Phosphorylation was carried out by transferring 5 μl of annealed oligonucleotides in 12 μl of water and adding 2 μl of 10x T4 ligase buffer and 1 μl of polynucleotide kinase prior to incubation at 37°C for 30 min. The enzyme was heat-inactivated by heating the samples to 70°C for 10 min.

The pLVTHM vector was double-digested with the MluI and ClaI endonucleases and the reaction product purified by preparative agarose gel electrophoresis. The desired band was cut out from the agarose gel, and DNA was isolated with the QIAquick gel extraction kit according to the manufacturer's instructions (4.2.14.8.).

The pLVTHM vector DNA and the phosphorylated oligonucleotides were ligated by T4 ligase, the ligation product was transferred into NovaBlue Singles™ competent cells and transformed cells were selected on carbenicillin-containing agar plates (50 mg/ml of 1000-fold carbenicillin). Agar streak plates were prepared from colonies growing after overnight incubation, which were in turn used to start bacterial liquid cultures, from which the recombinant plasmid DNA was isolated with the NucleoSpin® Plasmid miniprep kit from Macherey-Nagel according to the manufacturer's protocol (4.2.14.5.). The isolated recombinant plasmid DNA was subjected to digestion with BamHI and ClaI and then analysed on an analytical 1% agarose gel. The insert regions of the plasmids showing the expected band pattern were commercially sequenced by MWG Biotech sequencing service, München, Germany. One of the bacterial clones bearing the mutation-free recombinant plasmid was used to prepare a bacterial glycerol stock that was stored frozen at -80°C.

#### **4.2.14.14. Replacement of the promoter in the pWPXL vector**

The EF1 $\alpha$  promoter region in the pWPXL vector, located between recognition sites for the restriction endonucleases Sall and PacI, was replaced either with the human FOXJ1 promoter region or the rat wdr16 putative promoter region, respectively. The pWPXL vector was simultaneously digested with Sall and PacI and the larger digestion product purified by preparative agarose gel electrophoresis.

A genomic DNA fragment containing 1008 bp of the human FOXJ1 promoter region was amplified using genomic DNA isolated from HEK293T cells (4.2.14.7.) with the PCR primers which also contain recognition sites for Sall and PacI as shown below.

5'-ATGTCGACTGAGCCGAGCCGGGACTTAG-3'

5'-AGATTAATTAAGTCCCCAGACTCCCGTTACACGG-3'

*PfuUltra™* hot start high-fidelity DNA polymerase was used. The cycling parameters were: 95°C, 30 s; 62°C, 45 s; 72°C, 70 s (30 times); final elongation (72°C, 8 min). Before thermal cycling, the samples were heated to 95°C for 2 min. The PCR product was then purified with the NucleoSpin® Extract II kit from Macherey-Nagel according to the manufacturer's

instructions (4.2.14.9.). The purified FOXJ1 promoter PCR products were digested with Sall, followed by a phenol/chloroform/isoamyl alcohol extraction with subsequent ethanol precipitation and a further digestion with Pacl.

The rat genomic DNA fragment of 758 bp between the syntaxin8 and wdr16 genes was amplified with the PCR primers as shown below.

5'-GTCGACAACCTGTTTTATTGACCTCAGAA-3'  
5'-GAGTTGAGGAATCAACCAGCTGAATTAATTAA-3'

*PfuUltra™* hot start high-fidelity DNA polymerase was used during the PCR. The cycling parameters were: 95°C, 30 s; 45°C, 30 s; 72°C, 1 min (35 times); final elongation (72°C, 10 min). Before thermal cycling, the samples were heated to 95°C for 2 min. The PCR product was then purified with the NucleoSpin® Extract II kit from Macherey-Nagel according to the manufacturer's instructions. The purified putative wdr16 promoter PCR products were digested with Sall, followed by a phenol/chloroform/isoamyl alcohol extraction with subsequent ethanol precipitation and a further digestion with pacl.

The pWPXL vector DNA and the amplified FOXJ1 or wdr16 promoter PCR products were ligated by T4 ligase, the respective ligation products transferred into E.coli DH5α competent cells and transformed cells were selected on carbenicillin-containing agar plates (50 mg/ml of 1000-fold carbenicillin). Agar streak plates were prepared from colonies growing after overnight incubation, which were in turn used to start bacterial liquid cultures, from which the recombinant plasmid DNA was isolated with the NucleoSpin® Plasmid kit according to the manufacturer's protocol (4.2.14.5.). The isolated recombinant plasmid DNAs were subjected to digestion with either MfeI or SmaI, and the respective products analysed on analytical 1% agarose gels. The plasmids showing the expected band pattern were commercially sequenced over their insert region. The bacterial clones bearing the mutation-free recombinant plasmids were used to prepare bacterial glycerol stocks that were stored frozen at -80°C.

#### **4.2.14.15. Restriction digestion of DNA**

##### **Preparative digestion of vector DNA and PCR product**

Five micrograms of vector DNA or a PCR product that had previously been purified with the QIA quick purification kit according to the manufacturer's instructions (see 4.2.14.8. and 4.2.14.9; eluted with 44  $\mu$ l H<sub>2</sub>O), respectively, were digested with 10 U of the corresponding restriction enzymes in the appropriate buffers for 4 h. The total reaction volume was 50  $\mu$ l.

##### **Analytical digestion of recombinant DNA**

Five micrograms of the recombinant plasmid DNA were digested with 10 U of the corresponding restriction endonuclease in the appropriate buffer for 2 - 4 h at 37°C. The total reaction volume was 50  $\mu$ l.

If a sequential digestion was necessary, (due to the incompatibility of the reaction conditions for different restriction endonucleases) a phenol / chloroform / isoamyl alcohol extraction with subsequent ethanol precipitation was performed after digestion with the first endonuclease. The extracted and precipitated DNA was subsequently subjected to the digestion with the second endonuclease.

#### **4.2.14.16. Phenol / chloroform / isoamyl alcohol extraction of DNA with subsequent ethanol precipitation**

DNA solution after the first restriction enzymatic digestion was mixed with 1 volume phenol / chloroform / isoamyl alcohol (25: 24: 1, v/v/v), "Vortex"-mixed and centrifuged (13,000 rpm, RT, 5 min) in a table top centrifuge. The upper, aqueous, DNA-containing phase was transferred to a new 1.5 ml reaction tube and combined with 3 volumes of pure ethanol. The DNA was allowed to precipitate for 2 h at -20°C. After centrifugation (13,000 rpm, 4°C, 10 min), the pellet was washed with 80% ethanol, air-dried and dissolved in 44  $\mu$ l ddH<sub>2</sub>O, before it was finally subjected to a further digestion with another enzyme.



#### **4.2.14.17. Dephosphorylation of vector DNA**

Dephosphorylation buffer: 500 mM Tris / HCl, 1 mM EDTA; pH 8.0

To the 50 µl of restriction digestion reaction mix, 5 µl dephosphorylation buffer and 1 µl CIAP (1U/µl) were added, followed by incubation at 37°C for 1 h. Subsequently, the enzyme was heat-denatured at 85°C for 15 min.

#### **4.2.14.18. Agarose gel electrophoresis**

##### **Solutions**

50-fold concentrated TAE: 2 M Tris, 0.1 M EDTA, Na salt; pH 8.5 (pH adjusted with glacial acetic acid)

5-fold concentrated DNA loading buffer: 40% (w/v) sucrose, 0.25% (w/v) bromophenol blue

##### **Experimental procedure**

Agarose gel electrophoresis was used for analytical purposes as well as for preparative DNA purification. Agarose concentrations varied between 1.0% and 1.2%, depending on the expected size of the DNA fragments. Agarose was dissolved in 100 ml of TAE by heating the mixture in a microwave oven. A gel comb was then placed into the tray to generate gel pockets. After cooling down to approximately 50°C, the solution was poured into a gel slide (110 mm x 90 mm). The samples were mixed (5: 1) with 5-fold concentrated DNA loading buffer. Electrophoresis was conducted at 100 V in TAE buffer (550 ml) for approximately 1.5 h. “Fermentas 100 bp Plus DNA ladder” or “1 kb plus DNA ladder” were used as size standards. To visualise nucleic acids, the gels were incubated in 0.005% (v/v) ethidium bromide / TAE for 10 min and then inspected on a UV transilluminator. Photographs were taken with a digital camera.

#### 4.2.14.19. Ligation of PCR products into vector DNA

Based on 25 ng vector DNA, a 5-fold molecular excess of insert DNA was used for the ligation reaction. The corresponding amount of insert was calculated with the equation:

$$\text{Amount}_{\text{insert}} = 25 \text{ ng Vector} \times \text{length}_{\text{insert}} (\text{bp}) / \text{length}_{\text{vector}} (\text{bp}).$$

25 ng of vector DNA and the corresponding amount of insert DNA were supplemented with 1  $\mu\text{l}$  10-fold concentrated ligation buffer and 1  $\mu\text{l}$  T<sub>4</sub>-ligase (5 U/ $\mu\text{l}$ ). The reaction mixture was then filled up to a total volume of 10  $\mu\text{l}$  with ddH<sub>2</sub>O. The ligation reaction was incubated overnight at 16°C. On the next day, the enzyme was heat-inactivated at 65°C for 10 min.

#### 4.2.14.20. Preparation of E.coli competent cells

##### Solutions

TFB I buffer: 30 mM potassium acetate / 100 mM RbCl / 10 mM CaCl<sub>2</sub> / 50 mM MnCl<sub>2</sub> / 15% (v/v) glycerol; pH 5.8

TFB II buffer: 10 mM MOPS / 10 mM RbCl / 75 mM CaCl<sub>2</sub> / 15% (v/v) glycerol; pH 7.0

##### Experimental procedure

E. coli DH5 $\alpha$  cells were kindly provided by F. Madeo on an agar streak plate. From this, a 5 ml bacteria liquid overnight culture was started in antibiotic-free LB medium. For preparation of competent cells, 500 ml antibiotic-free LB medium was inoculated with 1 ml of the overnight culture and incubated on a shaking platform at 37°C until the bacteria suspension reached an OD of 0.5 at a wavelength of 595 nm. Afterwards, the cells were spun down in a Heraeus/Christ Varifuge K (3,000 rpm, 4°C, 15 min). The resulting pellet was resuspended in 150 ml TFB I buffer, incubated 15 min on ice and centrifuged again under the aforementioned conditions. Subsequently the pellet was resuspended in 20 ml TFB II buffer. Finally, 100  $\mu\text{l}$  aliquots of DH5 $\alpha$  competent cells were frozen in liquid nitrogen and stored at -80°C until further use.

#### **4.2.14.21. Transformation of competent bacterial cells with plasmid DNA**

##### **Transformation of NovagenBlue Singles™ competent cells**

NovagenBlue Singles™ competent cells were thawed on ice, mixed carefully with 1.5 µl of the ligation solution and incubated on ice for 5 min. Subsequently the cells were heat-shocked at 42°C for 30 s. After incubation on ice for 2 min, the cells were mixed with 250 µl SOC medium (provided with the cells) and incubated at 37°C for 1 hour on a shaking platform. Volumes of 50-120 µl were streaked out on carbenicillin-containing agar plates, and the plates were incubated overnight at 37°C. On the next day, the plates were checked for the presence of colonies.

##### **Transformation of DH5α competent cells**

E. coli DH5α competent cells were thawed on ice, carefully mixed with 10 µl of the ligation solution and kept on ice for 10 min. The heat-shock was conducted at 42°C for 2 min. Afterwards, 900 µl antibiotic-free LB medium was added, and the suspension was incubated at 37°C for 1 h on a shaking platform. The process was continued as described for the transformation of NovagenBlue Singles™ competent cells.

#### **4.2.15. Reverse transcription of RNA**

Total RNA was isolated with the RNeasy RNA isolation kit according to the manufacturer's advice (4.2.14.6). The reaction mixture for reverse transcription of RNA contained 5 mM MgCl<sub>2</sub>, 10 mM each of dATP, dGTP, dCTP and dTTP, 25 U Avian Myoblastosis Virus Reverse Transcriptase (AMV RT), 0.6 µg oligo(dT<sub>15</sub>) primer, 0.6 µg random hexamer primer and 1 µg total RNA in 50 µl of PAN Script NH<sub>4</sub> buffer. After pipetting on ice, the mixture was heated to 42°C, incubated for 1 h, inactivated by heating to 95°C for 5 min, diluted 1:2 with H<sub>2</sub>O and stored frozen at -80°C. For control purposes, the process was repeated without addition of RT.

#### 4.2.16. Real-time PCR

Real-time PCR was performed with the FastStart DNA Master SYBR Green I kit. The reaction mixture contained 3 mM MgCl<sub>2</sub>, 0.2 μM of each primer and 2 μl of cDNA. PCR was carried out in the LightCycler<sup>®</sup> instrument over 45 cycles under the following conditions: denaturation at 95°C for 10 s, step-down annealing (67°-57°C; 1°/cycle) over 10 cycles and constant annealing temperature of 57°C thereafter for 10 s, elongation at 72°C for 12 s. The primer sequences used were

Target	Primer sequence
E71	5'-CAAAGACAGCGACTCGCTCACCC-3' 5'-ACTCACGGAGACGCTAAGTGCGC-3'
Cyclophilin	5'-GGGGAGAAAGGATTTGGCTA-3' 5'-ACATGCTTGCCATCCAGCC-3'

The specificity of the PCR reaction was verified by melting point analysis (Pfaffl, 2001) and agarose gel electrophoresis. To monitor inter-run variability, a standard with a known invariant crossing point was included with each run. To generate the standard, RNA from 3 different testes and 3 different EPC were reverse-transcribed and finally combined, resulting in a total volume of 300 μl as invariant standard. PCR efficiencies, derived from regression lines  $R^2 \geq 0.98$  after plotting crossing points against the logarithms of concentrations were used to calculate the amounts of E71 mRNA relative to that of the mRNA for cyclophilin as the standard according to the formula  $A_t/A_c \cdot A_t = E_{\text{target}}^{-\text{CP}(+)} - E_{\text{target}}^{-\text{CP}(-)}$ ;  $A_c = E_{\text{cyclophilin}}^{-\text{CP}(+)} - E_{\text{cyclophilin}}^{-\text{CP}(-)}$  (+, presence of RT; -, absence of RT).

#### 4.2.17. Generation of E71 peptide antibodies

For generating peptide antibodies, peptides with the rat E71 subsequences SSEFLSELHWEDGFAIC (positions 2-17), CSSGSNSNIPKGKLNK (positions 921-936), CEDSIPISPPTAKVIELR (positions 891-907), and CKEIYALQNTLQVLSS (positions 690-704) were coupled to sulfosuccinimidyl 4-[N-maleimidomethyl]cyclohexane-1-carboxylate-activated keyhole limpet hemocyanin (KLH) or likewise-activated bovine serum albumin (BSA) with the

Inject Maleimide Activated Immunogen Conjugation kit according to the manufacturer's advice as following. Briefly, maleimide activated KLH carrier protein was reconstituted by adding ddH<sub>2</sub>O. 2 mg peptide / 2 mg of activated KLH was used. The peptides were dissolved in conjugation buffer or DMSO. While using DMSO, care was taken not to exceed a DMSO concentration of more than 30% in the final conjugation solution. The peptide and activated KLH solutions were mixed immediately and allowed to react at RT for 2 h. The conjugate was purified by gel filtration over a D-Salt™ polyacrylamide desalting column to remove EDTA carried over from activated KLH. The column was washed 5 times with purification buffer supplied with the kit. The hapten-carrier mix was applied on top of the column, followed by the repeated addition of 500 µl aliquots of buffer. The corresponding fractions were collected in separate tubes, and the absorbance at 280 nm was measured to identify the fractions containing conjugate. The fractions with high levels of the conjugate were pooled and stored frozen at -20°C. Immunisation of rabbits was carried out commercially by Charles River Laboratories, Kisslegg, Germany. Initial immunisations were performed with Freund's complete adjuvant and the subsequent boosts (additional injections of the antigenic peptide) at day 28 and day 56 were performed with Freund's incomplete adjuvant. For the injection, 0.1 mg of the KLH-conjugated peptide was used, and final bleeding was carried out at day 70. The BSA-conjugate was stored at -20°C until it was used in ELISA experiments.

#### **4.2.18. ELISA for determining the peptide antibody titer**

##### **Solutions**

Borate buffer: 100 mM boric acid, 25 mM borax, 75 mM NaCl, 0.01% NaN<sub>3</sub>; pH 8.4

Blocking solution: 1% BSA in borate buffer

Washing buffer: 0.2% Tween 20 in borate buffer

Substrate buffer: 100 mM glycine / NaOH, 1 mM MgCl<sub>2</sub>, 1 mM ZnCl<sub>2</sub>; pH 10.4

Substrate solution: 1 mg/ml p-nitrophenylphosphate in substrate buffer

##### **Experimental procedure**

The ELISA was performed in 96-well round-bottom microtiter plates. All amounts listed below refer to an individual well.

The wells of the microtiter plate were incubated overnight with 250 ng antigen dissolved in 100 µl borate buffer at 4°C. After removal of the antigen solution from the plate by “beating out”, free binding sites were blocked with 200 µl blocking solution at 37°C for 1 h. In the meantime, a dilution series of the corresponding antiserum was prepared by diluting it in borate-buffer as follows: 1:10, 1: 30, 1:100, 1:300, 1: 10<sup>3</sup>, 1: 10<sup>3.5</sup>, 1:10<sup>4</sup>, 1: 10<sup>4.5</sup>, 1: 10<sup>5</sup>, 1: 10<sup>5.5</sup>, 1: 10<sup>6</sup>. After the microtiter plate had been washed four times with 200 µl washing buffer, the rinsed wells were incubated with 100 µl of the diluted antiserum at 37°C for 2 h, washed four times with 200 µl washing buffer and subsequently incubated at 37°C for 1 h with 100 µl of the secondary antibody (goat anti-rabbit IgG-AP conjugate, diluted 1: 1,000 in borate buffer). After washing four times with 200 µl washing buffer, 100 µl of p-nitrophenylphosphate substrate solution was added to the vials, followed by incubation at 37°C for 10 min. Finally, the product of the enzymatic reaction was measured in a microplate reader at a wavelength of 405 nm.

#### **4.2.19. ELISA for determining HIV-1-p24 antigen**

##### **Solutions**

Coating buffer: 100 mM NaHCO<sub>3</sub>; pH 8.5

10x TBS: 1.44 M NaCl, 0.5% Tween 20, 250 mM Tris; pH 7.5

Blocking buffer: 2% milk powder in 1x TBS

Substrate buffer: 0.1% “Empigen”, 20% FCS in 1x PBS

Anti-p24-Biotin buffer: 2% milk powder, 40% FCS in 1x TBS

SA-AP buffer: 2% milk powder, 1% BSA in 1x TBS

Reaction buffer: 1 mM MgCl<sub>2</sub>, 1 mM ZnCl<sub>2</sub>, 100 mM glycine / NaOH; pH 10.4

Substrate: 1 mg/ml p-nitrophenol phosphate in reaction buffer

##### **Sample preparation for HIV-1-p24 ELISA**

The virus-containing samples were treated with 0.2% “Empigen” detergent, and the virus was heat-inactivated by incubating the samples at 65°C for 30 min.

### **Experimental procedure**

Anti-HIV-1-p24 (3.33 µl/ml) was dissolved in coating buffer. The wells of the micotiter plates were coated with 100 µl of the diluted antibody each and incubated at room temperature for 6 h. After washing three times with 200 µl of 1x TBS, the free binding sites were blocked with 200 µl of blocking buffer for 45 min. In the meantime, a dilution series of the corresponding samples and standards were prepared with substrate buffer. After the microtiter plate had been washed three times with 200 µl of 1x TBS, the rinsed wells were incubated with 100 µl of the diluted samples and standards at room temperature overnight. The following day, biotinylated anti-p24 antibody was diluted 1:500 in anti-p24-biotin buffer, and 100 µl were placed into each well after washing six times with 200 µl of 1x TBS. Subsequently, the plate was incubated for 2 h at room temperature and washed six times with 200 µl of 1x TBS. Following washings, 100 µl of diluted 1:1,000 streptavidin-alkaline phosphatase conjugate in SA-AP buffer was added to each well, incubated at room temperature for 1 h and washed thoroughly six times with 200 µl of 1x TBS. Before adding the substrate, the microtiter wells were washed once with 200 µl of reaction buffer. 100 µl of substrate solution containing 1 mg/ml p-nitrophenol phosphate in reaction buffer was added to each well and incubated approximately 45 min at room temperature. Finally, the product of the enzymatic reaction was measured in a microplate reader at 405 nm. The p24 concentrations were calculated from a standard curve prepared with HIV-1-p24.

### **4.2.20. Protein assay (Bradford assay)**

The assay was performed according to Bradford (1976) using the commercially available Bio-Rad dye reagent concentrate. The diluted reagent (1:6 in water) was mixed with 10 µl of the sample (prediluted in ddH<sub>2</sub>O if necessary) to yield a final volume of 1 ml, and incubated at RT for 15 min. Afterwards, 400 µl of the reaction mixture were transferred to a 96-well plate and the absorbance was measured at a wavelength of 595 nm in a microplate reader. The protein concentrations were calculated from a standard curve prepared with BSA.

#### 4.2.21. Discontinuous SDS-PAGE

SDS PAGE was carried out as described by Laemmli (1970) with the modifications by Garfin (1990).

##### Solutions

Acrylamide solution: 29.2% (w/v) acrylamide, 0.8% (w/v) bisacrylamide (Rotiphorese Gel 30)

SDS: 10% (w/v)

APS solution: 10% (w/v)

TEMED

Running gel buffer: 0.5 M Tris / HCl, pH 8.9

Stacking gel buffer: 1.5 M Tris /HCl, pH 6.8

Electrode buffer: 25 mM Tris, 192 mM glycine, 0.1% (w/v) SDS

Five-fold concentrated sample buffer: 0.16 M Tris / HCl, 4% (w/v) SDS, 20% (w/v) glycerol, 0.38 M mercaptoethanol, 0.008 (w/v) bromophenol blue; pH 6.8

##### **Preparation of the gels**

The gel size was 8 cm x 10 cm x 1 mm. The stacking gels were prepared with 3% acrylamide at pH 6.8, the running gels with 10% acrylamide at pH 8.9. The following scheme was used for casting the gels:

<b>Solution</b>	<b>10% running gel</b>	<b>3% stacking gel</b>
Acrylamide solution	3.33 ml	0.50 ml
Running gel buffer	2.5 ml	
Stacking gel buffer		1.25 ml
Water	4.05 ml	3.0 ml
degassing (2 min)		
10% (w/v) SDS	100 µl	50 µl
TEMED	20 µl	5 µl
10% (w/v) APS solution	37.5 µl	200 µl



### **Preparation of the samples**

Protein solution was mixed with 5-fold concentrated sample buffer and filled up with ddH<sub>2</sub>O to yield a final concentration of 1-fold sample buffer in a maximal volume of 18 µl. The mixture was then heated to 95°C for 7 min. After collecting the condensate by brief centrifugation, the samples were applied to the gel.

### **Electrophoresis**

Electrophoresis was carried out under constant current (20 mA) at RT. When the bromophenol blue front had reached the end of the running gel, the process was stopped. The gels were either stained with Coomassie Brilliant Blue R 250 or used for Western blotting.

## **4.2.22. Coomassie blue staining of polyacrylamide gels**

### **Solutions**

Staining solution: 50% methanol, 40% H<sub>2</sub>O, 10% glacial acetic acid, 1% (w/v) Coomassie Brilliant Blue R 250 (in water)

Destaining solution: Methanol: H<sub>2</sub>O: glacial acetic acid (3: 6: 1)

### **Experimental procedure**

Polyacrylamide gels were incubated with staining solution at RT for 10 min. Afterwards, gels were briefly rinsed with water and transferred to destaining solution. When the blue background had disappeared and single protein bands became visible, the destaining solution was discarded and the gel was washed with ddH<sub>2</sub>O. Protein bands were documented by a digital camera.

## 4.2.23. Western blot analysis with chemiluminescence detection

### Protein Transfer

#### Solutions

Transfer buffer: 25 mM Tris / HCl, 192 mM glycine; pH 9.0

Ponceau S solution: 0.2% (w/v) Ponceau S in 3% (w/v) trichloroacetic acid

#### Experimental procedure

Proteins (20 µg) were separated by discontinuous SDS PAGE. The protein bands were then transferred from the gel to a nitrocellulose membrane using a modification of the protocol described by Burnette (1981) as detailed below.

The nitrocellulose membrane was rinsed in transfer buffer. The transfer “sandwich” was packed by piling a plastic lattice, a synthetic fiber mat, a filter paper, the SDS polyacrylamide gel, the nitrocellulose membrane, a filter paper, a synthetic fiber mat and a final plastic lattice. Air bubbles were strictly avoided in the process. The arrangement was inserted into an electroblot chamber filled with transfer buffer. Electrophoretic protein transfer was performed with a current of 140 mA at 4°C for 2 h.

After transfer, the membrane was removed from the transfer chamber and stained by brief immersion in Ponceau S solution. Subsequently the membrane was destained with 0.05% (v/v) Tween 20 / PBS, washed with PBS and processed as described in the following.

### Detection of protein bands with the enhanced chemiluminescence (ECL) reagent

#### Solutions

Washing buffer: 20 mM Tris / HCl, 150 mM NaCl, 0.02% (v/v) Tween 20; pH 7.4

Blocking solution: 1-fold concentrated Roti-Block / PBS

Substrate solution: 1 ml ECL solution I + 1 ml ECL solution II

**Experimental procedure**

The membrane was incubated overnight with 20 ml blocking solution at RT in order to block unspecific binding sites. It was then washed three times for 5 min with 20 ml washing buffer, and 20 ml of the the guinea pig Wdr16 antiserum was added at a dilution of 1:10,000 in washing buffer. The incubation time was 1 h. The membrane was washed three times for 5 min with 20 ml washing buffer, before 20 ml of the secondary antibody solution were applied. The secondary antibody was donkey anti-guinea pig IgG conjugated with peroxidase, diluted 1:120,000 in washing buffer. The incubation time was 1 h. The membrane was washed again three times for 5 min with 20 ml washing buffer, rinsed briefly with PBS and then the ECL detection solution was added dropwise to cover the membrane. After 2 min, the solution was removed and the membrane wrapped in transparent plastic foil. An X-ray film was exposed to it for approximately 5 min in an exposure cassette. The film was developed in an X-ray film developing machine. As loading controls, the same membranes were also probed with anti- $\beta$ -actin antibody according to the procedure described above.



## 5. References

Afzelius, B. A. (1985) The immotile-cilia syndrome: a microtubule-associated defect. *CRC Crit. Rev. Biochem.* **19**, 63-87.

Afzelius, B. A. (2004) Cilia-related diseases. *J. Pathol.* **204**, 470-477.

Akli, S., Caillaud C., Vigne E., Stratford-Perricaudet L. D., Poenaru L., Perricaudet M., Kahn A. and Peschanski M. R. (1993) Transfer of a foreign gene into the brain using adenovirus vectors. *Nat. Genet.* **3**, 224-228.

Alisky, J. M., Hughes S. M., Sauter S. L., Jolly D., Dubensky T. W Jr., Staber P. D., Chiorini J. A. and Davidson B. L. (2000) Transduction of murine cerebellar neurons with recombinant FIV and AAV5 vectors. *Neuroreport* **11**, 2669-2673.

Arya, M., Ahmed H., Silhi N., Williamson M. and Patel H. R. (2007) Clinical importance and therapeutic implications of the pivotal CXCL12-CXCR4 (chemokine ligand-receptor) interaction in cancer cell migration. *Tumour Biol* **28**, 123-131.

Banizs, B., Pike M. M., Millican C. L., Ferguson W. B., Komlosi P., Sheetz J., Bell P. D., Schwiebert E. M. and B. K. Yoder (2005) Dysfunctional cilia lead to altered ependyma and choroid plexus function, and result in the formation of hydrocephalus. *Development* **132**, 5329-5339.

Banziger, C., Soldini, D., Schutt, C., Zipperlen, P., Hausmann, G., and Basler, K. (2006) Wntless, a conserved membrane protein dedicated to the secretion of Wnt proteins from signalling cells. *Cell* **125**, 509-522.

Bartlett, J. S., Samulski R. J. and McCown T. J. (1998) Selective and rapid uptake of adeno-associated virus type 2 in brain. *Hum. Gene. Ther.* **9**, 1181-1186.

Baskar, J. F., Smith P. P., Nilaver G., Jupp R. A., Hoffmann S., Peffer N. J., Tenney D. J., Colberg-Poley A. M., Ghazal P. and Nelson J. A. (1996) The enhancer domain of the human cytomegalovirus major immediate-early promoter determines cell type-specific expression in transgenic mice. *J. Virol.* **70**, 3207-3214.

Beck, K. and Brodsky B. (1998) Supercoiled protein motifs: the collagen triple-helix and the alpha-helical coiled coil. *J. Struct. Biol.* **122**, 17-29.

Berkner, K. L. (1988) Development of adenovirus vectors for the expression of heterologous genes. *Biotechniques* **6**, 616-629.

Beyer, W. R., Westphal M., Ostertag W. and von Laer D. (2002) Oncoretrovirus and lentivirus vectors pseudotyped with lymphocytic choriomeningitis virus glycoprotein: generation, concentration, and broad host range. *J. Virol.* **76**, 1488-1495.

Blatt, E. N., Yan X. H., Wuerffel M. K., Hamilos D. L. and Brody S. L. (1999) Forkhead transcription factor HFH-4 expression is temporally related to ciliogenesis. *Am. J. Respir. Cell Mol. Biol.* **21**, 168-176.

Bledsoe, A. W., Jackson C. A., McPherson S. and Morrow C. D. (2000) Cytokine production in motor neurons by poliovirus replicon vector gene delivery. *Nat. Biotechnol.* **18**, 964-969.

Blomer, U., Naldini L., Kafri T., Trono D., Verma I. M. and Gage F. H. (1997) Highly efficient and sustained gene transfer in adult neurons with a lentivirus vector. *J. Virol.* **71**, 6641-6649.

Boussif, O., Lezoualc'h F., Zanta M. A., Mergny M. D., Scherman D., Demeneix B. and Behr J. P. (1995) A versatile vector for gene and oligonucleotide transfer into cells in culture and in vivo: polyethylenimine. *Proc. Natl. Acad. Sci. U S A* **92**, 7297-7301.

Bradford, M. M (1976) A rapid and sensitive method for quantitation of microgram quantities of protein using the principle of protein-dye binding. *Anal. Biochem.* **72**, 248-254.

Brody, S. L., Yan X. H., Wuerffel M. K., Song S. K. and Shapiro S. D. (2000) Ciliogenesis and left-right axis defects in forkhead factor HFH-4-null mice. *Am. J. Respir. Cell. Mol. Biol.* **23**, 45-51.

Brooks, A. I., Stein C. S., Hughes S. M., Heth J., McCray P. M. Jr., Sauter S. L., Johnston J. C., Cory-Slechta D. A., Federoff H. J. and Davidson B. L. (2002) Functional correction of established central nervous system deficits in an animal model of lysosomal storage disease with feline immunodeficiency virus-based vectors. *Proc. Natl. Acad. Sci. U S A* **99**, 6216-6221.

Brown, P. D., Davies S. L., Speake T. and Millar I. D. (2004) Molecular mechanisms of cerebrospinal fluid production. *Neuroscience* **129**, 957-970.

Brummelkamp, T. R., Bernards R. and Agami R. (2002) A system for stable expression of short interfering RNAs in mammalian cells. *Science* **296**, 550-553.

Bruni, J. E. (1998) Ependymal development, proliferation, and functions: a review. *Microsc. Res. Tech.* **41**, 2-13.

Bryson, D. G., McNulty M. S., McCracken R. M. and Cush P. F. (1983) Ultrastructural features of experimental parainfluenza type 3 virus pneumonia in calves. *J. Comp. Pathol.* **93**, 397-414.

Bukrinsky, M. I., Haggerty S., Dempsey M. P., Sharova N., Adzhubei A., Spitz L., Lewis P., Goldfarb D., Emerman M. and Stevenson M. (1993) A nuclear localization signal within HIV-1 matrix protein that governs infection of non-dividing cells. *Nature* **365**, 666-669.

- Burnette W.N. (1981) "Western blotting": Electrophoretic transfer of proteins from sodium dodecylsulfate polyacrylamide gels to unmodified nitrocellulose and radiographic detection with antibody and radioiodinated protein A. *Anal. Biochem.* **112**, 195-203.
- Burns, J. C., Friedmann T., Driever W., Burrascano M. and Yee J. K. (1993) Vesicular stomatitis virus G glycoprotein pseudotyped retroviral vectors: concentration to very high titer and efficient gene transfer into mammalian and nonmammalian cells. *Proc. Natl. Acad. Sci. U S A* **90**, 8033-8037.
- Burton, E. A., Wechuck J. B., Wendell S. K., Goins W. F., Fink D. J. and Glorioso J. C. (2001) Multiple applications for replication-defective herpes simplex virus vectors. *Stem Cells* **19**, 358-377.
- Capela, A. and Temple S. (2002) LeX/ssea-1 is expressed by adult mouse CNS stem cells, identifying them as nonependymal. *Neuron* **35**, 865-875.
- Carbonell, W. S., Murase S. I., Horwitz A. F. and Mandell J. W. (2005) Infiltrative microgliosis: activation and long-distance migration of subependymal microglia following periventricular insults. *J. Neuroinflammation* **2**, 5-14.
- Cataldo, A. M. and Broadwell R. D. (1986) Cytochemical identification of cerebral glycogen and glucose-6-phosphatase activity under normal and experimental conditions. II. Choroid plexus and ependymal epithelia, endothelia and pericytes. *J. Neurocytol.* **15**, 511-524.
- Cathcart, R. S. and Worthington W. C., Jr. (1964) Ciliary movement in the rat cerebral ventricles: clearing action and directions of currents. *J. Neuropathol. Exp. Neurol.* **23**, 609-618.
- Chen, Y., McNeill J. R., Hajek I. and Hertz L. (1992) Effect of vasopression on brain swelling at the cellular level: Do astrocytes exhibit a furosemide-vasopressin-sensitive mechanism for volume regulation? *Can. J. Physiol. Pharmacol.* **70**(Suppl.), S367-S373.



Chiasson, B. J., Tropepe V., Morshead C. M. and van der Kooy D. (1999) Adult mammalian forebrain ependymal and subependymal cells demonstrate proliferative potential, but only subependymal cells have neural stem cell characteristics. *J. Neurosci.* **19**, 4462-4471.

Cifuentes, M., Fernandez L. P., Perez J., Perez-Figares J. M. and Rodriguez E. M. (1992) Distribution of intraventricularly injected horseradish peroxidase in cerebrospinal fluid compartments of the rat spinal cord. *Cell. Tissue. Res.* **270**, 485-494.

Cooray, S., Best J. M. and Jin L. (2003) Time-course induction of apoptosis by wild-type and attenuated strains of rubella virus. *J. Gen. Virol.* **84**, 1275-1279.

Cornish, T. E., Stallknecht D. E., Brown C. C., Seal B. S. and Howerth E. W. (2001) Pathogenesis of experimental vesicular stomatitis virus (New Jersey serotype) infection in the deer mouse (*Peromyscus maniculatus*). *Vet. Pathol.* **38**, 396-406.

Cornwell, R. D., Gollahon K. A. and Hickstein D. D. (1993) Description of the leukocyte function-associated antigen 1 (LFA-1 or CD11a) promoter. *Proc. Natl. Acad. Sci. U S A* **90**, 4221-4225.

Crews, L., Wyss-Coray T. and Masliah E. (2004) Insights into the pathogenesis of hydrocephalus from transgenic and experimental animal models. *Brain Pathol.* **14**, 312-316.

Cronin, J., Zhang X. Y. and Reiser J. (2005) Altering the tropism of lentiviral vectors through pseudotyping. *Curr. Gene. Ther.* **5**, 387-398.

Dai, C., McAninch R. E. and Sutton R. E. (2004) Identification of synthetic endothelial cell-specific promoters by use of a high-throughput screen. *J. Virol.* **78**, 6209-6221.

Danik, M., Chabot J. G., Hassan-Gonzalez D., Suh M. and Quirion R. (1993) Localization of sulfated glycoprotein-2/clusterin mRNA in the rat brain by in situ hybridization. *J. Comp. Neurol.* **334**, 209-227.

Davidson, B. L., Allen E. D., Kozarsky K. F., Wilson J. M. and Roessler B. J. (1993) A model system for in vivo gene transfer into the central nervous system using an adenoviral vector. *Nat. Genet.* **3**, 219-223.

Davidson, B. L., Stein C. S., Heth J. A., Martins I., Kotin R. M., Derksen T. A., Zabner J., Ghodsi A. and Chiorini J. A. (2000) Recombinant adeno-associated virus type 2, 4, and 5 vectors: transduction of variant cell types and regions in the mammalian central nervous system. *Proc. Natl. Acad. Sci. U S A* **97**, 3428-3432.

Davidson, L. and Breakefield O. (2003) Viral vectors for gene delivery to the nervous system. *Nat. Rev. Neurosci.* **4**, 353-364.

Davson, H. and Segal M. (1996) Physiology of the CSF and Blood-Brain Barriers. CRC Press, Boca Raton.

Del Bigio, M. R. (1995) The ependyma: a protective barrier between brain and cerebrospinal fluid. *Glia* **14**, 1-13.

Dellmann, H. D. and Simpson J. B. (1979) The subfornical organ. *Int. Rev. Cytol.* **58**, 333-421.

Diatchenko, L., Lau Y. F., Campbell A. P., Chenchik A., Moqadam F., Huang B., Lukyanov S., Lukyanov K., Gurskaya N., Sverdlov E. D. and Siebert P. D. (1996) Suppression subtractive hybridization: a method for generating differentially regulated or tissue-specific cDNA probes and libraries. *Proc. Natl. Acad. Sci. U S A* **93**, 6025-6030.

Diringer, M. N., Kirsch J. R., Ladenson P. W., Borel C. and Hanley D. F. (1990) Cerebrospinal fluid atrial natriuretic factor in intracranial disease. *Stroke* **21**, 1550-1554.

Doetsch, F. and Alvarez-Buylla A. (1996) Network of tangential pathways for neuronal migration in adult mammalian brain. *Proc. Natl. Acad. Sci. U S A* **93**, 14895-14900.

Doetsch, F., Petreanu L., Caille I., Garcia-Verdugo J. M. and Alvarez-Buylla A. (2002) EGF converts transit-amplifying neurogenic precursors in the adult brain into multipotent stem cells. *Neuron* **36**, 1021-1034.

Downward, J (2004) RNA interference. *British Medical Journal* **328**, 1245-1248.

Dubensky, T. W., Jr. (2002) (Re-)Engineering tumor cell-selective replicating adenoviruses: a step in the right direction toward systemic therapy for metastatic disease. *Cancer Cell* **1**, 307-309.

Dull, T., Zufferey R., Kelly M., Mandel R. J., Nguyen M., Trono D. and Naldini L. (1998) A third-generation lentivirus vector with a conditional packaging system. *J. Virol.* **72**, 8463-8471.

Dunn-Meynell, A. A., Routh V. H., Kang L., Gaspers L. and Levin B. E. (2002) Glucokinase is the likely mediator of glucosensing in both glucose-excited and glucose-inhibited central neurons. *Diabetes* **51**, 2056-2065.

Dutcher, S. K. (2003) Elucidation of basal body and centriole functions in *Chlamydomonas reinhardtii*. *Traffic* **4**, 443-451.

Dziegielewska, K. M., Ek J., Habgood M. D. and Saunders N. R. (2001) Development of the choroid plexus. *Microsc. Res. Tech.* **52**, 5-20.

Ehrengruber, M. U. (2002) Alphaviral vectors for gene transfer into neurons. *Mol. Neurobiol.* **26**, 183-201.

Evan, G. and Littlewood T. (1998) A matter of life and cell death. *Science* **281**, 1317-1322.

Fajac, I., Thevenot G., Bedouet L., Danel C., Riquet M., Merten M., Figarella C., Dall'Ava-Santucci J., Monsigny M. and Briand P. (2003) Uptake of plasmid/glycosylated polymer complexes and gene transfer efficiency in differentiated airway epithelial cells. *J. Gene. Med.* **5**, 38-48.

Fasbender, A., Zabner J., Zeiher B. G. and Welsh M. J. (1997) A low rate of cell proliferation and reduced DNA uptake limit cationic lipid-mediated gene transfer to primary cultures of ciliated human airway epithelia. *Gene. Ther.* **4**, 1173-1180.

Feistel, K. and Blum M. (2006) Three types of cilia including a novel 9+4 axoneme on the notochordal plate of the rabbit embryo. *Dev. Dyn.* **235**, 3348-3358.

Fink, D. J., DeLuca N. A., Goins W. F. and Glorioso J. C. (1996) Gene transfer to neurons using herpes simplex virus-based vectors. *Annu. Rev. Neurosci.* **19**, 265-287.

Fliegau, M. and Omran H. (2006) Novel tools to unravel molecular mechanisms in cilia-related disorders. *Trends. Genet.* **22**, 241-245.

Frommer, K (2003) Identifizierung und Charakterisierung ependymspezifisch exprimierter Gene. Diplomarbeit, Universität Tübingen.

Furtado, L. M., Somwar R., Sweeney G., Niu W. and Klip A. (2002) Activation of the glucose transporter GLUT4 by insulin. *Biochem. Cell. Biol.* **80**, 569-578.

Garfin, D.E. (1990) One-dimensional gel electrophoresis. *Meth. Enzymol.* **182**, 425-441.

Gee, P., Rhodes C. H., Fricker L. D. and Angeletti R. H. (1993) Expression of neuropeptide processing enzymes and neurosecretory proteins in ependyma and choroid plexus epithelium. *Brain. Res.* **617**, 238-248.

Geiger, H., Bahner U., Palkovits M., Hugo C., Niklas E. and Heidland A. (1989) Atrial natriuretic peptide in brain preoptic areas: implications for fluid and salt homeostasis. *J. Cardiovasc. Pharmacol.* **13**, S20-23.

Gelderblom, H.R., Hausmann E.H.S., Özel M., Pauli G. and Koch M.A. 1987a. Fine structure of human immunodeficiency virus (HIV) and immunolocalization of structural proteins. *Virology* **156**, 171-176.

Gill, D. R., Smyth S. E., Goddard C. A., Pringle I. A., Higgins C. F., Colledge W. H. and Hyde S. C. (2001) Increased persistence of lung gene expression using plasmids containing the ubiquitin C or elongation factor 1alpha promoter. *Gene Ther.* **8**, 1539-1546.

Goldman, M. J., Lee P. S., Yang J. S. and Wilson J. M. (1997) Lentiviral vectors for gene therapy of cystic fibrosis. *Hum. Gene Ther.* **8**, 2261-2268.

Greenstone, M. A., Jones R. W., Dewar A., Neville B. G. and Cole P. J. (1984) Hydrocephalus and primary ciliary dyskinesia. *Arch. Dis. Child.* **59**, 481-482.

Grimm, D. and Kleinschmidt J. A. (1999) Progress in adeno-associated virus type 2 vector production: promises and prospects for clinical use. *Hum. Gene Ther.* **10**, 2445-2450.

Grimm, D., Streetz K. L., Jopling C. L., Storm T. A., Pandey K., Davis C. R., Marion P., Salazar F. and Kay M. A. (2006) Fatality in mice due to oversaturation of cellular microRNA/short hairpin RNA pathways. *Nature* **441**, 537-541.

Grondona, J. M., Perez-Martin M., Cifuentes M., Perez J., Jimenez A. J., Perez-Figares J. M. and Fernandez-Llebrez P. (1996) Ependymal denudation, aqueductal obliteration and hydrocephalus after a single injection of neuraminidase into the lateral ventricle of adult rats. *J. Neuropathol. Exp. Neurol.* **55**, 999-1008.

Guichard, C., Harricane M. C., Lafitte J. J., Godard P., Zaegel M., Tack V., Lalau G. and Bouvagnet P. (2001) Axonemal dynein intermediate-chain gene (DNAI1) mutations result in situs inversus and primary ciliary dyskinesia (Kartagener syndrome). *Am. J. Hum. Genet.* **68**, 1030-1035.

Gundlach, A. L. and Knobe K. E. (1992) Distribution of preproatrial natriuretic peptide mRNA in rat brain detected by in situ hybridization of DNA oligonucleotides: enrichment in hypothalamic and limbic regions. *J. Neurochem.* **59**, 758-761.

Gurok, U., Steinhoff C., Lipkowitz B., Ropers H. H., Scharff C. and Nuber U. A. (2004) Gene expression changes in the course of neural progenitor cell differentiation. *J. Neurosci.* **24**, 5982-6002.

Hackett, B. P., Brody S. L., Liang M., Zeitz I. D., Bruns L. A. and Gitlin J. D. (1995) Primary structure of hepatocyte nuclear factor/forkhead homologue 4 and characterization of gene expression in the developing respiratory and reproductive epithelium. *Proc. Natl. Acad. Sci. U S A* **92**, 4249-4253.

Hartigan-O'Connor, D., Barjot C., Salvatori G. and Chamberlain J. S. (2002) Generation and growth of gutted adenoviral vectors. *Methods. Enzymol.* **346**, 224-246.

Hatskelzon, L., Dalal B. I., Shalev A., Robertson C. and Gerrard J. M. (1993) Wide distribution of granulophysin epitopes in granules of human tissues. *Lab. Invest.* **68**, 509-519.

Hay, S. and Kannourakis G. (2002) A time to kill: viral manipulation of the cell death program. *J. Gen. Virol.* **83**, 1547-1564.

Hirschner, W (2007) Identification and characterisation of ependyma-specific genes and their proteins. Doktorarbeit, Universität Tübingen.

Hirschner, W., Pogoda H. M., Kramer C., Thiess U., Hamprecht B., Wiesmuller K. H., Lautner M. and Verleysdonk S. (2007) Biosynthesis of Wdr16, a marker protein for kinocilia-bearing cells, starts at the time of kinocilia formation in rat, and wdr16 gene knockdown causes hydrocephalus in zebrafish. *J. Neurochem.* **101**, 274-288.

Ibanez-Tallon, I., Heintz N. and Omran H. (2003) To beat or not to beat: roles of cilia in development and disease. *Hum. Mol. Genet.* **12**, 27-35.

Ibanez-Tallon, I., Pagenstecher A., Fliegauf M., Olbrich H., Kispert A., Ketelsen U. P., North A., Heintz N. and Omran H. (2004) Dysfunction of axonemal dynein heavy chain Mdnah5 inhibits ependymal flow and reveals a novel mechanism for hydrocephalus formation. *Hum. Mol. Genet.* **13**, 2133-2141.

Jackson, A. L. and Linsley P. S. (2004) Noise amidst the silence: off-target effects of siRNAs? *Trends Genet.* **20**, 521-524.

Jetton, T. L., Liang Y., Pettepher C. C., Zimmerman E. C., Cox F. G., Horvath K., Matschinsky F. M. and Magnuson M. A. (1994) Analysis of upstream glucokinase promoter activity in transgenic mice and identification of glucokinase in rare neuroendocrine cells in the brain and gut. *J. Biol. Chem.* **269**, 3641-3654.

Johanson, C. E., Donahue J. E., Spangenberg A., Stopa E. G., Duncan J. A. and Sharma H. S. (2006) Atrial natriuretic peptide: its putative role in modulating the choroid plexus-CSF system for intracranial pressure regulation. *Acta. Neurochir. Suppl.* **96**, 451-456.

Johansson, C. B., Momma S., Clarke D. L., Risling M., Lendahl U. and Frisen J. (1999) Identification of a neural stem cell in the adult mammalian central nervous system. *Cell* **96**, 25-34.

Johnson, L. G., Olsen J. C., Naldini L. and Boucher R. C. (2000) Pseudotyped human lentiviral vector-mediated gene transfer to airway epithelia in vivo. *Gene. Ther.* **7**, 568-574.

Jordan, M., Schallhorn A. and Wurm F. M. (1996) Transfecting mammalian cells: optimization of critical parameters affecting calcium-phosphate precipitate formation. *Nucleic Acids Res.* **24**, 596-601.

Kahl, C. A., Marsh J., Fyffe J., Sanders D. A. and Cornetta K. (2004) Human immunodeficiency virus type 1-derived lentivirus vectors pseudotyped with envelope glycoproteins derived from Ross River virus and Semliki Forest virus. *J. Virol.* **78**, 1421-1430.

Keep, R. F. and Jones H. C. (1990) A morphometric study on the development of the lateral ventricle choroid plexus, choroid plexus capillaries and ventricular ependyma in the rat. *Brain Res. Dev. Brain Res.* **56**, 47-53.

Kimchi-Sarfaty, C., Ben-Nun-Shaul O., Rund D., Oppenheim A. and Gottesman M. M. (2002) In vitro-packaged SV40 pseudovirions as highly efficient vectors for gene transfer. *Hum. Gene. Ther.* **13**, 299-310.

Knowles, F. (1972) Ependyma of the third ventricle in relation to pituitary function. *Prog. Brain Res.* **38**, 255-270.

Kobayashi, Y., Watanabe M., Okada Y., Sawa H., Takai H., Nakanishi M., Kawase Y., Suzuki H., Nagashima K., Ikeda K. and Motoyama N. (2002) Hydrocephalus, situs inversus, chronic sinusitis, and male infertility in DNA polymerase lambda-deficient mice: possible implication for the pathogenesis of immotile cilia syndrome. *Mol. Cell. Biol.* **22**, 2769-2776.

Kobinger, G. P., Weiner D. J., Yu Q. C. and Wilson J. M. (2001) Filovirus-pseudotyped lentiviral vector can efficiently and stably transduce airway epithelia in vivo. *Nat. Biotechnol.* **19**, 225-230.

Kohn, D. F., Chinookoswong N. and Magill L. S. (1981) Pathogenicity of influenza A virus in ependymal organ culture. *Teratology* **24**, 201-213.



Koutoulis, A., Pazour G. J., Wilkerson C. G., Inaba K., Sheng H., Takada S. and Witman G. B. (1997) The *Chlamydomonas reinhardtii* ODA3 gene encodes a protein of the outer dynein arm docking complex. *J. Cell Biol.* **137**, 1069-1080.

Kremer, K. L., Dunning K. R., Parsons D. W. and Anson D. S. (2007) Gene delivery to airway epithelial cells in vivo: a direct comparison of apical and basolateral transduction strategies using pseudotyped lentivirus vectors. *J. Gene Med.* **9**, 362-368.

Laemmli U. K. (1970) Cleavage of structural proteins during the assembly of the head of bacteriophage T4. *Nature* **227**, 680-685.

Lademann, U., Cain K., Gyrð-Hansen M., Brown D., Peters D. and Jaattela M. (2003) Diarylurea compounds inhibit caspase activation by preventing the formation of the active 700-kilodalton apoptosome complex. *Mol. Cell. Biol.* **23**, 7829-7837.

Lampson, L. A., Grabowska A. and Whelan J. P. (1994) Class I and II MHC expression and its implications for regeneration in the nervous system. *Prog. Brain Res.* **103**, 307-317.

Laywell, E. D., Rakic P., Kukekov V. G., Holland E. C. and Steindler D. A. (2000) Identification of a multipotent astrocytic stem cell in the immature and adult mouse brain. *Proc. Natl. Acad. Sci. U S A* **97**, 13883-13888.

Lee, E. R., Marshall J., Siegel C. S., Jiang C., Yew N. S., Nichols M. R., Nietupski J. B., Ziegler R. J., Lane M. B., Wang K. X., Wan N. C., Scheule R. K., Harris D. J., Smith A. E. and Cheng S. H. (1996) Detailed analysis of structures and formulations of cationic lipids for efficient gene transfer to the lung. *Hum. Gene Ther.* **7**, 1701-1717.

Lehmann, G. L., Gradilone S. A. and Marinelli R. A. (2004) Aquaporin water channels in central nervous system. *Curr. Neurovasc. Res.* **1**, 293-303.

Leloup, C., Orosco M., Serradas P., Nicolaidis S. and Penicaud L. (1998) Specific inhibition of GLUT2 in arcuate nucleus by antisense oligonucleotides suppresses nervous control of insulin secretion. *Brain Res. Mol. Brain Res.* **57**, 275-280.

Lenardo, M. J., Angleman S. B., Bounkeua V., Dimas J., Duvall M. G., Graubard M. B., Hornung F., Selkirk M. C., Speirs C. K., Trageser C., Orenstein J. O. and Bolton D. L. (2002) Cytopathic killing of peripheral blood CD4(+) T lymphocytes by human immunodeficiency virus type 1 appears necrotic rather than apoptotic and does not require env. *J. Virol.* **76**, 5082-5093.

Leonhardt, H. (1980) Ependym und circumventriculäre Organe. Handbuch der mikroskopischen Anatomie des Menschen, Neuroglia I. Nervensystem IV/10. A 4: pp. 177-665. Springer Verlag, Berlin.

Li, D and Roberts, R (2001) WD-repeat proteins: structure characteristics, biological function, and their involvement in human diseases. *Cell. Mol. Life Sci.* **58**, 2085-2097.

Lim, L., Zhou H. and Costa R. H. (1997) The winged helix transcription factor HFH-4 is expressed during choroid plexus epithelial development in the mouse embryo. *Proc. Natl. Acad. Sci. U S A* **94**, 3094-3099.

Lindemann, C. B. and Kanous K. S. (1997) A model for flagellar motility. *Int. Rev. Cytol.* **173**, 1-72.

Lippoldt, A., Jansson A., Kniesel U., Andbjør B., Andersson A., Wolburg H., Fuxe K. and Haller H. (2000) Phorbol ester induced changes in tight and adherens junctions in the choroid plexus epithelium and in the ependyma. *Brain Res.* **854**, 197-206.

Lois, C. and Alvarez-Buylla A. (1994) Long-distance neuronal migration in the adult mammalian brain. *Science* **264**, 1145-1148.

Look, D. C., Walter M. J., Williamson M. R., Pang L., You Y., Sreshta J. N., Johnson J. E., Zander D. S and Brody S. L. (2001) Effects of paramyxoviral infection on airway epithelial cell Foxj1 expression, ciliogenesis, and mucociliary function. *Am. J. Pathol.* **159**, 2055-2069.

Loser, P., Jennings G. S., Strauss M. and Sandig V. (1998) Reactivation of the previously silenced cytomegalovirus major immediate-early promoter in the mouse liver: involvement of NFkappaB. *J. Virol.* **72**, 180-190.

Lotti, F., Menguzzato E., Rossi C., Naldini L., Ailles L., Mavilio F. and Ferrari G. (2002) Transcriptional targeting of lentiviral vectors by long terminal repeat enhancer replacement. *J. Virol.* **76**, 3996-4007.

Lupas, A. (1996) Coiled coils: new structures and new functions. *Trends. Biochem. Sci.* **21**, 375-382.

Lupas, A. N. and Gruber M. (2005) The structure of alpha-helical coiled coils. *Adv. Protein. Chem.* **70**, 37-78.

Lupas, A., Van Dyke M. and Stock J. (1991) Predicting coiled coils from protein sequences. *Science* **252**, 1162-1164.

Luskin, M. B. (1993) Restricted proliferation and migration of postnatally generated neurons derived from the forebrain subventricular zone. *Neuron* **11**, 173-189.

Maekawa, F., Toyoda Y., Torii N., Miwa I., Thompson R. C., Foster D. L., Tsukahara S., Tsukamura H. and Maeda K. (2000) Localization of glucokinase-like immunoreactivity in the rat lower brain stem: for possible location of brain glucose-sensing mechanisms. *Endocrinology* **141**, 375-384.

Manthorpe, C. M., Wilkin G. P. and Wilson J. E. (1977) Purification of viable ciliated cuboidal ependymal cells from rat brain. *Brain Res.* **134**, 407-415.

Marchler-Bauer, A., Anderson J. B., Derbyshire M. K., DeWeese-Scott C., Gonzales N. R., Gwadz M., Hao L., He S., Hurwitz D. I., Jackson J. D., Ke Z., Krylov D., Lanczycki C. J., Liebert C. A., Liu C., Lu F., Lu S., Marchler G. H., Mullokandov M., Song J. S., Thanki N., Yamashita R. A., Yin J. J., Zhang D. and Bryant S. H. (2007) CDD: a conserved domain database for interactive domain family analysis. *Nucl. Acid. Res.* **35**(Database issue), D237-240.

Marshall, W. F. and Nonaka S. (2006) Cilia: Tuning in to the Cell's Antenna. *Curr. Biol.* **16**, R604-R614.

Marumo, F., Masuda T. and Ando K. (1987) Presence of the atrial natriuretic peptide in human cerebrospinal fluid. *Biochem. Biophys. Res. Commun.* **143**, 813-818.

Massion, P. P., Funari C. C., Ueki I., Ikeda S., McDonald D. M. and Nadel J. A. (1993) Parainfluenza (Sendai) virus infects ciliated cells and secretory cells but not basal cells of rat tracheal epithelium. *Am. J. Respir. Cell. Mol. Biol.* **9**, 361-370.

Mata, M., Glorioso J. C. and Fink D. J. (2003) Gene transfer to the nervous system: prospects for novel treatments directed at diseases of the aging nervous system. *J. Gerontol. A. Biol. Sci. Med. Sci.* **58**, M1111-1118.

Matsui, H., Johnson L. G., Randell S. H. and Boucher R. C. (1997) Loss of binding and entry of liposome-DNA complexes decreases transfection efficiency in differentiated airway epithelial cells. *J. Biol. Chem.* **272**, 1117-1126.

Maxwell, D. S. and Pease D. C. (1956) The electron microscopy of the choroid plexus. *J. Biophys. Biochem. Cytol.* **2**, 467-474.

McGrane, M. M., de Vente J., Yun J., Bloom J., Park E., Wynshaw-Boris A., Wagner T., Rottman F. M. and Hanson R. W. (1988) Tissue-specific expression and dietary regulation of a chimeric phosphoenolpyruvate carboxykinase/bovine growth hormone gene in transgenic mice. *J. Biol. Chem.* **263**, 11443-11451.

McGrath, J., Somlo S., Makova S., Tian X. and Brueckner M. (2003) Two populations of node monocilia initiate left-right asymmetry in the mouse. *Cell* **114**, 61-73.

Meiniel, A. (2007) The secretory ependymal cells of the subcommissural organ: which role in hydrocephalus? *Int. J. Biochem. Cell. Biol.* **39**, 463-468.

Meiniel, A., Meiniel R., Didier R., Creveaux I., Gobron S., Monnerie H. and Dastugue B. (1996) The subcommissural organ and Reissner's fiber complex. An enigma in the central nervous system? *Prog. Histochem. Cytochem.* **30**, 1-66.

Mestres, P. (1998) Introduction to histology of the ventricular walls of the brain. *Microsc. Res. Tech.* **41**, 1.

Miekka S.I., Ingham K. C and Menche D. (1982) Rapid methods for isolation of human plasma fibronectin. *Thrombosis Res.* **27**, 1-14.

Michael Pfaffl W. (2001) A new mathematical model for relative quantification in real-time RT-PCR. *Nucleic Acids Research* **29**, 2003-2007.

Milhorat, T. H. (1976) Structure and function of the choroid plexus and other sites of cerebrospinal fluid formation. *Int. Rev. Cytol.* **47**, 225-288.

Mims, C. A. and Murphy F. A. (1973) Parainfluenza virus Sendai infection in macrophages, ependyma, choroid plexus, vascular endothelium and respiratory tract of mice. *Am. J. Pathol.* **70**, 315-328.

Morral, N., Parks R. J., Zhou H., Langston C., Schiedner G., Quinones J., Graham F. L., Kochanek S. and Beaudet A. L. (1998) High doses of a helper-dependent adenoviral vector yield supraphysiological levels of alpha1-antitrypsin with negligible toxicity. *Hum. Gene. Ther.* **9**, 2709-2716.

Muller, F. and O'Rahilly R. (1990) The human brain at stages 18-20, including the choroid plexuses and the amygdaloid and septal nuclei. *Anat. Embryol. (Berl)* **182**, 285-306.

Murray, J. W., Edmonds B. T., Liu G. and Condeelis J. (1996) Bundling of actin filaments by elongation factor 1 alpha inhibits polymerization at filament ends. *J. Cell Biol.* **135**, 1309-1321.

Naldini, L. (1998) Lentiviruses as gene transfer agents for delivery to non-dividing cells. *Curr. Opin. Biotechnol.* **9**, 457-463.

Naldini, L., Blomer U., Gage F. H., Trono D. and Verma I. M. (1996) Efficient transfer, integration, and sustained long-term expression of the transgene in adult rat brains injected with a lentiviral vector. *Proc. Natl. Acad. Sci. U S A* **93**, 11382-11388.

Nguyen, T., Chin W. C., O'Brien J. A., Verdugo P. and Berger A. J. (2001) Intracellular pathways regulating ciliary beating of rat brain ependymal cells. *J. Physiol.* **531**, 131-140.

Nicholson, C. (1999) Signals that go with the flow. *Trends Neurosci.* **22**, 143-145.

Nicklin, S. A., Reynolds P. N., Brosnan M. J., White S. J., Curiel D. T., Dominiczak A. F. and Baker A. H. (2001) Analysis of cell-specific promoters for viral gene therapy targeted at the vascular endothelium. *Hypertension* **38**, 65-70.

Nielsen, S. L. and Baringer J. R. (1972) Reovirus-induced aqueductal stenosis in hamsters. Phase contrast and electron microscopic studies. *Lab. Invest.* **27**, 531-537.

Nualart, F., Hein S., Rodriguez E. M. and Oksche A. (1991) Identification and partial characterization of the secretory glycoproteins of the bovine subcommissural organ-Reissner's fiber complex. Evidence for the existence of two precursor forms. *Brain Res. Mol. Brain Res.* **11**, 227-238.

O'Callaghan, Sikand C., K. and Rutman A. (1999) Respiratory and brain ependymal ciliary function. *Pediatr. Res.* **46**, 704-707.

Ogata H and Mitsudoe A. (1992) Hydrocephalus due to acute aqueductal stenosis following mumps infections: report of a case and review of the literature. *Brain Dev.* **14**, 417-419.

Ohashi, Y., Nakai Y., Esaki Y., Ohno Y., Sugiura Y. and Okamoto H. (1991) Influenza A virus-induced otitis media and mucociliary dysfunction in the guinea pig. *Acta Otolaryngol. Suppl.* **486**, 135-148.

Oksche, A. (1969) The subcommissural organ. *J. Neurovisc. Relat.* **31**, 111-139.

Oksche, A. (1973) Circumventricular structures and pituitary functions. In Ariens-Kappers, J., (ed.): Proceedings of the Fourth International Congress of Endocrinology. Excerpta Medica, Amsterdam: pp 73-79.

Oldfield, B. J., Allen A. M., Hards D. K., McKinley M. J., Schlawe I. and Mendelsohn F. A. (1994) Distribution of angiotensin II receptor binding in the spinal cord of the sheep. *Brain Res.* **650**, 40-48.

Ostrowski, L. E., Hutchins J. R., Zakel K. and O'Neal W. K. (2003) Targeting expression of a transgene to the airway surface epithelium using a ciliated cell-specific promoter. *Mol. Ther.* **8**, 637-645.

Oudrhiri, N., Vigneron J. P., Peuchmaur M., Leclerc T., Lehn J. M. and Lehn P. (1997) Gene transfer by guanidinium-cholesterol cationic lipids into airway epithelial cells in vitro and in vivo. *Proc. Natl, Acad, Sci, U S A* **94**, 1651-1656.

Papadopoulos, M. C., Krishna S. and Verkman A. S. (2002) Aquaporin water channels and brain edema. *Mt. Sinai. J. Med.* **69**, 242-248.

Pattisapu, J. V. (2001) Etiology and clinical course of hydrocephalus. *Neurosurg. Clin. North Am.* **12**, 651-659.

Perez-Figares, J. M., Jimenez A. J. and Rodriguez E. M. (2001) Subcommissural organ, cerebrospinal fluid circulation, and hydrocephalus. *Microsc. Res. Tech.* **52**, 591-607.

Peters, A. and Swan R. C. (1979) The choroid plexus of the mature and aging rat: the choroidal epithelium. *Anat. Rec.* **194**, 325-353.

Pfeiffer, B., Elmer K., Roggendorf W., Reinhart P. H. and Hamprecht B. (1990) Immunohistochemical demonstration of glycogen phosphorylase in rat brain slices. *Histochemistry* **94**, 73-80.

Philippon, V., Vellutini C., Gambarelli D., Harkiss G., Arbuthnott G., Metzger D., Roubin R. and Filippi P. (1994) The basic domain of the lentiviral Tat protein is responsible for damages in mouse brain: involvement of cytokines. *Virology* **205**, 519-529.

Pollard, H., Remy J. S., Loussouarn G., Demolombe S., Behr J. P. and Escande D. (1998) Polyethylenimine but not cationic lipids promotes transgene delivery to the nucleus in mammalian cells. *J. Biol. Chem.* **273**, 7507-7511.

Poole, C. A., Flint M. H. and Beaumont B. W. (1985) Analysis of the morphology and function of primary cilia in connective tissues: a cellular cybernetic probe? *Cell Motil.* **5**, 175-193.

Preston, J. E. (2001) Ageing choroid plexus-cerebrospinal fluid system. *Microsc. Res. Tech.* **52**, 31-37.

Prothmann, C. (1995) Charakterisierung ependymaler Zellkulturen und Untersuchungen zu ihrem Glycogenstoffwechsel. Diplomarbeit, Universität Tübingen.



Prothmann, C., Wellard J., Berger J., Hamprecht B. and Verleysdonk S. (2001) Primary cultures as a model for studying ependymal functions: glycogen metabolism in ependymal cells. *Brain Res.* **920**, 74-83.

Purves, D., Augustine G. J., Fitzpatrick D., Katz L. C., LaMantia A.S., McNamara J. O. and Williams S. M (2001) *Neuroscience*. (2nd edition). Sinauer Associates, Inc. Sunderland, MA.

Qiao, J., Moreno J., Sanchez-Perez L., Kottke T., Thompson J., Caruso M., Diaz R. M. and Vile R. (2006) VSV-G pseudotyped, MuLV-based, semi-replication-competent retrovirus for cancer treatment. *Gene Ther.* **13**, 1457-1470.

Qin, L., Ding Y., Pahud D. R., Chang E., Imperiale M. J. and Bromberg J. S. (1997) Promoter attenuation in gene therapy: interferon-gamma and tumor necrosis factor-alpha inhibit transgene expression. *Hum. Gene. Ther.* **8**, 2019-2029.

Randell, S. H. (1992) Progenitor-progeny relationships in airway epithelium. *Chest* **101**, 11S-16S.

Rao, M. K., Pham J., Imam J. S., MacLean J. A., Murali D., Furuta Y., Sinha-Hikim A. P. and Wilkinson M. F. (2006) Tissue-specific RNAi reveals that WT1 expression in nurse cells controls germ cell survival and spermatogenesis. *Genes Dev.* **20**, 147-152.

Rao, M. K. and Wilkinson M. F. (2006) Tissue-specific and cell type-specific RNA interference in vivo. *Nat. Protoc.* **1**, 1494-1501.

Rawlins, E. L., Ostrowski L. E., Randell S. H. and Hogan B. L. (2007) Lung development and repair: contribution of the ciliated lineage. *Proc. Natl. Acad. Sci. U S A* **104**, 410-417.

Reader, J. R., Tepper J. S., Schelegle E. S., Aldrich M. C., Putney L. F., Pfeiffer J. W. and Hyde D. M. (2003) Pathogenesis of mucous cell metaplasia in a murine asthma model. *Am. J. Pathol.* **162**, 2069-2078.

Rodriguez, E. M. (1976) The cerebrospinal fluid as a pathway in neuroendocrine integration. *J. Endocrinol.* **71**, 407-443.

Rodriguez, E. M., Oksche A., Hein S., Rodriguez S. and Yulis R. (1984) Spatial and structural interrelationships between secretory cells of the subcommissural organ and blood vessels. An immunocytochemical study. *Cell Tissue Res.* **237**, 443-449.

Rodriguez, E. M., Oksche A., Hein S. and Yulis C. R. (1992) Cell biology of the subcommissural organ. *Int. Rev. Cytol.* **135**, 39-121.

Rodriguez, E. M., Rodriguez S. and Hein S. (1998) The subcommissural organ. *Microsc. Res. Tech.* **41**, 98-123.

Rodriguez, S. and Caprile T. (2001) Functional aspects of the subcommissural organ-Reissner's fiber complex with emphasis in the clearance of brain monoamines. *Microsc. Res. Tech.* **52**, 564-572.

Rosenbaum, J. L. and Witman G. B. (2002) Intraflagellar transport. *Nat. Rev. Mol. Cell Biol.* **3**, 813-825.

Rosenberg, G. A., Kyner W. T., Fenstermacher J. D. and Patlak C. S. (1986) Effect of vasopressin on ependymal and capillary permeability to tritiated water in cat. *Am. J. Physiol.* **251**, F485-489.

Roth, Y., Kimhi Y., Edery H., Aharonson E. and Priel Z. (1985) Ciliary motility in brain ventricular system and trachea of hamsters. *Brain Res.* **330**, 291-297.

Roux, K H (1995) Optimization and trouble shooting in PCR. *Genome Research* PCR Methods Appl **4**, S185-194.

Sankar, R., Thamotharan S., Shin D., Moley K. H. and Devaskar S. U. (2002) Insulin-responsive glucose transporters-GLUT8 and GLUT4 are expressed in the developing mammalian brain. *Brain Res. Mol. Brain Res.* **107**, 157-165.

Sapiro, R., Kostetskii I., Olds-Clarke P., Gerton G. L., Radice G. L. and Strauss I. J. (2002) Male infertility, impaired sperm motility, and hydrocephalus in mice deficient in sperm-associated antigen 6. *Mol. Cell Biol.* **22**, 6298-6305.

Sapiro, R., Tarantino L. M., Velazquez F., Kiriakidou M., Hecht N. B., Bucan M. and Strauss J. F. (2000) Sperm antigen 6 is the murine homologue of the *Chlamydomonas reinhardtii* central apparatus protein encoded by the PF16 locus. *Biol. Reprod.* **62**, 511-518.

Sarnat, H. B. (1992) Regional differentiation of the human fetal ependyma: immunocytochemical markers. *J. Neuropathol. Exp. Neurol.* **51**, 58-75.

Sarnat, H. B. (1995) Ependymal reactions to injury. A review. *J. Neuropathol. Exp. Neurol.* **54**, 1-15.

Sarnat, H. B. (1998) Histochemistry and immunocytochemistry of the developing ependyma and choroid plexus. *Microsc. Res. Tech.* **41**, 14-28.

Sarnat, H. B. and Menkes J. H. (2000) How to construct a neural tube. *J. Child Neurol.* **15**, 110-124.

Satir, P. and Christensen S. T. (2007) Overview of structure and function of mammalian cilia. *Annu. Rev. Physiol.* **69**, 377-400.

Saunders, N. A., Smith R. J. and Jetten A. M. (1994) Differential responsiveness of human bronchial epithelial cells, lung carcinoma cells, and bronchial fibroblasts to interferon-gamma in vitro. *Am. J. Respir. Cell Mol. Biol.* **11**, 147-152.

Sawamoto, K., Wichterle H., Gonzalez-Perez O., Cholfin J. A., Yamada M., Spassky N., Murcia N. S., Garcia-Verdugo J. M., Marin O., Rubenstein. J. L., Tessier-Lavigne M., Okano H. and Alvarez-Buylla A. (2006) New neurons follow the flow of cerebrospinal fluid in the adult brain. *Science* **311**, 629-632.

Scholey, J. M. and Anderson K. V. (2006) Intraflagellar transport and cilium-based signaling. *Cell* **125**, 439-442.

Segal, M. B. (2001) Transport of nutrients across the choroid plexus. *Microsc. Res. Tech.* **52**, 38-48.

Senut, M. C., Jazat F., Choi N. H. and Lamour Y. (1992) Protein SP40,40-like immunoreactivity in the rat brain: progressive increase with age. *Eur. J. Neurosci.* **4**, 917-928.

Shinagawa, T. and Ishii S. (2003) Generation of Ski-knockdown mice by expressing a long double-strand RNA from an RNA polymerase II promoter. *Genes Dev.* **17**, 1340-1345.

Silva, F. P., Hamamoto R., Nakamura Y. and Furukawa Y. (2005) WDRPUH, a novel WD-repeat-containing protein, is highly expressed in human hepatocellular carcinoma and involved in cell proliferation. *Neoplasia* **7**, 348-355.

Simpson, J. C., Wellenreuther R., Poustka A., Pepperkok R. and Wiemann S. (2000) Systematic subcellular localization of novel proteins identified by large-scale cDNA sequencing. *EMBO Rep* **1**, 287-292.

Sledz, C. A., Holko M., de Veer M. J., Silverman R. H. and Williams B. R. (2003) Activation of the interferon system by short-interfering RNAs. *Nat. Cell. Biol.* **5**, 834-839.

Smith, E. F. and Lefebvre P. A. (1997) The role of central apparatus components in flagellar motility and microtubule assembly. *Cell Motil. Cytoskeleton* **38**, 1-8.

Smith, T. F., Gaitatzes C., Saxena K. and Neer E. J. (1999) The WD repeat: a common architecture for diverse functions. *Trends Biochem. Sci.* **24**, 181-185.

Snell, W. J., Pan J. and Wang Q. (2004) Cilia and flagella revealed: from flagellar assembly in *Chlamydomonas* to human obesity disorders. *Cell* **117**, 693-697.

Spassky, N., Merkle F. T., Flames N., Tramontin A. D., Garcia-Verdugo J. M. and Alvarez-Buylla A. (2005) Adult ependymal cells are postmitotic and are derived from radial glial cells during embryogenesis. *J. Neurosci.* **25**, 10-18.

Spector, R. and Eells J. (1984) Deoxynucleoside and vitamin transport into the central nervous system. *Fed. Proc.* **43**, 196-200.

Sterba, G. (1969) Morphologie und Funktion des Subcommissuralorgans. In: G. Sterba, ed. *Zirkumventriculare Organe und Liquor*. Gustav Fischer Verlag, Jena: pp 17-27.

Takano, T., Mekata Y., Yamano T. and Shimada M. (1993) Early ependymal changes in experimental hydrocephalus after mumps virus inoculation in hamsters. *Acta Neuropathol. (Berl)* **85**, 521-525.

Tam, L. W. and Lefebvre P. A. (2002) The *Chlamydomonas* MBO2 locus encodes a conserved coiled-coil protein important for flagellar waveform conversion. *Cell Motil. Cytoskeleton* **51**, 197-212.

Tarlow, M. J., Jenkins R., Comis S. D., Osborne M. P., Stephens S., Stanley P. and Crocker J. (1993) Ependymal cells of the choroid plexus express tumour necrosis factor-alpha. *Neuropathol. Appl. Neurobiol.* **19**, 324-328.

Taulman, P. D., Haycraft C. J., Balkovetz D. F. and Yoder B. K. (2001) Polaris, a protein involved in left-right axis patterning, localizes to basal bodies and cilia. *Mol. Biol. Cell* **12**, 589-599.

Thomas, C. E., Schiedner G., Kochanek S., Castro M. G. and Lowenstein P. R. (2000) Peripheral infection with adenovirus causes unexpected long-term brain inflammation in animals injected intracranially with first-generation, but not with high-capacity, adenovirus vectors: toward realistic long-term neurological gene therapy for chronic diseases. *Proc. Natl. Acad. Sci. U S A* **97**, 7482-7487.

Thomas, L. H., Wickremasinghe M. I., Sharland M. and Friedland J. S. (2000) Synergistic upregulation of interleukin-8 secretion from pulmonary epithelial cells by direct and monocyte-dependent effects of respiratory syncytial virus infection. *J. Virol.* **74**, 8425-8433.

Thompson, C. B. (1995) Apoptosis in the pathogenesis and treatment of disease. *Science* **267**, 1456-1462.

Tristram, D. A., Hicks, Jr W. and Hard R. (1998) Respiratory syncytial virus and human bronchial epithelium. *Arch. Otolaryngol. Head Neck Surg.* **124**, 777-783.

Tyner, J. W., Kim E. Y., Ide K., Pelletier M. R., Roswit W. T., Morton J. D., Battaile J. T., Patel A. C., Patterson G. A., Castro M., Spoor M. S., You Y., Brody S. L. and Holtzman M. J. (2006) Blocking airway mucous cell metaplasia by inhibiting EGFR antiapoptosis and IL-13 transdifferentiation signals. *J. Clin. Invest.* **116**, 309-321.

Verleysdonk, S., Hirschner W., Wellard J., Rapp M., de los Angeles Garcia M., Nualart F. and Hamprecht B. (2004) Regulation by insulin and insulin-like growth factor of 2-deoxyglucose uptake in primary ependymal cell cultures. *Neurochem. Res.* **29**, 127-134.

Vigna, E. and Naldini L. (2000) Lentiviral vectors: excellent tools for experimental gene transfer and promising candidates for gene therapy. *J. Gene Med.* **2**, 308-316.

Vogel R, Amar L, Thi AD, Saillour P and Mallet J (2004) A single lentivirus vector mediates doxycycline-regulated expression of transgenes in the brain. *Hum. Gene Ther.* **15**, 157-165.

Walther, W. and Stein U. (1996) Cell type specific and inducible promoters for vectors in gene therapy as an approach for cell targeting. *J. Mol. Med.* **74**, 379-392.

Wang, Q., Pan J. and Snell W. J. (2006) Intraflagellar transport particles participate directly in cilium-generated signaling in *Chlamydomonas*. *Cell* **125**, 549-562.

Watson, D. J., Kobinger G. P., Passini M. A., Wilson J. M. and Wolfe J. H. (2002) Targeted transduction patterns in the mouse brain by lentivirus vectors pseudotyped with VSV, Ebola, Mokola, LCMV, or MuLV envelope proteins. *Mol. Ther.* **5**, 528-537.

Watson, D. J., Passini M. A. and Wolfe J. H. (2005) Transduction of the choroid plexus and ependyma in neonatal mouse brain by vesicular stomatitis virus glycoprotein-pseudotyped lentivirus and adeno-associated virus type 5 vectors. *Hum. Gene Ther.* **16**, 49-56.

Weibel, M., Pettman, B., Artault, J. C., Sensenbrenner, M and Labourdette, G. (1986) Primary cultures of rat ependymal cells in serum-free defined medium. *Dev. Brain. Res.* **25**, 199-209.

Wellard, J., DeVente J., Hamprecht B. and Verleysdonk S. (2006) Natriuretic peptides, but not nitric oxide donors, elevate levels of cytosolic guanosine 3',5'-cyclic monophosphate in ependymal cells ex vivo. *Neurosci. Lett.* **392**, 187-192.

Wellard, J., Rapp M., Hamprecht B. and Verleysdonk S. (2003) Atrial natriuretic peptides elevate cyclic GMP levels in primary cultures of rat ependymal cells. *Neurochem. Res.* **28**, 225-233.

Wittkowski, W. (1998) Tanycytes and pituicytes: morphological and functional aspects of neuroglial interaction. *Microsc. Res. Tech.* **41**, 29-42.

Wiznerowicz, M., Szulc J. and Trono D. (2006) Tuning silence: conditional systems for RNA interference. *Nat. Methods* **3**, 682-688.

Worthington, W. C. and Cathcart R. S. (1963) Ependymal cilia: distribution and activity in the adult human brain. *Science* **139**, 221-222.

Yang, J., Liu X., Yue G., Adamian M., Bulgakov O. and Li T. (2002) Rootletin, a novel coiled-coil protein, is a structural component of the ciliary rootlet. *J. Cell Biol.* **159**, 431-440.

Yang Z Y, Duckers H J, Sullivan N J, Sanchez A, Nabel E G, Nabel G J (2000) Identification of the Ebola virus glycoprotein as the main viral determinant of vascular cell cytotoxicity and injury. *Nat. Med.* **6**, 886-889.

Yi, Y., Lee C., Liu Q. H., Freedman B. D. and Collman R. G. (2004) Chemokine receptor utilization and macrophage signaling by human immunodeficiency virus type 1 gp120: Implications for neuropathogenesis. *J. Neurovirol.* **10**, 91-96.

Young, L. S., Dawson C. W. and Eliopoulos A. G. (1997) Viruses and apoptosis. *Br. Med. Bull.* **53**, 509-521.

Zabner, J., Fasbender A. J., Moninger T., Poellinger K. A. and Welsh M. J. (1995) Cellular and molecular barriers to gene transfer by a cationic lipid. *J. Biol. Chem.* **270**, 18997-19007.

Zhang, B., Metharom P., Jullie H., Ellem K. A., Cleghorn G., West M. J. and Wei M. Q. (2004) The significance of controlled conditions in lentiviral vector titration and in the use of multiplicity of infection (MOI) for predicting gene transfer events. *Genet. Vaccines. Ther.* **2**, 6.

Zhang, J., Williams M. A. and Rigamonti D. (2006) Genetics of human hydrocephalus. *J. Neurol.* **253**, 1255-1266.

Zhang, X. Y., La Russa V. F. and Reiser J. (2004) Transduction of bone-marrow-derived mesenchymal stem cells by using lentivirus vectors pseudotyped with modified RD114 envelope glycoproteins. *J. Virol.* **78**, 1219-1229.



Zhang, Z., Jones B. H., Tang W., Moss S. B., Wei Z., Ho C., Pollack M., Horowitz E., Bennett J., Baker M. E. and Strauss J. F. (2005) Dissecting the axoneme interactome: the mammalian orthologue of Chlamydomonas PF6 interacts with sperm-associated antigen 6, the mammalian orthologue of Chlamydomonas PF16. *Mol. Cell. Proteomics* **4**, 914-923.

Zufferey, R., Nagy D., Mandel R. J., Naldini L. and Trono D. (1997) Multiply attenuated lentiviral vector achieves efficient gene delivery in vivo. *Nat. Biotechnol.* **15**, 871-875.



## 6. Summary

- Identification of E71, a coiled-coil domain containing protein, by screening of a subtractive ependymal cDNA library and its further analysis with quantitative RT-PCR studies revealed that the E71 gene is exclusively transcribed in kinocilia-bearing cells.
- Polyciliated ependymal cells in primary culture are completely resistant to nonviral gene transfer methods using naked plasmid DNA.
- In contrast to the nonviral gene transfer methods, lentiviral vector-mediated gene transfer significantly increases the number of transfected cells in the ependymal primary cultures (EPC).
- Transfection efficiency in the undifferentiated ependymal primary cultures is significantly higher than in the differentiated cultures when lentiviruses are employed as gene transfer vectors.
- Infection of ependymal primary cultures with lentiviral vectors may result in a significant loss of ciliated cells.
- The loss of cilia or ciliated cells in the ependymal primary cultures after infection with virus are likely not caused by apoptosis via the apoptosome-mediated pathway, since it is not affected by an apoptosis inhibitor.
- Transfection of ependymal primary cultures with lentivirus encoding green fluorescent protein as a marker under the control of the EF1 $\alpha$  promoter resulted in the expression of the transgene in more than 75% of cells, of which very few, however, were kinociliated.
- By using lentiviral vectors encoding GFP under the control of promoters specific for ciliated cells (FOXJ1, wdr16), the transgene expression in cells without kinocilia could be suppressed and the transfection efficiency with respect to kinociliated cells was increased significantly.

## *Summary*

- The genomic DNA fragment of 766 bp between the transcription start sites of the rat syntaxin8 and wdr16 genes is capable of driving the transgene expression specifically in kinociliated cells.
- The wdr16 promoter seems to be activated specifically in kinociliated cells but not in monociliated cells, similar to the known kinociliated cell-specific promoter FOXJ1.
- In EPC, the wdr16 and FOXJ1 promoters drive transgene expression not only in kinociliated cells but also in some cells without surface cilia, which may be precursors of ciliated cells.

## **My academic teachers are:**

In India:

Prof. Dr. C. Annapurna  
Prof. Dr. D.E. Babu  
Prof. Dr. B. Bharatha Lakshmi  
Prof. Dr. Ch. Bharathi  
Prof. Dr. G. Gnana Mani  
Prof. Dr. A. Joseph  
Prof. Dr. R. Kameswara Rao  
Prof. Dr. B. Kishore  
Prof. Dr. M. Lakshmi Narasu  
Dr. S. C. Lali  
Dr. C. Manjulatha  
Prof. Dr. Y. Prabhakara Rao  
Prof. Dr. A. V. Raman  
Dr. T. B. Ratna Kumari  
Dr. Rekha Chaturvedi  
Prof. Dr. B. V. Sandeep  
Prof. Dr. U. Shameem  
Prof. Dr. K. Sreeramulu  
K. Subbaraya Sharma  
Dr. Subeer S Majumdar  
Prof. Dr. C. Vijaya Lakshmi  
Dr. Vinod Agarkar  
Udaya Bhaskar

In Germany:

Prof. Dr. Bernd Hamprecht  
PD Dr. Stephan Verleysdonk

## Curriculum Vitae

---

Name: Bhavani Shankar Kowtharapu

Date of birth: 18-08-1975

Birth place: Repalle (Andhra Pradesh, India)

Education:

1980-1990: Board of Secondary School Education, B.S.S.S. High School, Repalle, AP, India

1990-1992: Board of Intermediate Education, V.R.S & Y.R.N. College, Chirala, AP, India

1993-1996: Bachelor of Science, S.V.R.M. College, Nagaram, AP, India

1996-1998: Master of Science (Zoology), Andhra University, Visakhapatnam, AP, India

1999-2001: Master of Technology (Bio-Technology), J.N.T.University, Hyderabad, AP, India  
Master Thesis: "Studies on pentachlorophenol degrading bacterial isolates of marine origin" (at the Institute of Genomics and Integrative Biology, New Delhi, India).

2003-2008: Preparation of this doctoral thesis under the guidance of Prof. Dr. Bernd Hamprecht and PD Dr. Stephan Verleysdonk at the Interfaculty Institute for Biochemistry, University of Tuebingen, Germany.